

5-2021

Genetic Pathway Analysis Of Abnormal Facial Development In Nonsyndromic Cleft Lip And Palate

lorena maili

Follow this and additional works at: https://digitalcommons.library.tmc.edu/utgsbs_dissertations



Part of the [Developmental Biology Commons](#), [Genetics Commons](#), and the [Medicine and Health Sciences Commons](#)

Recommended Citation

maili, loren, "Genetic Pathway Analysis Of Abnormal Facial Development In Nonsyndromic Cleft Lip And Palate" (2021). *Dissertations and Theses (Open Access)*. 1100.
https://digitalcommons.library.tmc.edu/utgsbs_dissertations/1100

This Dissertation (PhD) is brought to you for free and open access by the MD Anderson UTHealth Houston Graduate School at DigitalCommons@TMC. It has been accepted for inclusion in Dissertations and Theses (Open Access) by an authorized administrator of DigitalCommons@TMC. For more information, please contact digcommons@library.tmc.edu.

Genetic Pathway Analysis of Abnormal Facial Development in
Nonsyndromic Cleft Lip and Palate

by

Lorena Maili, M.S.

APPROVED:

Jacqueline Hecht, Ph.D.

Ariadne Letra, D.D.S., M.S., Ph.D.

George Eisenhoffer, Ph.D.

Brett Chiquet, D.D.S., Ph.D.

Ralf Krahe, Ph.D.

APPROVED:

Michael Blackburn, PhD, The University of Texas
MD Anderson Cancer Center UTHealth Graduate School of Biomedical Sciences

Genetic Pathway Analysis of Abnormal Facial Development in
Nonsyndromic Cleft Lip and Palate

A

Dissertation

Presented to the Faculty of

The University of Texas

MD Anderson Cancer Center UTHealth

Graduate School of Biomedical Sciences

in Partial Fulfillment

of the Requirements

for the Degree of

Doctor of Philosophy

by

Lorena Maili, M.S.
Houston, Texas

May, 2021

Acknowledgements

First, I would like to thank my advisor, Dr. Jacqueline Hecht, for being an outstanding mentor, supervisor, advocate and role model during the last ten years, both while I was a research assistant and a graduate student. I would not have been able to accomplish my goals without your around-the-clock dedication, passion for teaching, extensive experience and patience -- working with you has made me a better scientist and person.

Thank you to my committee Drs. Jacqueline Hecht, Brett Chiquet, Ariadne Letra, George Eisenhoffer, Gil Cote and Ralf Krahe for your time, your advice and your investment in my academic growth. Thank you to everyone in the Hecht Lab, both past and present members, Dr. Brett Chiquet, Dr. Qiuping Yuan, Dr. Bhavna Tandon, Dr. Vershanna Morris, Dr. Katelyn Weymouth, Christian Urbina, Rachel Willeford, Dr. Wei Lu, Dr. Shea Posey, Dr. Francoise Coustry, Alka Veerisetty, Mohammad Hossain, Frankie Chiu, Elena Serna and Rosa Martinez for contributing to my training, teaching me lab techniques, reading over written drafts, creating a space where I could openly discuss scientific ideas and ask questions of various scopes, and for all other support. Special thanks to Dr. Syed Hashmi and our collaborator, Dr. Susan Blanton for your teaching and your contributions to the statistical analyses.

Thank you to Drs. Eric Swindell, George Eisenhoffer and Oscar Ruiz for all the education and advice on everything zebrafish related. Also, thank you to Dr. Ariadne Letra and her lab for collaborating with us on multiple projects, helping me with experiments and sharing protocols. Dr. Rachel Miller her lab, especially Mark Corkins, were extremely helpful in assisting me with the confocal microscope and I am very grateful to you all. Thank you to Dr. Yoshi Komatsu for your co-sponsor role (along with Dr. Jacqueline Hecht, Dr.

George Eisenhoffer and Dr. Susan Blanton) in my F31 application and for your career advice.

Everyone at GSBS makes up an incredible team and a fantastic academic program for students, and I am lucky to have been part of the school. Special thank you to both the Human and Molecular Genetics and the Genetics and Epigenetics programs for welcoming me and providing so much support over the years, especially the program directors (Drs. Subrata Sen, Ann Killary, Eduardo Vilar-Sanchez, Richard Behringer, Jichao Chen and Francesca Cole) and program coordinators (Bert Shaw and Elisabeth Lindheim), you are exemplary in your dedication to students.

Thank you to all my friends and classmates for encouraging me to work hard but also enjoy life outside the lab and for being patient with my schedule through all these years of school.

Lastly, thank you to my parents, Dr. Eduard Maili and Zhaneta Maili, my sister Alkesta Belknap and brother-in-law Curtis Belknap, and my partner Chris Fulkerson, for all your love, your belief in me and your unconditional support.

Genetic Pathway Analysis of Abnormal Facial Development in Nonsyndromic Cleft Lip and Palate

Lorena Maili, M.S.

Advisory Professor: Jacqueline Hecht, Ph.D.

Nonsyndromic cleft lip with or without cleft palate (NSCLP) is the most common craniofacial birth defect resulting from incomplete fusion of the facial prominences during development, which leaves a gap in the lip, primary palate and/or the secondary palate. NSCLP affects 135,000 NSCLP newborns worldwide each year based on a birth prevalence of 1 per 700 live births. While surgical treatments have dramatically improved, many long-term health issues persist, imposing significant medical, psychosocial and economic burdens. Familial aggregation and segregation analyses suggest genetic contributions underlie NSCLP, but despite decades of study, only a small portion of the NSCLP genetic liability has been identified leaving a large knowledge gap. Following a pathway-based approach to identify NSCLP etiologic genes, this dissertation examined gene networks regulating facial morphogenesis. Three different pathways were assessed and found to have etiologic roles in NSCLP. The PBX pathway, implicated in murine midfacial development, was confirmed to be associated with NSCLP in our family-based and case-control datasets. The second gene, identified in the CRISPLD2 network, was found to play a novel role in regulating oral and facial development, with perturbation causing abnormal oral morphogenesis in zebrafish. The final study used bioinformatic, cell-based and transgenic zebrafish approaches together to identify noncoding variants in *FZD6*, *LRP5*, *LRP6* and *DKK1* driving allele-specific expression during craniofacial

development. Testing of these variants in our extensive family-based NSCLP dataset identified, for the first time, associations between *LRP5* and *DKK1* and NSCLP, and confirmed the previously identified association with *FZD6* and *LRP6*. These results support the analysis of gene networks rather than individual genes to identify the missing heritability underlying NSCLP. This approach is critical towards understanding the polygenic contributions that are known to underlie NSCLP and other complex disorders. The goal of these studies is to construct and map all of the noncoding and coding variants contributing to NSCLP, with the ultimate goal of determining individual and family risks, so that the information can be used in the clinic setting.

Table of Contents

Approval Page.....	i
Title Page	ii
Acknowledgements	iii
Abstract	v
Table of Contents	vii
List of Figures.....	x
List of Tables.....	xii
CHAPTER 1: BACKGROUND AND SIGNIFICANCE	13
1.1 Introduction.....	14
1.2 Clinical Features of Orofacial Clefts.....	14
1.3 Nonsyndromic Cleft Lip and Palate	15
1.3 Genetic studies of NSCLP.....	16
1.4 Gene Pathways implicated NSCLP	16
1.5 Noncoding variants in NSCLP.....	17
1.8 Craniofacial embryology.....	17
1.9 WNT signaling in facial development.....	19
1.10 WNT pathway genes.....	21
1.11 Significance.....	22
CHAPTER 2: MATERIALS AND METHODS.....	24
2.1 Prioritization of noncoding variants	25
2.2 Electrophoretic mobility shift assay (EMSA)	26
2.3 Luciferase assays	26
2.4 Zebrafish care and husbandry	27
2.5 Morpholino and CRISPR/Cas9 injections.....	27
2.6 Zebrafish Facial Analytics based on Coordinate Extrapolate system (zFACE)	28
2.7 Skeletal staining.....	29
2.8 Generation of transgenic reporter lines.....	30
2.9 Drug treatments	30
2.10 Family dataset	31
2.11 Genotyping	31
2.12 Statistical Analysis for Association Studies.....	32
CHAPTER 3: PBX-WNT-P63-IRF6 pathway in nonsyndromic cleft lip and palate	33

3.0 Introduction.....	34
3.1 Materials and methods	35
3.1.1 Family discovery and case control validation datasets	36
3.1.2 SNVs genotyped	37
3.1.3 Single SNV and haplotype association testing.....	37
3.1.4 Gene-gene interaction analysis	37
3.2 Results	40
3.2.1 Single SNV associations	40
3.2.2 Haplotype associations.....	40
3.2.3 Gene-gene interactions	43
3.2.4 Predicted functional consequences of associated SNVs	44
3.3 Discussion	46
CHAPTER 4: Fostering the face: the role of <i>FOS</i> in craniofacial morphogenesis and nonsyndromic cleft lip and palate	51
4.1 Introduction.....	52
4.1 Materials and methods	54
4.2 Results	54
4.2.1 <i>Fos</i> knockdown causes craniofacial abnormalities in zebrafish	54
4.2.2 <i>Fos</i> morphants have abnormally-shaped mouths and craniofacies	60
4.2.3 Human <i>fos</i> mRNA rescues morphant phenotype.....	65
4.2.4 <i>Fos</i> CRISPR/Cas9 F0 mutants recapitulate morphant craniofacial phenotype at 5 dpf	67
4.2.5 Cranial neural crest cells are reduced in <i>fos</i> morphant and mutant embryos.....	69
4.3 Discussion	71
CHAPTER 5: The role of regulatory variants in <i>FZD6</i> and interacting genes in nonsyndromic cleft lip and palate.....	76
5.0 Introduction.....	77
5.1 Materials and methods	79
5.2 Results	80
5.2.1 Twenty one putatively functional variants prioritized for study.....	80
5.2.2 Protein-DNA binding assays showed allele-specific effects for ten variants	81
5.2.3 Luciferase assays identified six variants with allele-specific effects on expression.....	82
5.2.4 Establishment of timeline for mouth development and β -catenin expression	84
5.2.5 Knockdown of <i>FZD6</i> and related genes caused similarly abnormal facial phenotypes	85
5.2.6 Small molecule inhibition and activation of WNT signaling alters facial phenotype	88

5.2.7 Transgenic reporter zebrafish assays supported functionality of four variants	89
5.2.5 Association in NSCLP families	93
5.3 Discussion	95
CHAPTER 6: Summary and Future Directions.....	99
BIBLIOGRAPHY.....	103
Vita	130

List of Figures

Figure 1: Clinical manifestations of orofacial clefts

Figure 2: Embryonic facial development

Figure 3: The Wnt signaling pathway

Figure 4: PBX study methodology workflow

Figure 5. Violin plots from GTEx for the significant SNVs in this study

Figure 6. Gene pathway model linking human and mouse findings

Figure 7. Overview of experimental approach in the *fos* study

Figure 8. *Fos* knockdown caused craniofacial and dental abnormalities

Figure 9. Phenotype severity increased with higher doses of *fos* morpholino

Figure 10. *Fos* morphants showed abnormal arches and reduced ossification

Figure 11. Zebrafish pharyngeal dentition at 5 and 7 days post fertilization

Figure 12. Developmental timeline of *fos* morphant dentition

Figure 13. *Fos* morphants had abnormal facial morphology with a keyhole shaped mouth

Figure 14. Graph of two mouth angles altered in *fos* morphants at 5 and 6 dpf

Figure 15. Summary of altered zFACE dimensions in *fos* morphants

Figure 16. PC plot showing *fos* morphants separating from both controls and resulting shape changes along PC1

Figure 17. DFA results showed significantly different face shape in *fos* morphants

Figure 18. Human *FOS* mRNA rescued facial abnormalities associated with *fos* knockdown

Figure 19. PC plot results confirmed the rescue group was more similar to controls

Figure 20. DFA showed the rescue group had a more normal average face shape

Figure 21. CRISPR/Cas9 mutants recapitulated the morphant phenotype

Figure 22. CNCC populations were altered in *fos* morphants and mutants

Figure 23. *Sox10* expression was significantly reduced in *fos* morphants and mutants

Figure 24. Approach to identify and test noncoding variants in *FZD6* and related genes

Figure 25. Results for *LRP6* rs7136380 showed allele-specific banding and luciferase expression

Figure 26. β -catenin activation during orofacial development in zebrafish embryos

Figure 27. Knockdown of *fzd6* and related genes caused abnormal facial phenotypes

Figure 28. Morphometric measurements altered after knockdown of *fzd6*, *lrp5*, *lrp6* and *dkk1*

Figure 29. DFA results showed that all morphants had a significantly different face shape compared to controls but a similar face shape compared to each other

Figure 30. Wnt drugs altered facial phenotype and β -catenin activation in the oral cavity

Figure 31. *FZD6* rs139557689 expression results showed alternate allele-driven mCherry expression in F1 transgenic embryos

Figure 32. Transgenic reporter expression results at 3 dpf.

Figure 33. Transgenic reporter expression results at 3 dpf in stable F1 embryos

List of Tables

Table 1: Description of family-based and case-control NSCLP datasets

Table 2: SNV alleles and frequencies by ethnicity

Table 3: *WNT3*, *WNT9B* and *IRF6* SNVs used in gene-gene interaction calculations

Table 4. Association results by ethnicity and pedigree type

Table 5. Haplotype results from NSCLP families

Table 6. Summary of gene-gene interaction calculations in NSCLP families

Table 7. Bioinformatic analysis results

Table 8. CB5 mineralization and pharyngeal tooth development is affected in *fos* morphants

Table 9. ZFACE analysis results for all morphometric measurements

Table 10. Bioinformatic prioritization results

Table 11. Details of selected variants and predicted allele-specific TF binding sites

Table 12. Summary of EMSA and luciferase assay results for prioritized variants

Table 13. ZFACE morphometric results in *FZD6*, *LRP5*, *LRP6* and *DKK1* morphants

Table 14. FBAT results on *FZD6*, *LRP5*, *LPR6* and *DKK1* variants

Table 15. Gene-gene interaction results for *FZD6* pathway variants

CHAPTER 1: BACKGROUND AND SIGNIFICANCE

1.1 Introduction

Nonsyndromic cleft lip with or without cleft palate (NSCLP) is the most common craniofacial birth defect, with a birth prevalence of 1 in 700 live births and affecting approximately 4000 newborns in the United States and 130,000 babies worldwide each year [1-3] (CDC 2006). Despite decades of research, the causative factors are largely unknown. The studies in this dissertation aim to increase our understanding of the underlying genetic causes of abnormal facial development in NSCLP in order to create better diagnostics for at-risk individuals and advance therapeutic interventions. The clinical features of NSCLP, facial development and molecular mechanisms that influence it as well as known genetic contributions are reviewed to set the stage for what was learned from this work.

1.2 Clinical Features of Orofacial Clefts

Orofacial clefts are structural malformations that arise from incomplete fusion of the facial prominences during development, leaving a gap in the lip, palate or a combination of both [4] (**Figure 1**). Clefts occur unilaterally in 80% of cases, more often affecting the left side of face and bilaterally in the remaining 20%; males are affected twice as frequently as females [5, 6]. The birth prevalence varies depending on geographic regions and ethnic populations with East Asian and Native Americans having the highest birth prevalence and African ancestry populations having the lowest [2, 7].

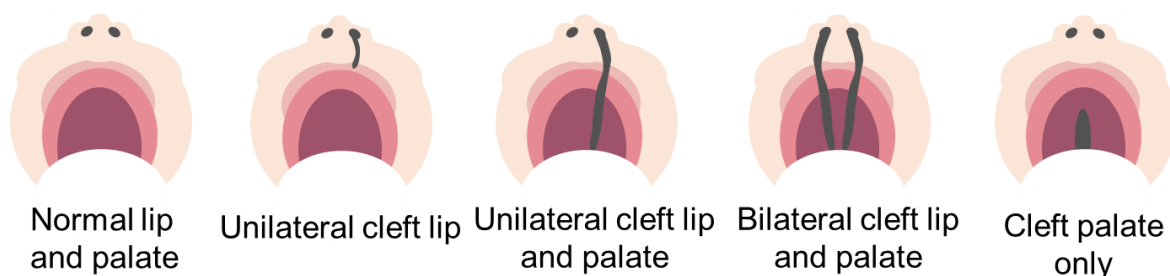


Figure 1: Clinical manifestations of orofacial clefts.

The mildest manifestation is a unilateral microform cleft lip, where a notch is present in the upper lip (vermillion) and a scar-like band of fibrous tissue occurs from the lip to the nostril (also minor nasal deformities can be present) [8, 9]. The fibrous tissue is thought to be a scar from delayed lip closure (as a mild form of the defect) or from spontaneous repair of the cleft in utero by unknown mechanisms [9]. The most severe form is bilateral complete cleft lip and palate, which requires the most extensive surgical and rehabilitative therapy [10].

In addition to the cleft anomaly, other structural abnormalities include a short philtrum, abnormal orbicularis oris muscle (muscle in the upper lip is inserted in parts of the nose), structural deformities that affect the appearance and function of the nose, disruptions in the alveolar bone and dental anomalies [11, 12].

Developmentally, orofacial clefts can be divided into cleft palate only or cleft lip with or without cleft palate. Additionally, in syndromic forms, clefts can be one of multiple clinical features. To date, over 400 syndromes include an orofacial cleft as a clinical feature, including van der Woude, Stickler and Treacher Collins syndromes [4, 7]. The majority of clefts, however, manifest without any other structural, functional or behavioral abnormalities and are the focus of this work.

1.3 Nonsyndromic Cleft Lip and Palate

Nonsyndromic cleft lip with or without cleft palate (NSCLP) is postulated to follow the multifactorial model of inheritance, which involves both genetic and environmental interacting factors that each have a small effect, but act together in an additive manner [6, 13-15] [16]. The genetic component is estimated to be high in NSLCP, with some heritability estimates of greater than 70% [17].

Family studies, the first of which were documented by Fogh Anderson in 1942, have shown a strong familial aggregation; individuals with an affected first degree relative have a 32 times

higher relative risk compared to the general population [18, 19]. This relative risk decreases with familial distance. Additionally, the concordance rate is higher in monozygotic twins (40-60%) compared to dizygotic twins (3-5%) strongly implicating genetic factors. Based on these findings, both candidate gene and genome-wide interrogations have been applied in the last several decades with some success in identifying genetic contributions to NSCLP [4, 20, 21].

1.3 Genetic studies of NSCLP

Approximately 30-40 genetic loci influencing risk to orofacial clefts have been identified through linkage and genome wide association studies (GWAS). Twelve GWAS loci have been replicated in other studies and meta-analyses [4, 22]. Candidate genes in/close to linkage and GWAS regions include *ARHGAP29*, *CRISPLD2*, *FOXE1*, *IRF6*, *MSX1*, *TGFA*, *RARA*, and *TP63* among others [4, 22, 23]. Surprisingly, *IRF6* is the only gene supported by both linkage and GWAS methods [24]. This could be due to high genetic heterogeneity contributing to NSCLP. Additionally, the identified genetic variation so far includes common single nucleotide variants (SNVs), low frequency variants, copy number variants and deNovo/rare mutations, the latter of which are usually restricted (private) to specific families [25-30].

1.4 Gene Pathways implicated NSCLP

Results from both human genetic studies and animal models support the dysregulation of genes and signaling pathways contributing to NSCLP, including WNT, FGF, BMP, and TGF- β among others [31, 32]. This is consistent with the multifactorial model, where multiple genes interact with each other or environmental factors to contribute to NSCLP. Pathway analyses or methods that detect gene-gene interactions have the potential to discover or amplify signals from combinatorial contributions from multiple genes [24]. We have successfully used this

approach to confirm previously nominated genes and to identify new candidate NSCLP gene networks [33, 34].

1.5 Noncoding variants in NSCLP

Interestingly, several loci identified in linkage studies are not near any genes and the majority of GWAS SNVs meeting genome-wide association thresholds are noncoding variants, found either upstream, downstream or in introns of genes [35]. Although they don't code for proteins or alter protein sequence, noncoding variants can harbor regulatory elements such as enhancers, silencers, promoters and noncoding RNAs which have the potential to modify transcription and alter the dosage of gene expression [36, 37]. It has been shown that enhancer elements alter facial morphology by fine-tuning gene expression during embryonic development to create circumstances that allow for nonsyndromic clefts to occur [38]. We and others have recently found support for craniofacial enhancer elements contributing to NSCLP [39, 40]. Further identification and interrogation of such variants, as well as their functional consequences, is an exciting direction for current/future research in the genetics of NSCLP.

1.8 Craniofacial embryology

Orofacial development is complex, involving multiple biological processes and growth factors with precise timing of tissue movement and fusion [41, 42]. The information pertaining to upper lip and palate development is derived from studies of human fetuses but also detailed experiments in animal models [43].

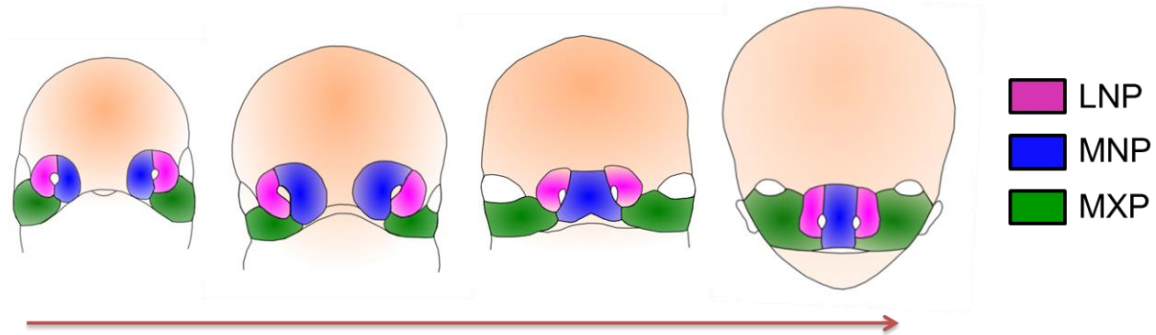


Figure 1: Embryonic facial development.

Facial development starts during the fourth gestational week, when the neural crest cells (NCCs), a transient population of multipotent cells, delaminate from the cephalic neural tube, migrate and combine with the core mesoderm and epithelial cover and proliferate to give rise to the 5 facial primordia [4, 5] (**Figure 2**). These primordia are the frontonasal prominence (FNP), the paired mandibular processes and the paired maxillary processes. At week 5, the nasal placodes appear and divide the medial (MNP) and lateral nasal processes (LNP) [4]. During weeks 6 and 7, the maxillary processes grow medially and fuse with the nasal processes to give rise to a complete upper lip and primary palate [4]. The secondary palate is formed when the palatal shelves grow out from the MXP during the sixth week and elevate above the tongue to subsequently fuse during weeks 9 - 12 to form the roof of the oral cavity [4]. Importantly, because the fusion of the lip and primary palate takes place first, the presence of a cleft in the lip can affect the fusion of structures in the palate, which is why cleft lip and palate often occur together [4].

Interestingly, as the facial primordia are growing and fusing, the brain is also developing and in turn, influencing the face through both physical and molecular interactions [44-46]. The brain acts as a platform and influences the shape, growth and displacement of the facial primordia [44]. One theory is that if the brain is growing very quickly, then the prominences have a smaller window to make contact and fuse and this scenario might increase the

likelihood of a cleft to occur [44, 45]. In the case of NSCLP, this is plausible as there are no other malformations, and minor/subtle changes in the brains of patients with NSCLP have been reported [47, 48].

1.9 WNT signaling in facial development

While many signaling pathways are known regulate craniofacial development, among them BMP, FGF, SHH and others, Wnt signaling, the focus of this dissertation, as it is one of the key pathways affecting many stages, from migration of NCCs to the growth and fusion of the facial prominences [49]. Wnt signaling transductions can be divided into canonical (β -catenin mediated) and non-canonical pathways and both are important during facial development [49, 50]. There are 19 secreted WNTs transcribed from closely related genes that are similar in size, which bind to 10 frizzled receptors coupled to 2 LDL co-receptors (LRP5 and LRP6) [51]. The interaction between the ligands and receptors is mediated by conserved residues and although several WNT ligands preferentially bind to certain FZD receptors this is driven mostly by cellular context and adds to the complexity of how and when this pathway functions [51].

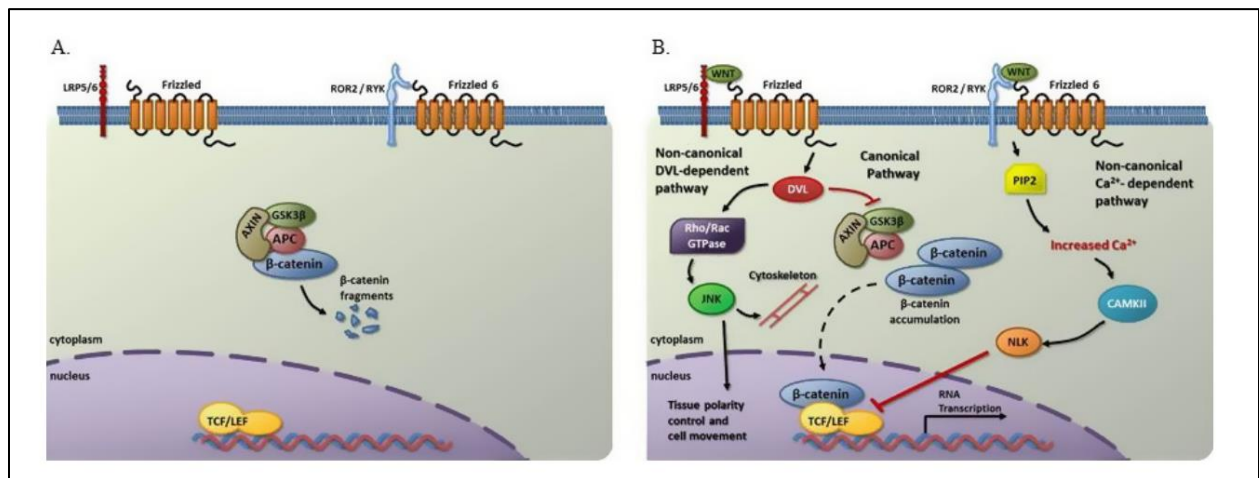


Figure 2: The WNT signaling pathway.

The β -catenin mediated Wnt pathway is activated when a Wnt ligand binds a frizzled (Fzd) receptor and a low-density lipoprotein-related protein 5 or 6 (LRP5/6) co-receptor, leading to inhibition of the β -catenin destruction complex [49, 50]. This allows for the accumulation of β -catenin in the cytoplasm [49, 50]. β -catenin can then translocate into the nucleus and interact with lymphoid enhancer-binding factor or T cell-specific transcription factor (TCF/LEF) in WNT-responsive DNA elements and regulate the transcription of specific genes [49, 50]. The inhibitors for this pathway, Dickkopf (DKK) family members, bind to LRP5/6 and antagonize Wnt ligands to downregulate β -catenin signaling [49].

Canonical (β -catenin) Wnt signaling is active in both the ectoderm and underlying mesenchyme of the facial prominences and palatal shelves [49]. This signaling marks areas of high growth and, in mammals, it is more intensely expressed in lateral regions such as the maxilla, and low or absent in the midline regions or the frontonasal prominence [52]. Wnt mutant mouse models highlight the importance of dosage (fine tuning) in signaling by revealing that both too little and too much canonical Wnt signaling can lead to craniofacial deformity phenotypes that include cleft lip and palate [49]. There is an inbred strain (A-) of mice that exhibits multifactorial nonsyndromic clefting (A/WySn and compound *Wnt9b/clf1* mutants) [53]. These mice have mutations that affect Wnt signaling through cis interference and epigenetic control of *Wnt9b* transcription [53-58]. They exhibit abnormalities in size and shape of the facial prominences during development and the frequency of clefts can be anywhere from 10%-90% [53]. A study investigating signaling at the mouse lamboidal junction, where the MXP, MNP and LNP make contact, found that the Pbx transcription factors dysregulated Wnt signaling and decreased apoptosis at the fusion site, triggering completely penetrant bilateral clefts [59]. Additionally, there is a long-range murine enhancer harbored by the 8q24 region that acts on *Myc* expression and causes dysregulation of Wnt pathway genes (*Fzd6*, *Wnt5A*, *Wnt9b*, *TCF4*, *Dkk1* and *Lef1*) [60]. Deletions in this enhancer lead to

cleft lip in 7% of mutant mice and alter facial features such as the snout, frontal bones, width of MPN and others in the rest [60].

In summary, Wnt β -catenin pathway genes are important for normal development of the upper lip and palate, and disturbances in this pathway lead to altered facial morphology, including orofacial clefts.

1.10 WNT pathway genes

WNT signaling genes have been identified as causative factors in both syndromic and nonsyndromic forms of CLP [31]. For example, while mutations in *WNT3* and *WNT5A* are associated with syndromic clefts in tetra-amelia and Robinow syndrome, noncoding variants in *WNT3*, *WNT3A*, *WNT5A*, *WNT9B* and *WNT11* have been associated with NSCLP in European, European American, Latin American, Hispanic and Chinese populations [31, 61-64]. All components of the pathway, including 9 ligand genes, 4 receptor and co-receptor genes, 3 β -catenin partners and *LEF1* have been implicated, through various studies of orofacial clefts, in the last 20 years [31].

A GWAS study identified a variant in *FZD6* that segregated through all 11 individuals with NSCLP in a large African American family [65]. This variant, rs138557689, is located in intron 1, approximately 700 bp upstream of the start site in exon 2 [65]. Experiments to understand the functional consequences of the C allele found that it created an additional protein binding site that led to ~80% reduction in promoter activity [65]. *Fzd6* is expressed in the mandible and maxilla during murine development [66-68]. It negatively regulates canonical WNT signaling and down-regulates TCF/LEF binding and subsequent transcription of WNT target genes [69]. Both knockdown and overexpression of *fzd6* in zebrafish cause craniofacial anomalies such as a reduced ethmoid plate and abnormal mandibular cartilages [65]. Taken

together these findings suggest that noncoding variants can modulate *FZD6* expression and dysregulate WNT signaling during development to contribute to nonsyndromic cleft formation. Frizzled receptors require LRP5/6 as co-receptors, with LRP6 being a key co-receptor for the β -catenin pathway [51, 70]. Mutations in *LRP5* are associated with craniosynostosis, torus palatinus and a thick mandibular ramus in humans while frameshift and missense mutations in *LRP6* are associated with orofacial clefts and tooth agenesis [71-74]. Zebrafish knockdown and mutant models of *lrp5* exhibit abnormal craniofacial cartilages while *lrp6* null mice have fully penetrant bilateral clefts and mandible defects [73, 75]. *Dkk1* is the major inhibitor of canonical Wnt signaling [76]. In *Xenopus*, it induces head formation, while *Dkk1* null mice display severe craniofacial abnormalities and completely lack facial structures [76, 77]. Overexpression of *Dkk1* in Wnt reporter mice showed an altered Wnt activation pattern in the developing craniofacies and changed the morphology of the facial prominences [52]. In humans, missense mutations in *DKK1* are found in patients with holoprosencephaly, a developmental disorder that affects the brain and face where a small percentage (~8%) of patients present with a median cleft [78, 79]. Taken together, this information nominates these 4 genes at the crux of Wnt signaling, which interact together at the receptor level, as strong NSLP candidate genes.

1.11 Significance

Although many susceptibility loci, genes and variants have been identified in NSLCP, our complete understanding of the genetic contributors is still lacking [40, 80]. As research efforts continue, gene pathway analysis and noncoding variants with regulatory effects on gene expression are becoming the focus of many research studies. Noncoding variants typically have effects in specific tissues at specific developmental timepoints, a concept of particular interest to understanding how nonsyndromic clefts might occur. Both the contribution of

multiple genes and the resulting alterations from noncoding variation fit the multifactorial model proposed more than five decades ago, where multiple factors with small effects push the phenotype to the threshold past which the disorder occurs. Precise control of gene expression is crucial, especially during development, when any perturbation in might lead to abnormalities.

The goal of this dissertation was to investigate gene pathways with supporting roles in craniofacial development, characterize such genes for their contributions to facial development, and to examine noncoding variation in a pathway of genes that work together at the receptor level of Wnt signaling, an important modulator of orofacial morphogenesis. The results are presented in the following chapters. Chapter 3 describes the confirmation of a *PBX*-driven pathway identified in mice for contributions to human NSCLP. Chapter 4 describes the characterization of a *CRISPLD2*-network gene, *FOS*, in vertebrate craniofacial development and morphogenesis. Chapter 5 combines approaches in Chapters 3 and 4 to examine functional noncoding variants for allele-specific expression in early craniofacial development and tests these variants for association in NSCLP families. Altogether, these studies demonstrate the usefulness of examining gene pathways and noncoding variants to understand the genetic etiology of complex disorders such as NSCLP and further the field in beginning to close the knowledge gap on NSCLPs heritability.

CHAPTER 2: MATERIALS AND METHODS

2.1 Prioritization of noncoding variants

DbSNP database was used to retrieve all variants upstream of the coding region of each gene [81]. Linkage disequilibrium for the upstream region of each gene was plotted using HapMap data in Haploview [82]. Global minor allele frequency was used to exclude rare variants so that the prioritized list would be informative for genotyping studies.

Genomic Evolutionary Rate Profiling (GERP) score was to estimate the evolutionary constraint rates for individual nucleotide positions [83, 84]. The base-wise genomic evolutionary rate profiling (GERP) was obtained from UCSC genome browser for each variant. GERP scores, which range from -12 to +6, indicate evolutionary constraint when positive; variants with positive scores were prioritized for use in this study [83, 84].

Ensembl Variant Effect Predictor (VEP) was used to identify the effect of each variant on the gene transcript. Genome Wide Annotation of Variants (GWAVA) was used to annotate variants in noncoding regions for potential functionality; this tool calculates a score for each SNV, with scores higher than 0.5 indicating functionality [85]. HaploReg V4.1, which employs Roadmap Epigenomics and ENCODE data, sequence conservation across mammals (SiPhy), and eQTL data, was used to further assess functionality annotations [86, 87]. HaploReg also annotates promoter histone marks, enhancer histone marks, DNase hypersensitivity, proteins bound by CHIP-seq experiments, binding motifs, and expression quantitative trait loci (eQTLs) on various cell lines and tissues [86, 87]. The Genotype-Tissue Expression (GTEx) portal was utilized to predict the effect of SNVs in different human tissues [88, 89].

Lastly *in silico* analysis of transcription factor binding sites was performed using Alibaba, Patch and Promo [90, 91]. Variants that were common, were evolutionarily conserved, designated

functional by predictor tools, and altered transcription factor binding sites in at least 2 in silico analyses were prioritized.

2.2 Electrophoretic mobility shift assay (EMSA)

Oligonucleotides were synthesized end-labeled with an infrared dye by Integrated DNA Technologies (Coralville, IA). They were annealed using standard protocols. Human embryonic kidney (HEK293) cell nuclear extracts were purchased from ActiveMotif (Carlsbad, CA). Electrophoretic mobility shift assays (EMSAs) were performed by incubating 2.5 μ g nuclear extract, labeled probe and 1 μ L of dG/dC in a 20 μ L mixture containing 20 mmol/L Tris pH 7.5, 50 mmol/L KCl, 10% glycerol, 0.5 mmol/L EDTA (ethylenediaminetetraacetic acid), 0.5 mmol/L DTT (dithiothreitol), 0.05% NP-40 (nonyl phenoxypolyethoxylethanol) and 1 mmol/L PMSF (phenylmethanesulfonylfluoride) for 1 h at 4°C. 10X Orange loading dye was added to monitor electrophoresis (Li-Cor, Lincoln, NE). Competition assays included 5-, 10-, and 50-fold excess of cold probe. Negative controls were prepared using the labeled probes and binding buffer without the nuclear extract. All samples were loaded on a prerun 5% polyacrylamide gel in 1X TBE. After electrophoresis for 3 h at 150 V, the gel was imaged using the Odyssey infrared scanner (Li-Cor, Lincoln, NE).

2.3 Luciferase assays

Luciferase reporter constructs were obtained from Switchgear Genomics (Carlsbad, CA) and 20-basepair sequences containing each variant was cloned upstream of its respective gene promoter by InFusion cloning (Takara Bio USA, Mountain View, CA). The alternate allele construct was created using the Quick Change II site-directed mutagenesis kit (Agilent, Santa Clara, CA). 293T, HeLa and MCF7 cells (ATCC, Manassas, VA) were seeded at 100,000 cells per well in a 96-well plate, and allowed to grow for 24 hours in complete media before being transfected with control and experimental constructs. Additionally, an internal control to

ensure the efficiency of transfection, was used by co-transfecting *Cypridina* TK. Each condition was transfected triplicate and each experiment was performed at least three times. The LightSwitch Luciferase Assay Kit (Switchgear Genomics, Carlsbad, CA) was used following the manufacturers protocol to measure both *Renilla* luciferase and *Cypridina* TK luciferase in the Tecan plate reader (Männedorf, Switzerland). For analysis, each well was normalized to the internal control and $p < 0.05$ was considered significant).

2.4 Zebrafish care and husbandry

Zebrafish (*D. rerio*) were housed and maintained at 28°C as previously described (Westerfield, 2000). All work involving the use of animals was performed with approval of the UTHealth Animal Welfare Committee (AWC-20-0052). Wild type controls were from the AB mapping reference strain. Tg(-4.9sox10:GFP) were obtained from ZIRC and Tg(7xTCF-Xla.Siam:GFP) transgenic lines were obtained from Moro et al [92].

2.5 Morpholino and CRISPR/Cas9 injections

Zebrafish antisense morpholinos (*fzd6* MO: TTAACCGCAAACCTCCTCCTCTTCC *Irp5* MO: CGGGCTTTAATTCCATAATCCCAGC, *Irp6* MO: AGAGAGTCTGAAGCACGGCACCCAT, and *dkk1* MO: AATTGTAGGATGTATTCCCTGGGTG) targeting the ATG start sites and mismatched control morpholinos were designed by GeneTools. Morpholinos were suspended in MilliQ water to a stock concentration of 16.67mg/mL or 2mM. Injections of morpholinos were diluted to 0.5 ng/uL to 3ng/nL in Danieau buffer.

mRNA was generated using the mMessage mMachine Sp6 kit (Ambion). mRNA was resuspended in nuclease-free water to a stock concentration of 2ng/nL and diluted to 0.5ng/nL in 0.1M KCl for injections.

Fzd6 F0 mutants were created using IDT Alt-R™ CRISPR-Cas9 System (Coralville, IA). Three CRISPR RNAs (crRNAs) specific to *fzd6* gene, one pair targeting exon 2 and the other exon 4 (A: GCTGTAGACGTGACCACGGC, B: CACGGGCCTGTACGACCTGA and C: CATGCTGGAGCACTACGACC) were hybridized separately with trans activating crRNA (tracrRNA) to form a functional gRNA complex. 60uM of each gRNA was incubated with 5ug/ul of Cas9 protein (Alt-R® S.p. Cas9 Nuclease, IDT) for 10 minutes at 37°C to generate the ribonucleoprotein (RNP) complex. Equimolar amounts of the two RNPs were mixed and injected into the zebrafish embryos. Mutagenesis was detected by PCR using primers TCTACACACATTAAACACACAGCA and CAGAGCGGCTCCTTCCT. Sanger sequencing was used to specify the mutations created and the Synthego ICE tool was used to estimate editing efficiency for each guide (Synthego, Redwood City, CA). For all zebrafish injections, one-cell embryos were injected with 1nL of MO, MM or RNPs.

2.6 Zebrafish Facial Analytics based on Coordinate Extrapolate system (zFACE)

Zebrafish embryos were fixed in 4% paraformaldehyde (PFA) (Millipore Sigma, Burlington, MA) in 1X phosphate buffered saline with Triton X-100 (PBST) at room temperature for 4 hours and stained with 0.2mg/L DAPI (Thermo Fisher, Waltham, MA) for 30 minutes at room temperature. Embryos were mounted rostrally in 1% low-melt agarose (Research Products International, Mount Prospect, IL) and imaged with Zeiss LSM800 Confocal Microscope (Dublin, CA). Twenty-six anatomic landmarks including eyes, olfactory pits, neuromasts and mouth were identified from the confocal images and measurements between these landmarks were calculated to extract phenotypic features and understand which anatomical structures were altered as a result of *fos* knockdown. ANOVA and Tukey test for multiple comparisons were applied on each measurement and Bonferroni correction for 39 measurements was

applied to determine statistical significance. GraphPad Prism 9.0.0 was used to plot and visualize the data.

After this feature-focused analysis, dimensionality reduction was performed using Principal Component Analysis (PCA) in StataC 14 (StataCorp. 2015). Components with an eigenvalue of greater than or equal to 1 (following the Kaiser-Guttman method) were retained for analysis. Promax rotation, which accounts for correlations between the different factors (zFace measurements) was used because a high correlation was observed/ expected between features calculated using shared landmarks. Principal component (PC) scores were predicted and logistic regression models were utilized to regress morphant/mutant status by PC scores.

Additionally, to focus on facial shape and remove variation due to size, position, or rotation, the 2D landmark data points from the 26 zFACE coordinates were uploaded into MorphoJ version 1.07A and principal axes Procrustes superimposition was performed [93]. After Procrustes transformation, PCA was used to examine general shape variation in the combined groups while discriminant function analysis (DFA) with 10,000 permutations for the mean Procrustes distance was used to assess significant differences between the groups.

2.7 Skeletal staining

Alcian blue (Anatech LTD) and alizarin red (Sigma-Aldrich) staining was performed to visualize the bone and cartilage structures using standard techniques [94]. Briefly, 5-8 dpf embryos were collected and fixed in 2% PFA/1X PBXT for 1 h at room temperature and stored in methanol over night at -20°C . After removing methanol, embryos were incubated in 0.04% alcian blue solution (100 mmol/L Tris, pH 7.5, 10 mmol/L MgCl_2 , 64% ethanol) overnight at room temperature. They were de-stained in 3% H_2O_2 /0.5% KOH for 10 min at room temperature and then stained in 0.02% alizarin red solution (100 mmol/L Tris, pH 7.5, 25% glycerol) for 30 min at room temperature. Embryos were then de-stained in 50% glycerol/0.1%

KOH for 30 min and stored in 50% glycerol. Imaging was performed using the LAS Montage Module (Leica).

2.8 Generation of transgenic reporter lines

Variant specific sequences containing each variant allele flanked by 25-50 bp and attB4 and attB1r recombination sequences were ordered from IDT Technologies (Coralville, IA). These variant sequences were recombined into pDONRP4-P1R using BP clonase (ThermoFisher, Waltham, MA). QuickChange II kit was used to create the alternate allele for each construct (Agilent, Santa Clara, CA). Each of these constructs were then recombined with donor constructs that contained a *gata2* promoter and either a eGFP or mCherry-polyA cassette (Bhatia et al 2014) into either pDestTol2CG2 or pMinTol2R4R2, destination vectors with Tol2 recombination sites. These resulting expression plasmids were then isolated, purified and diluted to 50 ng/uL and mixed with the same concentration of Tol2 transposase before injections. Injections of 1-2 nL were injected into fertilized embryos at the 1 cell stage. Embryos that were screened for reporter activity were raised for 3 months and in-crossed or outcrossed with wild type animals to produce stable germline transgenic reporter fish.

To detect reporter activity, F0 and F1 embryos were fixed, DAPI stained and mounted in 1% low melting agarose and imaged in the ZEISS LSM confocal microscope (Dublin, CA) from 1 to 5 days post fertilization (dpf). Fluorescence was quantified using ImageJ [95] and $p < 0.05$ was the threshold for statistical significance.

2.9 Drug treatments

The WNT activator drug BIO (Sigma, B1686) and WNT inhibitor IWR-1 (Sigma, I0161) were dissolved in DMSO to 1 uM and 10 uM concentrations, respectively, and added to E3 media of dechorinated embryos starting at 24 hours post fertilization for IWR-1 and 48 hours post

fertilization for BIO. Treatment was repeated up to day 5 post fertilization by changing the E3 media and drugs once a day until collection. Untreated and DMSO treated dishes were also used as controls to eliminate any toxicity due to the DMSO solvent. All dishes were incubated in the dark. Embryos were fixed in 4% PFA with PBST for 4 hours at 4°C and DAPI stained before being imaged in 1% agarose in the ZEISS LSM800 confocal microscope (Dublin, CA).

2.10 Family dataset

This study was approved by the University of Texas Health Science Center Committee for Protection of Human Subjects (HSC-MS-03-090). The family-based dataset consisted of 2,233 individuals belonging to 780 NSCLP families, 243 multiplex families (145 nonHispanic White (NHW); 87 Hispanic) and 564 simplex parent-child trios (335 NHW and 213 Hispanic). Each family was ascertained through a NSCLP proband from one of four craniofacial centers: Boston Children's Hospital, Texas Children's Hospital, Shriners Hospital for Children-Houston and the McGovern Medical School UTHealth Craniofacial Center. Probands and relatives were examined to exclude syndromic forms of orofacial clefting. Information about race/ethnicity was obtained by self-report. After informed consent, blood and/or saliva samples were collected and genomic DNA was extracted using established protocols.

2.11 Genotyping

The four single nucleotide variants (SNVs) upstream of *FZD6*, *LRP5*, *LRP6* and *DKK1* genes were genotyped using Taqman genotyping assays and genotypes were detected on a ViiA7 Automatic Sequence Detection System (Life Technologies, Foster City, CA, USA). Control individuals with known genotypes as well as non-template control samples were included on all plates for the genotyping experiments.

2.12 Statistical Analysis for Association Studies

Tests for Hardy Weinberg equilibrium were performed on all unaffected individuals in our family dataset that did not have parent data (unaffected individuals and married-in individuals) using Fisher's exact tests. Family-based single SNV association analyses were performed using the Family-Based Association Test (FBAT) [96]. The "- e" extension was applied to correct for complex pedigree structures [97]. Association in the Presence of Linkage (APL) was used in the individual and pairwise-association analyses [98, 99]. Analyses were stratified by ethnicity and presence/absence of family history of NSCLP [98]. For all analyses, the Bonferroni multiple testing corrected p-value ($0.05/\text{number of SNVs}$) was considered significant.

Transmission of all possible intragenic 2, 3 and 4-SNV haplotypes was examined using the Haplotype Based Association Test (HBAT) function in FBAT [96, 100-102]. The significance threshold was based on the number of possible gene-gene SNV combinations and was set at $p\text{-value} \leq 0.0125$ ($0.05/4$ total SNVs).

CHAPTER 3: PBX-WNT-P63-IRF6 pathway in nonsyndromic cleft lip and palate

Note: The information in this chapter was published as “PBX-WNT-P63-IRF6 pathway in nonsyndromic cleft lip and palate” in *Birth Defects Research* in 2019 for which I was the primary author. Authors of published Wiley articles “have the right to reuse the full text of [their] published article as part of [their] thesis or dissertation” (<https://authorservices.wiley.com/author-resources/Journal-Authors/licensing/licensing-info-faqs.html>)

3.0 Introduction

NSCLP has multifactorial etiology in which numerous genes and environmental factors individually or interactively may contribute to the phenotype [4, 103, 104]. Over the years, numerous studies have successfully identified many genes/loci contributing to NSCLP [4, 32, 105]. Previous linkage, candidate gene and genome-wide association studies using family-based or case-control populations, and studies in animal models have provided evidence for the role of *MSX1*, *IRF6*, *TFAP2A*, *CRISPLD2*, 8q24 locus, *TP63*, and *WNT* genes, among other genes/loci in NSCLP [4, 105-107]. More recently, whole exome sequencing (WES) studies have confirmed the role of variants in known NSCLP genes (*IRF6*, *CDH1*, *CRISPLD2*, *FGFR2* and *PAX7*) and identified novel candidate genes (*CTNND1*, *PLEKHA7*, *PLEKHA5* and *ESRP2*) [25, 108, 109]. Furthermore, there is increasing evidence supporting an additive role for gene-gene interactions in NSCLP, with modifier phenotypic effects [33, 110-114].

In this context, a novel genetic pathway comprised of *Pbx-Wnt-p63-Irf6* genes was shown to control murine facial morphogenesis and was proposed to be an important regulatory pathway for NSCLP [59]. *Pbx* genes (*Pbx1*, -2, -3) and their respective encoded proteins are considered Hox factors, which increase Hox DNA-binding specificity and are important players during skeletal development [115-117]. Compound *Pbx* mutant mice presented with craniofacial abnormalities and fully penetrant bilateral cleft lip and palate, which was attributed to altered Wnt signaling at the midfacial region [59]. Expression of *Wnt9b*, *Wnt3*, and *p63* was not detected in the midface of compound *Pbx* mutant mice in comparison to wild type littermates; meanwhile *Fgf8* and *Irf6* expression was dramatically reduced [59]. This led to the conclusion that loss of *Pbx* genes in the mouse midfacial region disrupts this *Wnt-p63-Irf6* regulatory pathway, which in turn causes facial morphogenesis defects resulting in cleft

lip/palate [59]. Based on these findings, we asked whether variation in genes in the proposed *PBX-WNT-P63-IRF6* pathway and their potential interactions might contribute to NSCLP.

3.1 Materials and methods

The methodology workflow is described in **Figure 4**.

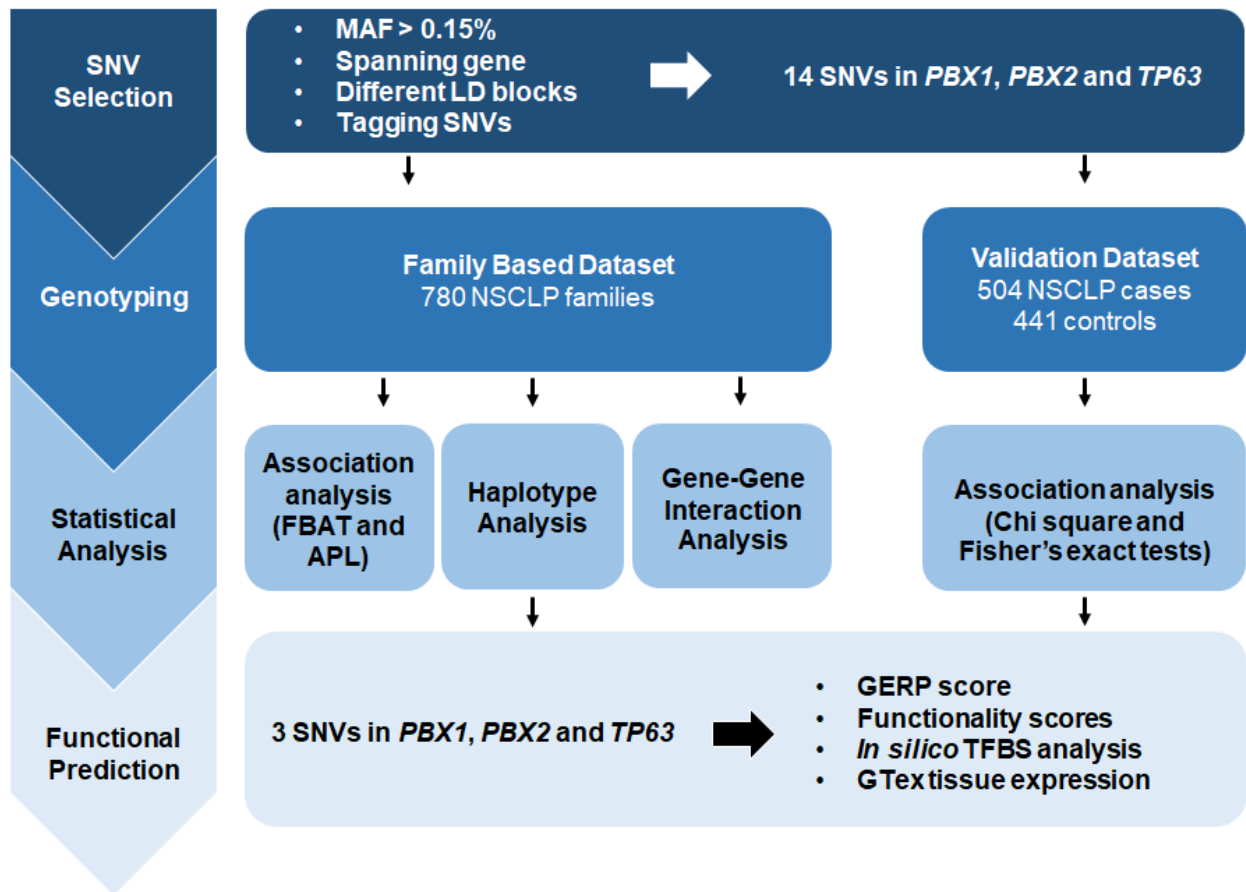


Figure 3: PBX study methodology workflow.

3.1.1 Family discovery and case control validation datasets

The details of the NSCLP family, sample collection, SNV selection criteria, genotyping and statistical analyses are described in Chapter 2. Briefly, for this study, 2,233 individuals belonging to 780 families, 243 multiplex families (145 nonHispanic White (NHW); 87 Hispanic) and 564 simplex parent-child trios (335 NHW and 213 Hispanic) were genotyped (**Table 1**).

A case-control NSCLP group, comprised of 945 unrelated individuals (504 individuals with NSCLP and 441 controls without NSCLP or family history of NSCLP), was used to validate the family-based results. Subjects were recruited under local IRB-approved protocols and written informed consent at the Hospital of Rehabilitation and Craniofacial Anomalies, Bauru Dental School, University of Sao Paulo, and at the Center for Treatment of Craniofacial Anomalies, Rio de Janeiro, Brazil. Only Caucasian individuals (from the Southeastern region of Brazil and of predominantly European ancestry) were included. Ethnicity was self-reported for up to 2 generations.

Table 1. Description of family-based and case-control NSCLP datasets

Ethnicity	NSCLP Datasets								
	Family-Based						Case-Control ²		
	Families			Individuals			Individuals		
	Simplex	Multiplex	Total	Unaffected	Affected	Total	Cases	Controls	Total
NHW¹	335	145	480	934	553	1487	504	441	945
Hispanic	213	87	300	531	315	846	--	--	--
Total	548	232	780	1465	868	2333	504	441	945

¹NHW = nonHispanic white

²Unrelated individuals of European Caucasian ancestry

3.1.2 SNVs genotyped

Fourteen single nucleotide variants (SNVs) in/nearby PBX1, PBX2, and TP63 genes were selected based on heterozygosity (minor allele frequency > 0.15%), location in gene, and linkage disequilibrium blocks surrounding each gene as previously described and elaborated in Chapter 2 [62]. These SNVs are described in **Table 2**.

3.1.3 Single SNV and haplotype association testing

Single SNV association analysis was performed using the Family-Based Association Test (FBAT) with and without the “-e” extension to correct for complex pedigree structures [96]. Transmission of all possible intragenic 2, 3 and 4-SNV haplotypes was examined using the Haplotype Based Association Test (HBAT) function in FBAT [96, 100, 102]. Association in the Presence of Linkage (APL) was used for the individual and pairwise-association analyses and stratified by ethnicity and presence/absence of family history of NSCLP [99]. The Bonferroni method for multiple testing was used and a corrected p-value ≤ 0.0036 ($0.05/14$ SNVs) was considered significant.

Chi square and Fisher’s exact tests, as implemented in PLINK v.1.07 [118] were used to detect differences in genotype and allele frequencies for each SNV between cases and controls, with p-values ≤ 0.05 considered significant.

3.1.4 Gene-gene interaction analysis

APL was used to detect gene-gene interactions between the studied SNVs with 14 variants in additional known NSCLP genes (*WNT3*, *WNT9B* and *IRF6*) for which genotype data was available (**Table 3**) [62, 119]. The significance threshold was based on the number of possible gene-gene SNV combinations and was set at p-value ≤ 0.0019 ($0.05/27$ total SNVs).

Table 2. SNV alleles and frequencies by ethnicity

Gene	Chr	Base position ^a	dbSNP ID	Alleles ^b	SNV Location ^c	NHW MAF ^d	Hispanic MAF ^e	Controls MAF
PBX1	1q23	164523953	rs6426870	CT	5' (- 867)	0.27	0.47	0.34
		164607346	rs1618566	AG	Intron 2	0.38	0.26	0.34
		164658057	rs10800043	CT	Intron 2	0.21	0.27	0.25
		164723835	rs7543038	GT	Intron 2	0.39	0.272	0.34
		164782006	rs3767367	AG	Intron 6	0.18	0.14	0.17
PBX2	6p21.3	32158319	rs176095	AG	5' (-340)	0.20	0.15	0.20
		32155581	rs204993	AG	Intron 4	0.26	0.18	0.22
		32151934	rs3131300	AG	3' (+576)	0.17	0.11	0.12
TP63	3q28	189341790	rs9332461	AG	5' (-7388)	0.38	0.26	0.33
		189421319	rs4575879	AG	Intron 1	0.37	0.31	0.37
		189451290	rs4607088	CT	Intron 1	0.39	0.49	0.43
		189497616	rs4686529	AG	Intron 3	0.46	0.38	0.50
		189596855	rs1515490	AG	Intron 10	0.24	0.22	0.24
		189641053	rs11706540	TC	3' (+25988)	0.29	0.22	0.29

Chr= chromosomal location

^a Ensembl GRCh37 reference assembly position

^b Most common allele listed first.

^c Distance from transcription start site in base pairs for upstream and downstream SNVs

^d Minor allele frequency

^e Corresponding frequency in Hispanic of nonHispanic White minor allele

Table 3. *WNT3*, *WNT9B* and *IRF6* SNVs used in gene-gene interaction calculations

Gene	Chr.	Base position ^a	dbSNP ID	Alleles ^b	NHW MAF Frequency ^c	Hispanic Frequency ^d
<i>WNT3</i>	17q21	44795234	rs142167	A/G	0.26	0.52
		44815743	rs7216231	A/G	0.06	0.41
		44847834	rs199525	G/T	0.22	0.16
		44859715	rs70602	C/T	0.22	0.15
		44865603	rs199498	C/T	0.24	0.49
		44871987	rs111769	C/T	0.42	0.26
		44891301	rs3851781	C/T	0.47	0.66
		44901449	rs9890413	A/G	0.36	0.22
<i>WNT9B</i>	17q21	44941366	rs2165846	A/G	0.42	0.72
		44951777	rs1530364	A/G	0.26	0.32
		44990522	rs197915	A/G	0.43	0.43
		44928053 [#]	rs12602434	C/G	0.14	0.34
<i>IRF6</i>	1q32.2	209989270	rs642961	A/G	0.25	0.22
		209964080	rs2235371	C/T	0.07	0.22

*Genotyped in Chiquet et al. 2008 (31) and Blanton et al. 2010 (38)

Genotyped in this study

^a Ensembl GRCh37 reference assembly position

^b Most common allele listed first.

^c Minor allele frequency

^d Corresponding frequency in Hispanics of NHW minor allele

3.2 Results

3.2.1 Single SNV associations

All SNVs were in Hardy-Weinberg equilibrium. In the family-based analysis, SNVs in all three genes interrogated met the nominal association threshold of $p \leq 0.05$ (**Table 4**). After Bonferroni correction, the most significant individual SNV associations were between *PBX2* rs3131300 ($p=0.003$) with NSCLP in Hispanic families (**Table 4**). In the case-control group, significant associations were found for *PBX1* rs6426870 ($p=0.007$) and *TP63* rs9332461 ($p=0.03$); no association was found for *PBX2* (**Table 4**).

3.2.2 Haplotype associations

Analyses of 2-, 3-, and 4-window haplotypes revealed altered transmission of *PBX2* alleles involving rs3131300 in both Hispanic and NHW families. Interestingly, the alternate allele G in rs3131300 was consistently over transmitted together with the ancestral alleles of rs176095 (A) and rs204993 (A) in NHW, whereas in Hispanic families over transmission of both alternate alleles in rs3131300 and rs204993 (G-G) was detected ($p<0.003$; **Table 5**). Additional *TP63* variant haplotypes were also significantly associated with NSCLP in Hispanics; in these families the transmission of the alternate alleles in rs4607088 and rs4686529 (T-G) were detected in combination with the ancestral alleles in rs9332461 (A), rs4575879 (A) and rs1515490 (A) ($p<0.003$; **Table 5**).

Table 4. Association results by ethnicity and pedigree type

Gene	SNV	Population															
		NHW [#]						Hispanic									NHW
		All			Multiplex			All			Multiplex			Simplex			Case - Control
		FBAT	FBAT -e	APL	FBAT	FBAT -e	APL	FBAT	FBAT -e	APL	FBAT	FBAT -e	APL	FBAT	FBAT -e	APL	PLINK
<i>PBX1</i>	rs6426870	--	--	--	--	--	--	--	--	--	--	--	--	--	--	--	0.006
	rs3767367	0.04	0.05	--	--	--	--	--	--	--	--	--	--	--	--	--	--
	rs1618566	--	--	--	--	--	--	<0.05	--	--	--	--	--	--	--	--	--
<i>PBX2</i>	rs204993	--	--	--	--	--	--	<0.05	<0.05	--	--	--	--	0.05	--	0.02	--
	rs176095	--	--	--	--	--	--	--	--	--	--	--	--	--	--	--	--
	rs3131300	--	--	--	0.02	0.02	0.04	0.003	0.003	0.03	--	--	--	0.01	0.014	0.02	--
<i>TP63</i>	rs9332461	--	--	--	--	--	--	--	--	--	0.005	0.01	--	--	--	--	0.03
	rs4686529	--	--	0.02	--	--	--	--	--	--	--	--	--	--	--	--	--

p-values ≤ 0.05 are shown

p-values ≤ 0.0036 are significant after Bonferroni correction (in bold)

FBAT = Family Based Association Test, FBAT -e = option for extended pedigrees

APL = Association in the Presence of Linkage

Results for NHW Simplex families are not shown because they were not significant

Table 5. Haplotype results from NSCLP families

Gene	Population	SNVs	Alleles[◊]	P-value*
<i>PBX2</i>	NHW All	rs3131300 rs204993	G A	0.0002
		rs3131300 rs176095	G A	0.0005
		rs3131300 rs204993 rs176095	G A A	0.0006
	NHW Simplex	rs3131300 rs204993	G A	0.0002
		rs3131300 rs176095	G A	0.002
		rs3131300 rs204993 rs176095	G A A	0.0003
Hispanic All	rs3131300 rs204993	G G	0.003	
<i>TP63</i>	Hispanic	rs9332461 rs4575879	A A	0.003
		rs9332461 rs4607088 rs4686529	A T G	0.003
	Multiplex	rs9332461 rs4607088 rs1515490	A T A	0.003
		rs9332461 rs4607088 rs4686529 rs1515490	A T G A	0.003

◊ Minor alleles shown in bold

* APL test, significant if p-values ≤ 0.0036 (in bold)

3.2.3 Gene-gene interactions

Gene-gene interaction analyses suggested numerous potential biological interactions, with the majority observed in the NHW families. In the NHW families, considering multiplex and all families, interactions were found between *PBX1/PBX2/TP63* with *IRF6*, followed by *PBX1* with *WNT9B* ($p \leq 0.0018$). In Hispanics, evidence of interaction was also found between *PBX1* and *WNT9B* ($p = 0.0007$). No significant interactions were observed between *TP63* and either *PBX* or *WNT* genes (**Table 6**).

Table 6. Summary of gene-gene interaction calculations in NSCLP families

Gene 1	SNV	Gene 2	SNV	NHW			Hispanic		
				All	multiplex	simplex	All	multiplex	simplex
<i>PBX1</i>	rs10800043	<i>WNT3</i>	rs199525				0.0026		
	rs6426870	<i>WNT9B</i>	rs1530364				0.0007		
	rs3767367		rs199498	0.0010					
	rs10800043	<i>IRF6</i>	rs2235371	0.0017		0.0026			
	rs1618566			0.0018		0.0008			
	rs3767367			0.0003					
	rs6426870			0.0004		0.0002			
	rs7543038			0.0013			0.0026		
rs6426870	rs642961							0.0023	
<i>PBX2</i>	rs176095	<i>WNT9B</i>	rs1530364				0.0023		
<i>PBX2</i>	rs176095	<i>IRF6</i>	rs2235371	0.0003		0.0007			
	rs204993			0.0001		0.0001			
	rs3131300			0.0007		0.0022			
<i>TP63</i>	rs1515490	<i>IRF6</i>	rs2235371	0.0009					
	rs4575879			0.0001		0.0001			
	rs4607088			0.0031		0.0011			
	rs4686529			0.0004					

*interactions with p-values ≤ 0.0036 are shown; significant if $p \leq 0.0018$ (in bold)

3.2.4 Predicted functional consequences of associated SNVs

Bioinformatic predictions of the potential functional effects of associated SNVs on gene expression are listed in **Table 7**. The downstream associated *PBX2* variant rs3131300 showed evidence of evolutionary conservation, with a GERP score of 2.9. This variant was classified as functional by GWAVA and as a modifier of the *PBX2* gene transcript by Ensembl VEP. The base pair change at this SNV affected 13 protein binding motifs, including BDP1, KLF4, KLF7, PLAG1 and p300. Enhancer histone marks were present at the SNV location, further implicating functionality. *PBX2* rs3131300 was also a significant expression quantitative trait locus (eQTL) in whole blood samples, where individuals with an A allele show higher *PBX2* expression (**Figure 5**) [88].

The 5' *PBX1* rs6426870 variant had a neutral GERP score but was classified as functional by GWAVA and harbored 6 altered binding motifs, including ones for FOXD1, FOXK1, FOXL1 and YY1. Additionally, this variant is also a significant eQTL in whole blood, and individuals with a C allele show higher *PBX1* expression (**Figure 5**).

The upstream *TP63* variant rs9332461 was predicted to affect the protein-binding motif for NKX2-1 and presented enhancer histone marks in blood and muscle tissues. This variant was also a significant eQTL in lung tissue, with the A allele leading to higher *TP63* expression (**Figure 5**).

Table 7. Bioinformatic analysis results

SNV	GERP ^a	Ensembl VEP ^b	GWAVA score ^c	Enhancer Histone Marks	Proteins bound	Motifs Changed	eQTL
<i>PBX2</i> rs3131300	2.9	Modifier, downstream gene variant	0.87	fetal brain, muscle	POL2 POL24H8	BDP1, CCNT2, Klf4, Klf7, LXR, PLAG1, PPAR, RREB- 1,UF1H3BETA, ZNF219, Zfp281, Zfp740, p300	brain, muscle, whole blood
<i>PBX1</i> rs6426870	-0.81	Modifier	0.69	-	-	Esr2, Foxd1, Foxf2, Foxk1, Foxl1, YY1	-
<i>TP63</i> rs9332461	-6.81	Modifier	0.12	blood, muscle	-	Nkx2.1	-

^a GERP scores suggesting high conservation are bolded

^b ENSEMBLE VEP designation is noted for effect on the gene of interest transcript

^c GWAVA scores suggestive of functionality are bolded

^d HaploReg functionality annotations

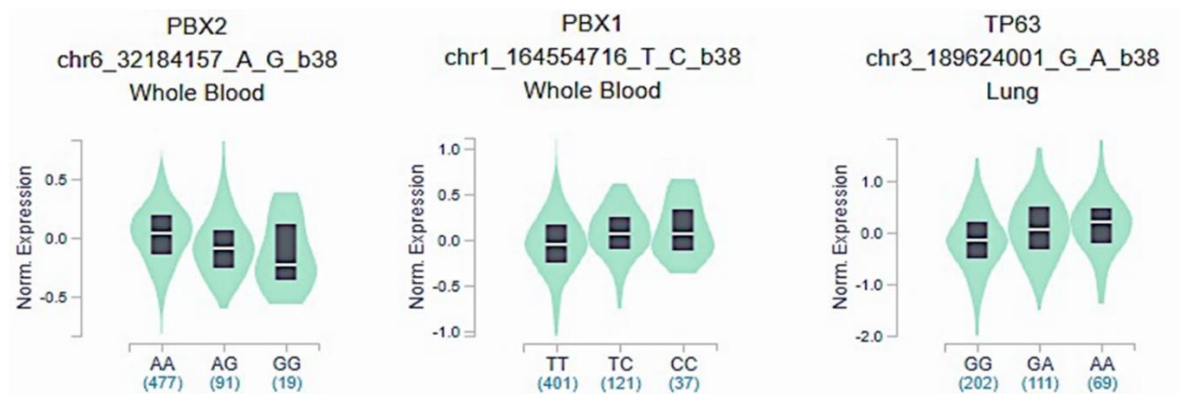


Figure 5. Violin plots from GTEx for the significant SNVs in this study.

3.3 Discussion

In this study, we investigated the role of the *PBX-WNT-TP63-IRF6* pathway in NSCLP because this gene module resulted in clefting in *Pbx*-deficient mice [59]. The contribution of *IRF6*, *TP63* and individual WNT genes has been extensively studied in NSCLP and data strongly supports them as cleft susceptibility genes in humans [4]. However, evidence regarding the role of *PBX* genes in NSCLP, individually and/or interactively with additional genes is still lacking. We tested whether variants in *PBX* and *TP63* were associated with NSCLP phenotypes in a large family-based group and in an independent case-control validation group. We also performed gene-gene interaction calculations considering the studied genes and additional known cleft genes. Overall, our results with two independent datasets provide additional support for the contribution of the proposed *PBX-WNT-TP63-IRF6* regulatory pathway to NSCLP risk. A significant association with *PBX2* was found in our NSCLP families and additional significant associations were found for *PBX1* and *TP63* in the case-control group. Additionally, we observed evidence of altered allele transmission and significant gene-gene interactions between *PBX2-IRF6*, *PBX1-WNT9B-IRF6*, and *TP63-IRF6*, that further support the biological mechanisms previously proposed [59].

In the family-based analysis, *PBX2* rs3131300 was significantly associated with NSCLP in Hispanics and nominally associated in NHW families. Interestingly, *PBX2* haplotypes including this variant were significantly associated in both ethnic groups. In multiplex Hispanic families, a marginal association was observed for *TP63* rs9332461, and four haplotypes containing this variant were significantly associated. Haplotype-based associations are thought to be powerful approaches in addition to single variant analysis for complex diseases because the inclusion of flanking variants has the potential to capture cis-interactions [120]. In the case-control analysis, the most significant associations were seen with *PBX1* rs6426870 and *TP63* rs9332461, whereas no association was found for *PBX2*.

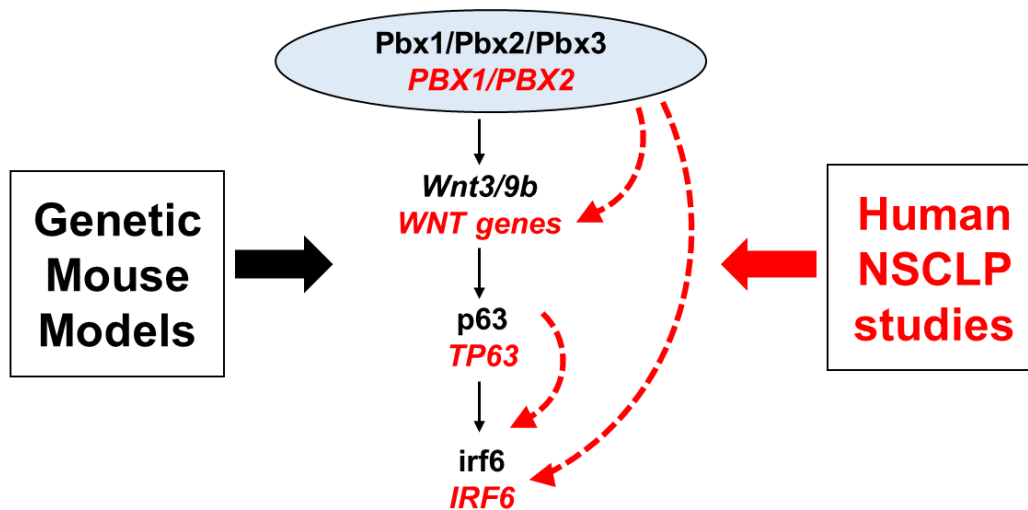


Figure 6. Gene pathway model linking human and mouse findings.

Family-based and case-control studies have different strengths in the types of associations detected. Family studies have the advantage that family members share a common genetic background and are also more likely to share environmental factors; whereas, case-control studies can be well-powered when of adequate sample size and controlled for population admixture effects [96, 121]. In this context, it is not unexpected to find that different variant associations from the family-based and case-control groups. The aim of validation studies is to obtain similar findings under modified influencing factors such as ethnic background, phenotype, or sampling scheme. As a consequence, results from validation studies can be different from those obtained with the discovery analysis because of both random and systematic variation [122].

The associated variants in this study are all located in noncoding regions, downstream (rs3131300) and upstream (rs6426870 and rs9332461) of their respective genes, and therefore of potential functional significance. Although determining the biological effects of these variants will require functional studies, their location and predicted functions suggest biological relevance to craniofacial development and/or NSCLP. *PBX2* rs3131300 is located

in a conserved region associated with enhancer histone marks in skin, muscle and nerve tissues, and predicted to alter 13 transcription factor binding motifs, including Klf4 and p300. Interestingly, missense variants in Klf4, an important regulator of periderm differentiation, have also been identified in NSCLP cases [123]. P300 is a multifunctional coactivator protein that exhibits protein/histone acetyltransferase activity and is essential for normal embryonic development and adult tissue homeostasis [124, 125]. Loss of p300 function in humans and in mice leads to craniofacial defects, possibly due to altered WNT and TGF- β signaling [124]. Craniofacial enhancer activity has recently been implicated in controlling facial morphogenesis during development and influencing the incidence of cleft phenotypes in mice [38, 126]. *PBX2* rs3131300 is noted as a significant eQTL in the GTEx database with allele-specific differences in gene expression, the A allele being associated with higher expression of *PBX2* in whole blood. In turn, the alternate allele G, associated with NSCLP in our family-based analysis, may be predicted to decrease *PBX2* expression. Although speculative, the association of this decreased function variant in humans would be in agreement with the observed effects of the reported murine Pbx regulatory module [59]. Bioinformatic analysis of *PBX1* rs6426870 also suggests potential functional effects with predicted alterations in 6 binding motifs, among them FOXD1, FOXF2, FOXX1, and FOXL1. Fox proteins have been shown to regulate palate, facial cartilage and tooth development [80, 127-129]. Among these, ample evidence exists suggesting that *FOXE1* is associated with NSCLP risk, therefore additional studies addressing the potential relationship between *PBX1* and *FOX* genes are warranted [114]. Additionally, in this study, NSCLP individuals had a higher frequency of the *PBX1* rs6426870 T allele, which was shown to be an eQTL associated with lower *PBX1* expression in whole blood. This suggests that this variant might contribute to lower *PBX1* expression, corroborating the findings in the mouse model [59]. Lastly, *TP63* rs9332461 alternate allele G was predicted to have preferential binding to NKX2-1, a transcription factor

in brain, lung and thyroid development [130, 131]. It was also located in enhancer mark-rich regions in bone and muscle tissues. Of note, these predictions are only suggestive as they obtained from gene expression data in whole blood, as there is currently a lack of a publicly available embryonic craniofacial cell/tissue database.

Evidence of multiple gene-gene interactions was detected between the studied variants in *PBX1*, *PBX2*, and *TP63* with variants in other known cleft genes for which genotype data was available in our NSCLP families [119, 132]. The majority of the interactions identified in the present study were found in the NHW families, and included multiple markers in *PBX1/PBX2/TP63* with *IRF6* rs2235371. Interactions between *PBX1* and *WNT9B* were also found in both NHW and Hispanic families. The *IRF6* rs2235371 variant results in a valine to isoleucine substitution at position 274 (V274I) of the protein and has been consistently reported in association with NSCLP in many populations [119, 132-137]. Moreover, previous studies have demonstrated the important role of *IRF6*, *TP63* and WNT pathway genes and their interactions in NSCLP and in craniofacial development [31, 43, 52, 75, 113, 129, 138-141]. The results of this study reflect statistical probabilities of gene-gene interactions, and yet revealed population-specific variant combinations in our NHW and Hispanic populations that further highlight the heterogeneous nature of NSCLP with many genes with etiologic and/or modifier roles contributing to the condition [4, 103, 104]. In the study by Ferretti et al., a *Pbx-Wnt-Tp63-Irf6* regulatory module was proposed based on the observations that mice lacking *Pbx* genes in the cephalic ectoderm exhibited fully penetrant cleft lip/palate and disruption of the Wnt-p63-Irf6 regulatory network caused by suppression of midfacial apoptosis [59]. In our study, this regulatory model in humans was mainly reflected on the observed interactions between *PBX1* with *WNT9B* and *IRF6*, and between *PBX2* with *IRF6* (Figure 7). Identification of potential biological interactions with purely statistical methods is easily overinterpreted, and utilizing a family-based approach limits the methods available [96,

142]. The observed statistical gene-gene interactions in the present study do not claim biological interactions; rather, they support the already existing biological evidence for the genes investigated [59]. Additional biological studies addressing the relevance of the interactions identified in this study should further our knowledge of the complex genetic architecture of NSCLP.

The results of this study provide the first evidence for a role of *PBX1/PBX2*, additional evidence for the role of *TP63*, and support for the proposed *PBX-WNT-TP63-IRF6* regulatory pathway in the etiology of human NSCLP. Studies focusing on identifying genes and regulatory networks that when disrupted lead to NSCLP have the potential to advance knowledge of the condition and directives for early diagnosis and prevention.

CHAPTER 4: Fostering the face: the role of *FOS* in craniofacial morphogenesis and nonsyndromic cleft lip and palate

Note: The information presented in this chapter is based on a manuscript prepared for submission, for which I am first author. Additional coauthors include Bhavna Tandon, Qiuping Yuan, Simone Menezes, Christian Urbina, George Eisenhoffer, Ariadne Letra and Jaqueline Hecht.

4.1 Introduction

Nonsyndromic cleft lip and/or palate (NSCLP) is the most common craniofacial birth defect, affecting 1 in 700 live births and more than 135,000 newborns worldwide each year [4, 20]. It results from the incomplete fusion of the facial prominences during development, which leaves a gap in the lip, primary palate and/or the secondary palate [143]. In addition to the cleft, other structural abnormalities including short philtrum, orbicularis oris muscle defects, nose irregularities, disruptions in the alveolar bone and dental anomalies [4, 5, 144]. The complexity of the lip and palatal defects and downstream effects require a multidisciplinary approach that includes not only surgery but also hearing, speech and dental evaluations and interventions [104, 145]. Despite improved intervention outcomes, affected individuals and their families face significant financial and psychosocial burdens [146].

Studies of NSCLP suggest a multifactorial mode of inheritance, involving genetic and environmental factors and their interactions [4]. Evidence for a genetic basis is supported by observations that NSCLP aggregates in families, has a higher concordance rate in monozygotic compared to dizygotic twins and presents an increased relative risk to individuals with an affected first-degree relative [24]. Heritability is estimated to be around 70% although varies by ethnicity [18, 147-149]. Currently, ~ 40 genetic risk loci have been associated with NSCLP, which only explains about 30% of the heritability and, these results are not consistent across populations [104, 150]. Thus, there is a critical need to broaden our understanding of the genetic factors contributing to NSCLP.

In previous studies, we reported that *CRISPLD2* was associated with NSCLP, which was independently replicated in separate populations [151-154]. Knockdown of *crispld2* in zebrafish showed that loss of *crispld2* caused severe craniofacial abnormalities [33, 155, 156], which resulted from altered the migration of neural crest cells, a critical population of

multipotent cells that give rise to the various tissues that make up craniofacial structures [41, 156]. Subsequently, morphant zebrafish were shown to differentially express seven genes that comprised an *in silico* network, with *Fosab*, the zebrafish homolog of human *FOS* identified. [33]. A positive association for *FOS/rs1046117* in NSCLP families nominated *FOS* as a candidate NSCLP gene [33].

FOS is known to play different roles, acting as a proto-oncogene, a transcription factor as part of activating protein-1 (AP-1) and as an activator in the lipid synthesis pathway in the ER [157-159]. In these roles *FOS* is involved in oncogenic processes such as tumor growth and progression but also biological processes like proliferation, differentiation, epithelial-to-mesenchymal transition and apoptosis [157-162]. *Fos* null mice display severe osteopetrosis, impaired gametogenesis, abnormal hematopoiesis and behavioral changes (Agamemnon et al 1994). Interestingly, craniofacial abnormalities such as a domed skull with a shorter snout, absence of tooth eruption and a reduced neocortex are also observed in these studies [158, 160, 163, 164]. Data from a *Fos-LacZ* mouse show expression of *Fos* in orofacial tissues such as the medial edge epithelium (MEE) of the palate, the dental papilla mesenchyme, the periderm, and cells at the midline of the nasal septum [165, 166]. Additionally, *Fos* immunostaining was present at the MEE just before elevation of the palatal shelves, the facial epidermis, Meckel's cartilage and the mesenchymal condensations that precede bone and muscle formation in a rat model [167]. While these studies provide strong evidence that *FOS* plays a role during craniofacial development, its specific contributions to mouth and palate formation are not known. This study investigated the role of *fos* during craniofacial development in zebrafish embryos to determine its potential involvement in craniofacial morphogenesis and NSCLP.

4.1 Materials and methods

Detailed methods of the techniques used in this study can be found in Chapter 2. **Figure 7** provides a brief summary of the experiments.

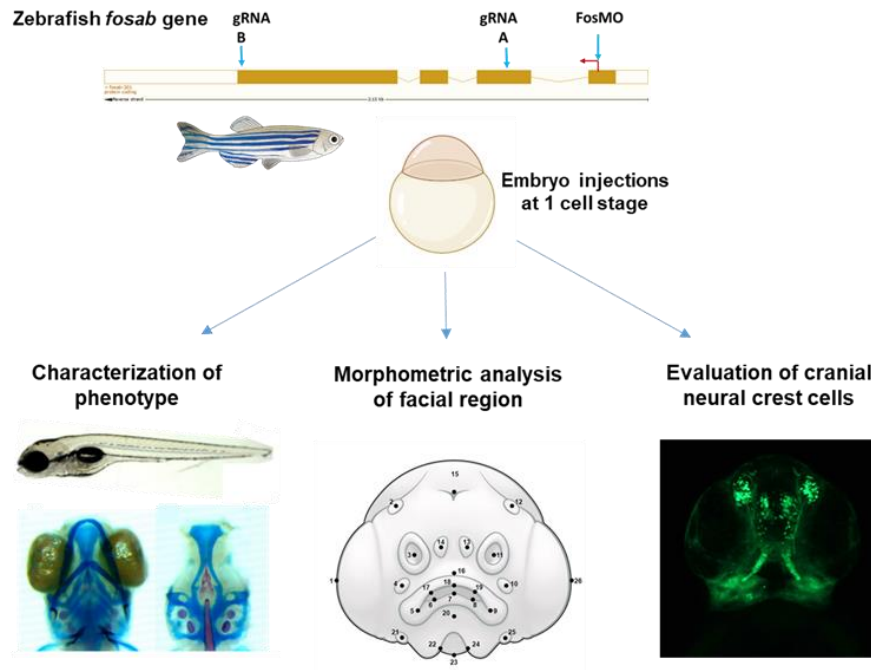


Figure 7. Overview of experimental approach for *fos* study.

4.2 Results

4.2.1 *Fos* knockdown causes craniofacial abnormalities in zebrafish

To define *Fos* in craniofacial development, knockdown was performed using a translation-blocking MO at the one-cell stage. As shown in **Figure 8**, morphant embryos displayed severe abnormalities at 5 days post fertilization (dpf) with smaller head and eyes, cardiac edema, abnormal yolk extension and missing swim bladder (**Figure 8C**) compared to uninjected (UIC) and mismatch morpholino (MM) controls (**Figure 8A and B**). Bone and cartilage staining revealed reduced and abnormally shaped jaw cartilages, including a diminished ethmoid

plate, trabeculae and parachordal cartilages, reduced Meckel's and palatoquadrate cartilages and missing basibranchial cartilages (**Fig. 8F-F' compared to D-D' and E-E'**). Impaired ossification was observed at the parasphenoid bone, branchiostegal rays and at ceratobranchial arch 5, where there were missing or smaller pharyngeal teeth (**Fig. 8F-F' asterisks compared to D-D' and E-E'**). Also observed were fused occipital bones and asymmetric neurocranial structures. These abnormalities were dose-dependent, with mild ones resulting from 0.5ng MO injections and the most severe from 2ngs (**Figure 9**).

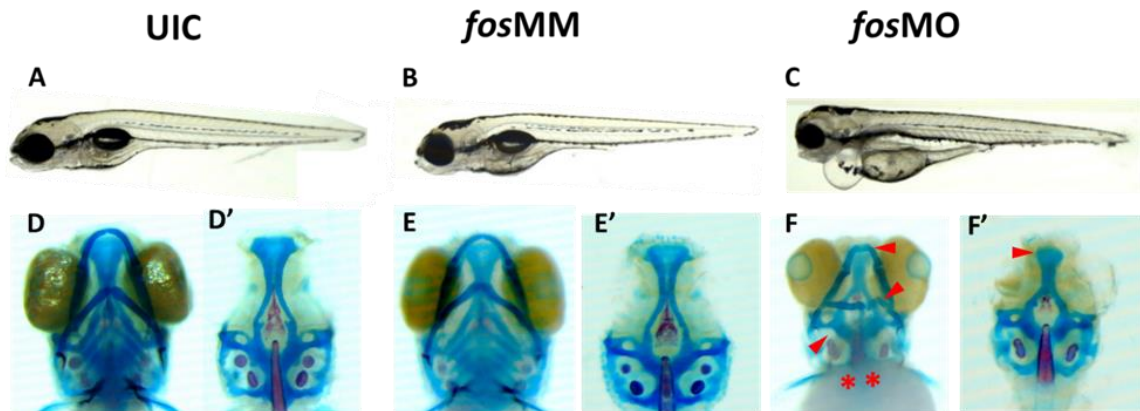


Figure 8. Fos knockdown caused craniofacial and dental abnormalities.

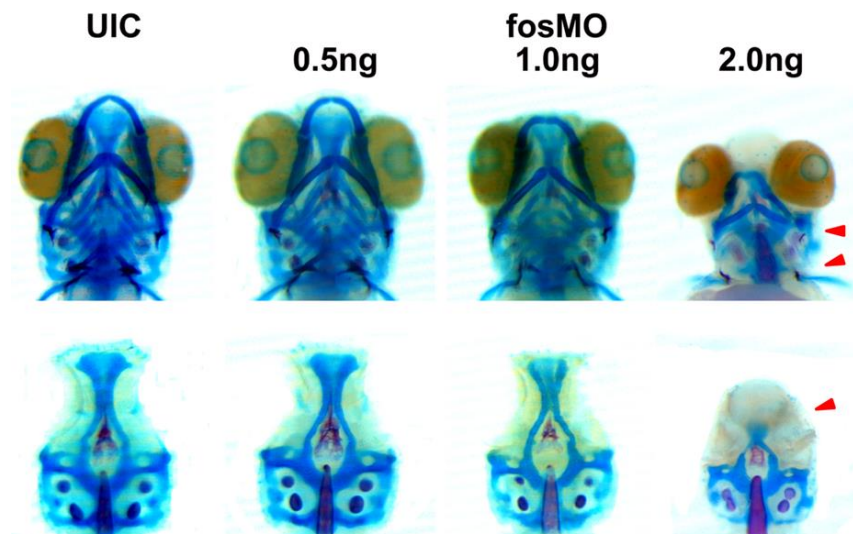


Figure 9. Phenotype severity increased with higher doses of fos morpholino.

To evaluate pharyngeal/ branchial arch formation and visualize tooth development in more detail, *fos* knockdown was performed in Tg(-4.9sox10:GFP), which allows for visualization of the neural crest cells that form the arches. These embryos were stained with alizarin red to examine mineralized tissues. At 5 dpf, pharyngeal arches (PA) 1 and 2 were the most affected in the MO injected embryos, with 37% of embryos showing merged PA1 and PA2 or absence of the structures (**Figure 10C1, C2** compared to **A** and **B**). The arches also showed disorganization, vertical and horizontal constriction and asymmetry. All morphant embryos had intact but similarly abnormal PA 3-7. Additionally, complete mineralization of the fifth ceratobranchial arch (CB5) was observed in 100% of the UIC and MM embryos (**Figure 10F1-F2** compared to **D** and **E, Table 8**), whereas mineralization was found in only 24% of *fos* morphant embryos. Diminished mineralization persisted to 8 dpf, with the MO group still showing only 68% mineralization (**Figure 11**). Smaller cleithrums and opercles (dermal bones) were observed further indicating abnormal ossification.

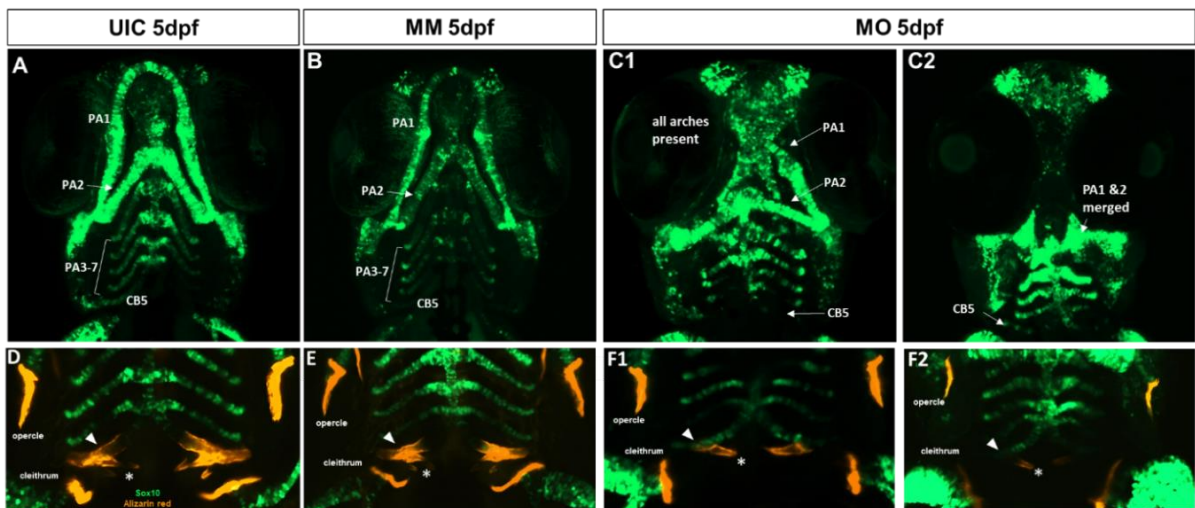


Figure 10. *Fos* morphants showed abnormal arches and reduced mineralization at 5 dpf.

The development of pharyngeal dentition was examined in detail from 5 to 8 dpf. At 5 dpf, 3 rows of pharyngeal teeth (one on each side –left and right pairs), termed 4V¹, 3V¹ and 5V¹, could be visualized in the UIC and MM injected controls, with 4V¹ ankylosed/attached to the perichondral bone of CB5 (**Figure 11**).

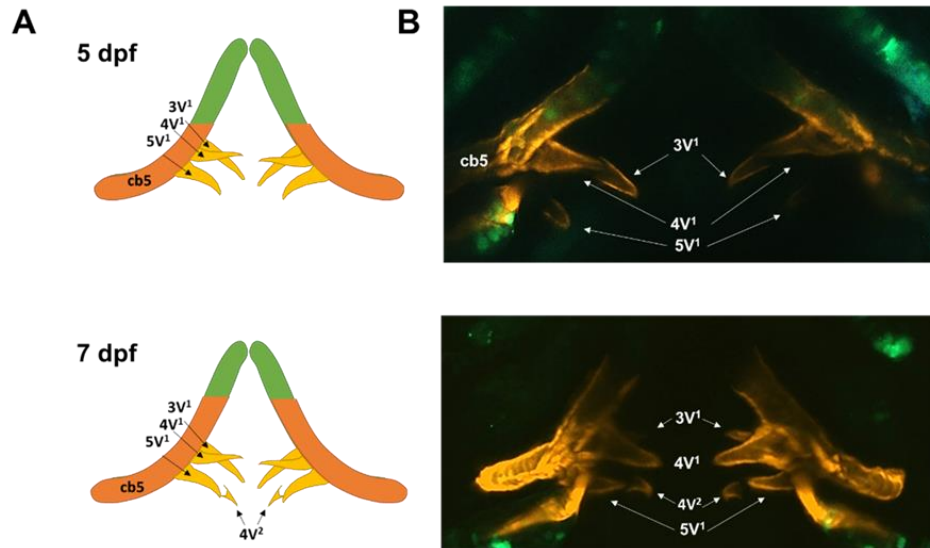


Figure 11. Zebrafish pharyngeal dentition at 5 and 7 dpf.

In comparison, MO embryos presented only 1 tooth on each side (4V¹ only) which was often smaller. In mild phenotypic morphants, 4V¹ had attached/deposited bone around the non-mineralized CB5 cartilage, while severe phenotype morphants only showed 4V¹ tips (**Figure 12**). At 6dpf, UIC and MM controls showed more bone deposition at CB5, with 4V¹ still the only tooth attached and 3V¹ and 5V¹ mineralizing towards CB5, but not yet attached. The mild phenotypic morphants looked similar to those at 5 dpf with the tip of 3V¹ observed, while the severe morphants showed only the tip of 4V¹ (**Figure 12**). By 7 dpf, UIC/MM showed 2 attached and 2 developing teeth, while the mild phenotypic morphants showed more bone deposit around 4V¹ at CB5. The severe morphants had unattached sets of 4V¹ and 3V¹ (**Figure 12**). Finally, at 8 dpf UIC and MM controls showed 3 sets of attached teeth and the

tips of replacement tooth 4V². Mild phenotype morphants resembled 5 dpf UIC/MM embryos but with less mineralization at CB5. The severe morphants showed unmineralized CB5, no attached teeth and the tips of 4V¹, 3V¹ and 5V¹ (**Figure 12**). These findings are presented in **Table 8**. Variability in left right symmetry of the teeth was seen in all groups, however the morphants showed a greater discrepancy between the number of left and right teeth. These observations together demonstrate abnormal tooth morphogenesis up to 8 dpf.

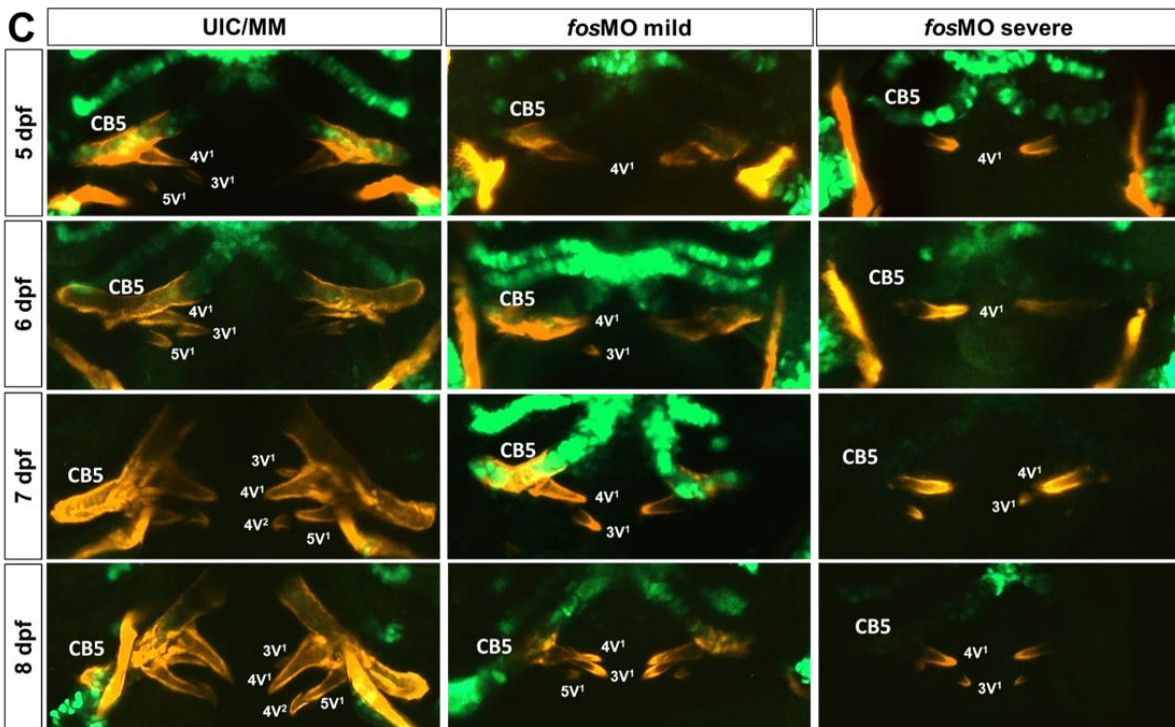


Figure 12. Developmental timeline of *fos* morphant dentition.

Table 8. CB5 mineralization and pharyngeal tooth development is affected in *fos* morphants. Pharyngeal teeth were counted in embryos at 5-8 dpf and tabulated the developmental timeline they appear (4V first and 4V² last). While UIC and MM embryos developed most of the pharyngeal teeth, *fos* morphants either failed to develop certain rows of teeth or showed asymmetry in their formation.

Developmental day	Tooth Id.	UIC		MM		MO	
		Left	Right	Left	Right	Left	Right
5 dpf	CB5	100%		100%		24%	
	4V	100	100	100	100	91	93
	3V	89	78	73	54	10	2
	5V	67	0	60	33	7	0
6 dpf	CB5	100%		100%		47%	
	4V	100	75	100	100	100	100
	3V	100	75	75	75	47	47
	5V	100	75	75	50	27	37
7 dpf	CB5	100%		100%		58%	
	4V	91	91	100	100	100	100
	3V	90	73	100	100	75	50
	5V	73	73	100	100	25	17
	4V2	64	55	88	88	0	0
8 dpf	CB5	100%		100%		69%	
	4V	100	100	100	100	93	100
	3V	100	86	100	100	69	66
	5V	86	86	100	100	41	45
	4V2	71	86	80	100	7	10

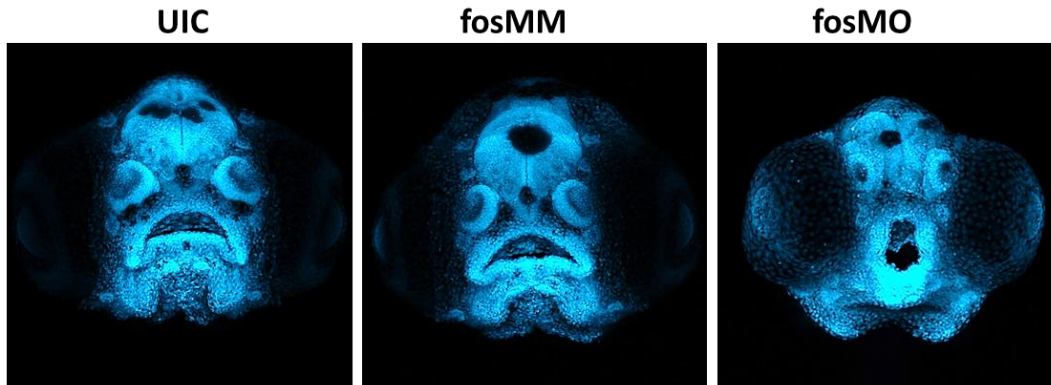


Figure 13. *Fos* morphants had abnormal facial morphology with a keyhole shaped mouth.

4.2.2 *Fos* morphants have abnormally-shaped mouths and craniofacies

The most striking abnormality was a keyhole-shaped mouth observed in the majority of morphant embryos (**Figure 13**) and resembled a previously reported hypoplastic upper lip or a median cleft observed in *Xenopus* embryos [168, 169]. zFACE, a novel tool to evaluate facial shape in zebrafish embryos was used to quantify the changes in facial morphometry in *fos* morphants and analyzed using feature-focused, PCA and shape analyses. Differences in zFACE measurements were first evaluated to determine which facial dimensions were affected as a result of *fos* knockdown. Univariate ANOVA revealed that 27 of the 39 zFACE measurements were significantly different in the morphant embryos compared to both UIC and MM groups ($p < 0.0013$). These included 15 parameters involving the oral cavity, 5 horizontal axis measurements, 5 midface angles, and 2 facial area measurements (**Figure 14, 15**). *Fos* morphants had a decreased mouth width but increased mouth height ($p < 0.0001$ for both) compared to the UIC/MM controls. The keyhole-shaped oral cavity was reflected by the increased chelion, crista philtri and labiale inferius and decreased labiale superius angles ($p < 0.0001$ for all), (**Figure 14**). Facial width, olfactory distance, neuromast width and chin width were also significantly reduced in the morphants reflecting a horizontally narrowed face ($p < 0.0001$).

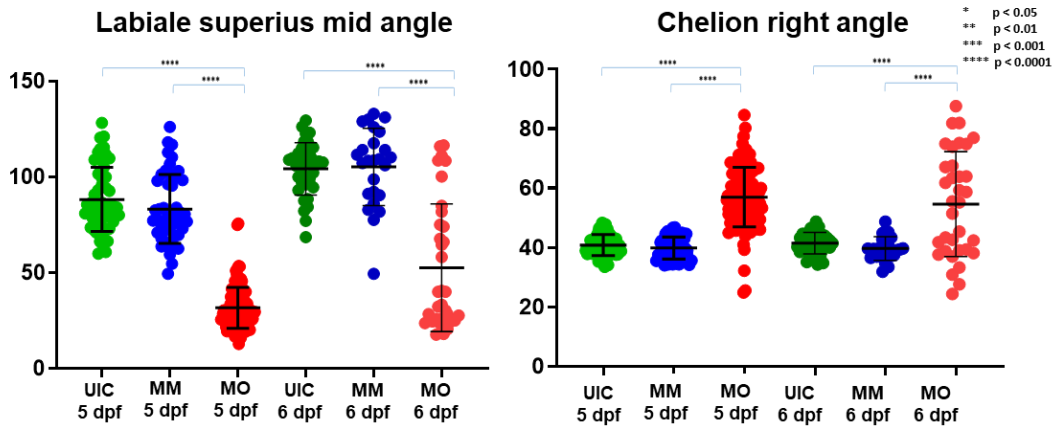


Figure 14. Graph of two mouth angles significantly altered in *fos* morphants at 5 and 6 dpf.

In contrast, measurements that involved the olfactory epithelium and neuromasts in the midface, such as left and right olfactory to mouth and neuromast angles were significantly increased ($p < 0.001$), reflecting abnormal midface dimensions. Interestingly, facial height ($p = 0.98$), mouth to chin distance ($p = 0.60$), neuromast height ($p = 0.97$) and mid olfactory to chin height ($p = 0.23$) were unchanged after *fos* knockdown indicating unaffected vertical axis dimensions. Analysis at 6 dpf showed similar results suggesting that developmental delay due to toxicity does not contribute to these differences in the morphant embryos.

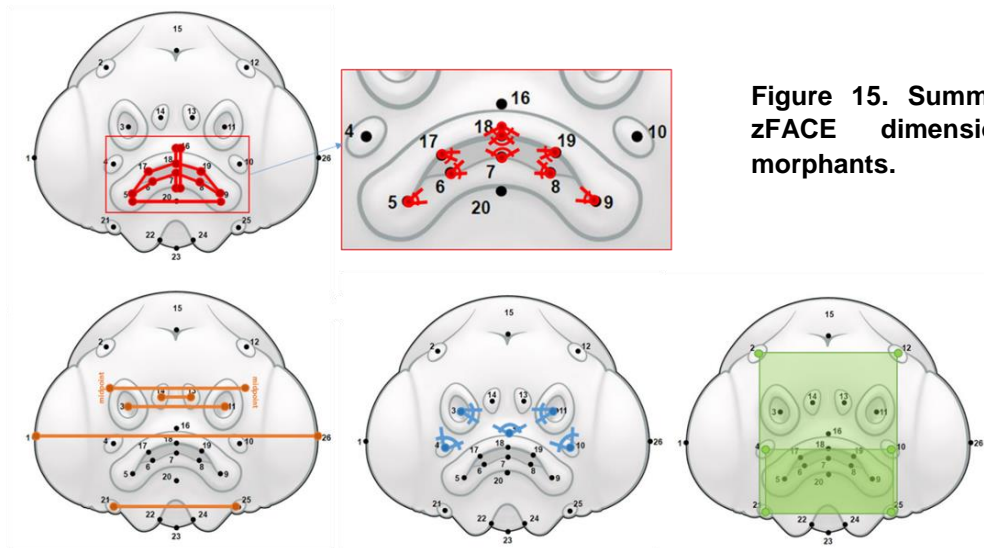


Figure 15. Summary of altered zFACE dimensions in *fos* morphants.

Table 9. zFACE analysis results for all morphometric measurements.

Morphometric feature	ANOVA	Tukey's multiple comparison test			Change in MO
		UIC vs. fosMM	UIC vs. fosMO	fosMM vs. fosMO	
Width		ns	****	****	↓
Height	ns				
Olfactory Distance		ns	****	****	↓
Upper Lip Width		ns	***	****	↑
Lower Lip Width		ns	****	****	↑
Mouth Width		ns	****	****	↓
Olfactory to Mouth		ns	****	***	↑
Olfactory to Mouth 2		ns	****	****	↑
Difference	ns				
Olfactory to Mouth 3		ns	****	****	↓
Chin Width		ns	****	****	↓
Mouth to Chin	ns				
Alternate Height	ns				
Mouth Height		ns	****	****	↑
Neuromast Angle 1		ns	****	****	↑
Neuromast Angle 2		ns	****	****	↑
Difference		ns	***	**	↑
Neuromast Height	ns				
Neuromast Width		ns	****	****	↓
Mid Neuromast Width		ns	****	****	↓
Avg Length Olf. to mouth	ns				
Area Top		ns	***	*	↓
Area Bottom		ns	****	****	↓
Area Combined		ns	****	****	↓
Mid Olfactory to Chin height	ns				
Mouth Area	ns				
Mouth Perimeter		ns	****	****	↓
Libiale Superius Angle		ns	****	****	↓
Chelion Left Angle		ns	****	****	↑
Chelion Right Angle		ns	****	****	↑
Chelion Diff		ns	****	****	↑
Labiale Inferius Angle		ns	****	****	↓
Crista Philtri Left Angle		ns	****	****	↑
Crista Philtri Right Angle		ns	****	****	↑
Crista Philtri Diff		ns	****	**	↑
Labiale Superius Mid Angle		ns	****	****	↓
Labiale Inferius Left Angle		ns	****	****	↑
Labiale Inferius Right Angle		ns	****	****	↑
Labiale Inferius Diff	ns				

**** p < 0.0001, *** p < 0.001, ** p < 0.01, * p < 0.05

Principal component analysis (PCA) of the total embryo group showed that the first principal component (PC1) explained 41% of the variability. The libiale superius angle, chelion right angle and crista philtri left angle measurements significantly loaded (eigenvector ≥ 0.30) into PC1 driving and explaining most of the variation. Logistic regression, with group as the dependent variable, and PC1 score as the independent variable, showed that PC1 score could be used to predict whether an embryo is a control or *fos* morphant, but could not distinguish between the UIC and MM controls (UIC and MO comparison $p = 0.001$; MM and MO comparison $p < 0.0001$; UIC and MM comparison, $p = 0.54$).

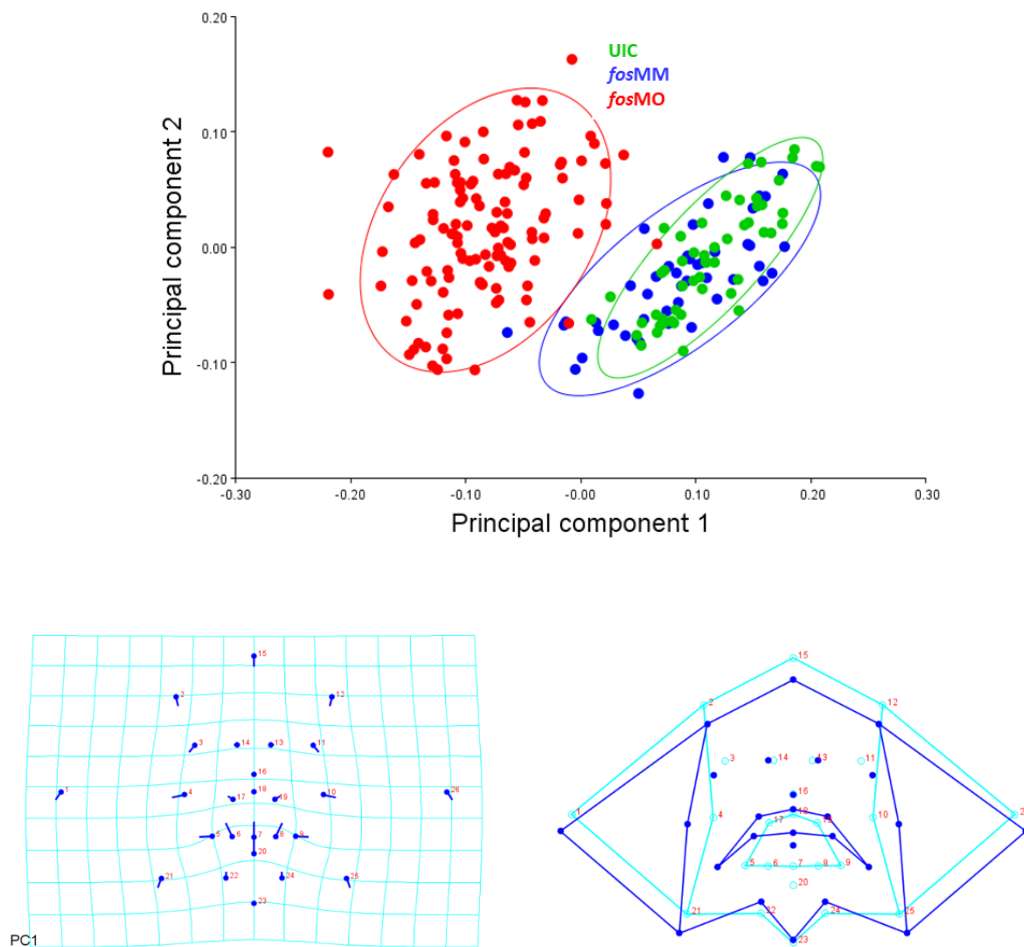


Figure 16. PC plot showed *fos* morphants separating from both controls and shape changes along PC1.

Procrustes transformed landmark analysis was additionally used because it removes variation in size, rotation and scale and aligns landmarks to a principal axis in order to compare only shape. Both PCA and discriminant function analysis (DFA) were performed with these superimposed landmarks (**Figure 16** and **17**). PCA of this scaled data was similar to the untransformed zFACE measurements PCA (**Figure 16**). Shape changes along PC1 were visualized with transformation grids with lollipop graphs (showing vectors of change) and wireframe diagrams and showed changes in landmarks around the mouth and midface, resulting in altered mouth shape and facial width (**Figure 16**). DFA confirmed that *fos* morphants had a significantly different mean face shape compared to both UIC and MM controls (**Figure 17**). Changes in 21 landmarks were observed between MO group with either UIC or MM controls and these changes were reflected in the wireframe diagrams showing a narrower face shape with an O-shaped mouth (**Figure 17**). The changes in Procrustes distance was significant ($p < 0.001$). These results together provide parallel evidence that *fos* knockdown significantly alters orofacial morphology.

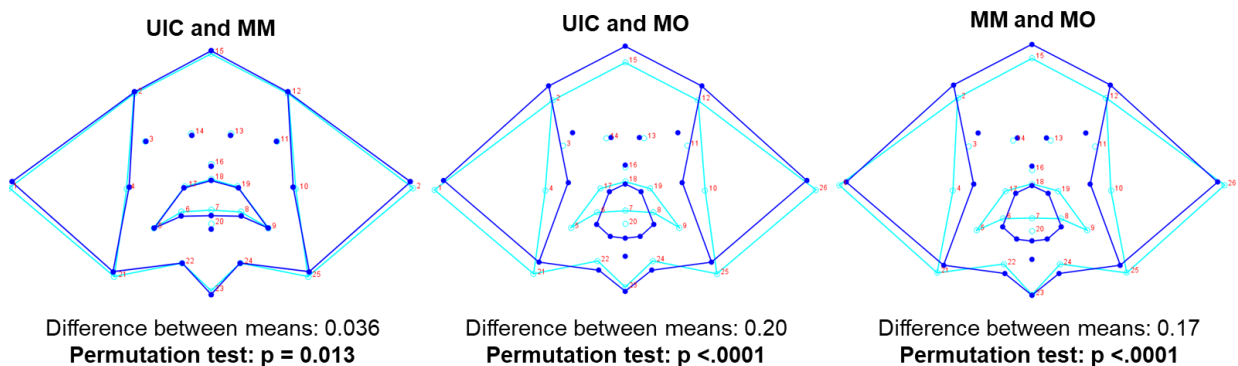


Figure 17. DFA results showed significantly different face shape in *fos* morphants.

4.2.3 Human *fos* mRNA rescues morphant phenotype

To test the specificity of the morphant phenotype to *fos* knockdown, an *in vitro* synthesized human *FOS* (Hu-*FOS*) mRNA was co-injected with the *fos* morpholino to rescue morphant abnormalities. Brightfield and DAPI-stained rostral images showed that Hu-*FOS* RNA significantly rescued the gross abnormal morphology, abnormal facial phenotype, including the size of the head and eyes, as well as finer facial features (**Figure 18**). While 82% of *fos* morphants had an abnormal mouth and face, human *FOS* mRNA co-injection rescue decreased abnormal embryos by 45%. Overexpression of human-*FOS* RNA in zebrafish embryos also caused severe abnormalities, including extended lower jaw and cyclopia. Morphometric analysis was not performed in the overexpression group because the anatomical facial landmarks were not present.

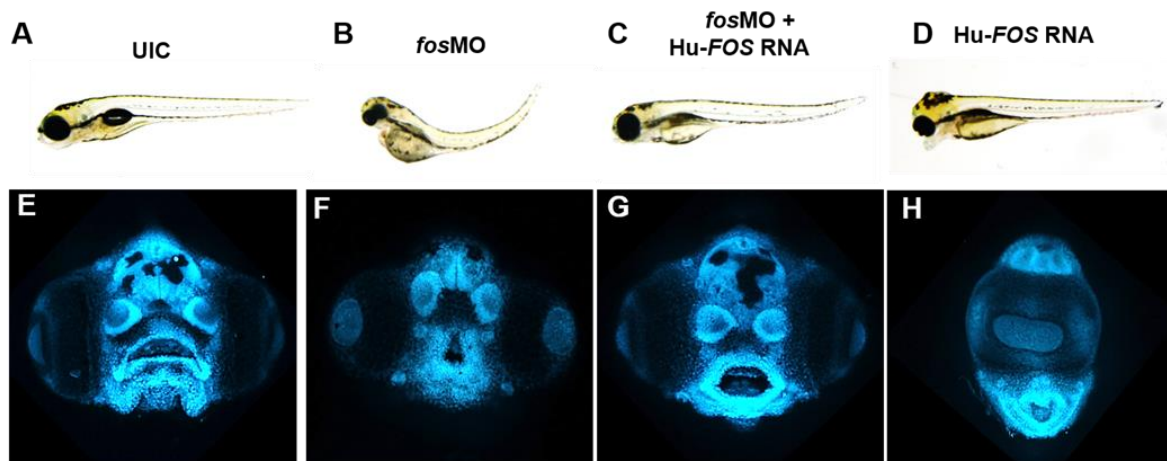


Figure 18. Human *FOS* mRNA rescued facial abnormalities associated with *fos* knockdown.

ZFACE analysis of UIC, MO and rescue groups identified 11 features that were rescued by co-injection of Hu-*FOS* (all 3 olfactory to mouth angles, neuromast angle 1, both chelion angles, labiale superius mid angle and both labiale inferius angles ($p > 0.0013$ comparing UIC and rescue groups). Thirteen additional features displayed a more normal, intermediate phenotype in the rescue group, but did not meet our statistical criteria for rescue ($p < 0.0013$ in UIC vs rescue comparison). The rescue embryos in this category were significantly different compared to UIC but they were also different compared to MO in measurements of facial width, olfactory distance, mouth width, chin width, mouth perimeter and others.

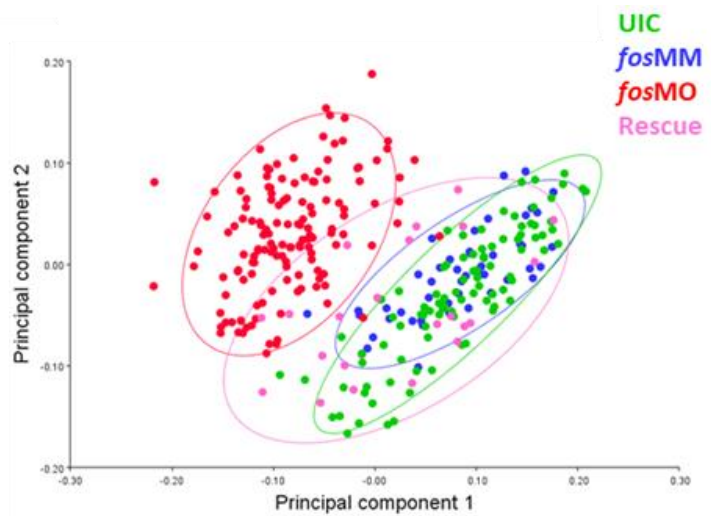


Figure 19. PC plot results confirmed the rescue group was more similar to controls.

Joint PCA of the rescue experiments together with the MO, MM and UIC data obtained for the initial morphometric analysis showed overlap of the rescue group with the UIC and MM groups when confidence ellipses were drawn in the plot (**Figure 19**). To determine face shape changes that were due to *fos* knockdown and concomitantly rescued by *fos* mRNA, DFA was used to compare the morphant and rescue groups as well as the rescue and control groups. When comparing rescue and MO, landmarks on the edges of the mouth as well as the top and middle neuromasts had the largest vectors of change, with the rescue embryos showing more normal mouths and wider midfaces (**Figure 20**). Comparing the rescue with the UIC

showed that rescue embryos had a less crescent shaped (more oval) mouth and narrower chin (**Figure 20**). Overall, these results demonstrate that the *fos* morphant phenotype, especially the abnormal mouth shape, is specific to *fos* knockdown in these embryos, can be rescued by human *FOS* mRNA co-injection, and not caused by any off-target effects of the morpholino or the injection process itself.

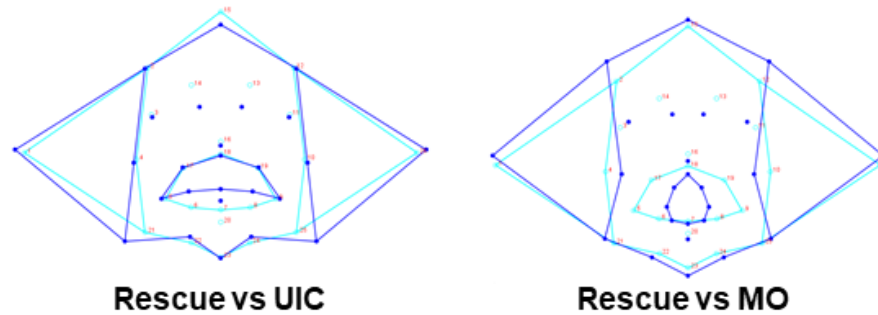


Figure 20. DFA showed the rescue group had a more normal average face shape.

4.2.4 *Fos* CRISPR/Cas9 F0 mutants recapitulate morphant craniofacial phenotype at 5 dpf

To generate a stable loss-of-function model for *fos*, CRISPR F0 mosaic mutants were generated using CRISPR/Cas9. Two single guide RNAs (sgRNAs) in exons 1 and 4 of the *fos* gene were designed to delete the entire *fos* coding region. F0 overall phenotypes ranged from mostly normal embryos to embryos with heart edema, smaller head, and smaller curved body axis, similar to morphant phenotypes. Genotyping revealed efficient mosaic mutagenesis in these F0s with most embryos showing a deletion of approximately 1500bp in the *fos* coding region.

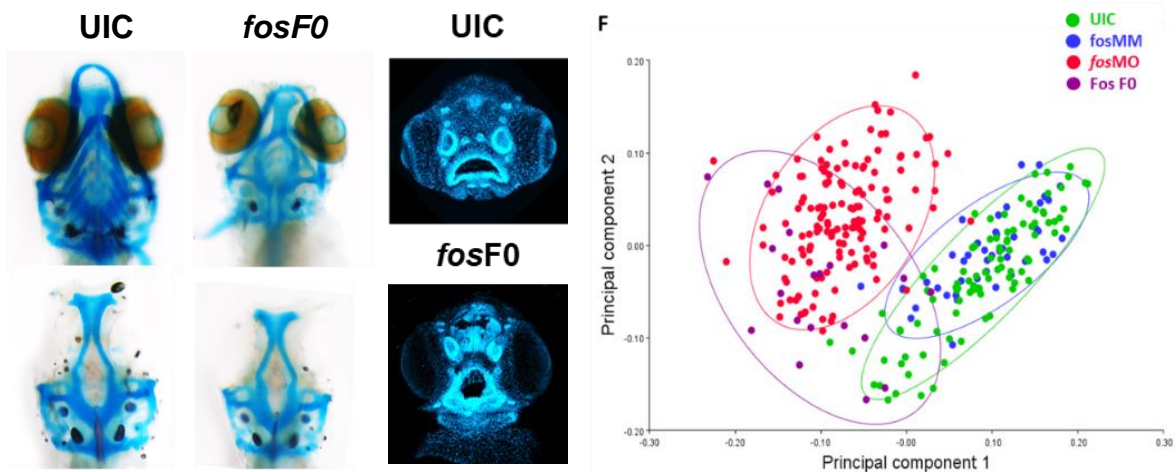


Figure 21. CRISPR/Cas9 mutants recapitulated the morphant phenotype.

The F0s were analyzed using bone and cartilage staining and zFACE morphometrics to determine if the CRISPR-induced genetic lesions recapitulated the morpholino knockdown phenotype. F0s showed reduced and abnormal jaw cartilages (**Figure 21**) as well as a range of dysfunctional facial features similar to the morphants. ZFACE measurement analysis showed 16 out of 39 significant changes after Bonferroni correction (Student's t test, $p < 0.00128$). These included olfactory distance, mouth width, olfactory to mouth angles, neuromast angles, mouth perimeter and labiale inferius and labiale superius mid angles ($p < 0.00128$). Nine additional parameters showed a trend ($p < 0.05$) but did not meet the Bonferroni corrected significance threshold.

A combined PCA plot (**Figure 21**) showed clustering of the F0s in the same area as the morphants, further confirming that the majority of mutants display similarly abnormal faces as the morphants. Only a few F0 embryos mapped to the same region as the controls likely related to mosaicism in the *fos* F0 mutants. Interestingly, DFA comparison of the F0 and morphant embryos showed only a few differences, with the overall mean face shape being very similar.

4.2.5 Cranial neural crest cells are reduced in *fos* morphant and mutant embryos

To further understand the mechanisms by which *fos* regulates craniofacial development, cranial neural crest cell (CNCC) populations were examined because craniofacial development is highly dependent on the correct formation, migration and differentiation of these cells [41]. The transgenic line *Tg(-4.9sox10:EGFP)* that contains GFP downstream of a *sox10* promoter/enhancer element and drives expression of GFP in pre-migratory and migrating NCCs was used in these experiments [170].

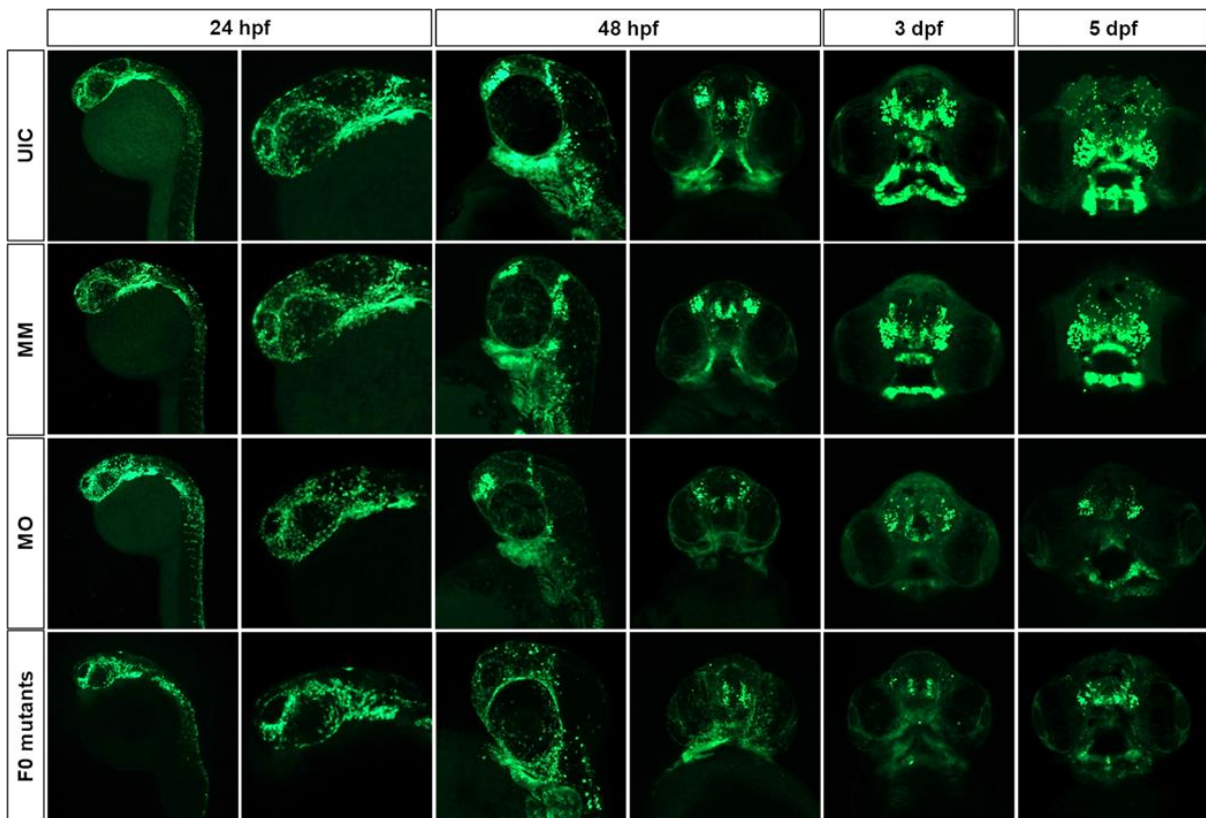


Figure 22. CNCC populations were altered in *fos* morphants and mutants.

As shown in **Figure 22**, NCC development and migration were unaffected in the morphants compared to the controls at 24 hours post fertilization (hpf) ($p = 0.27$). However, at 48 hpf, significant differences were found in both the number and migration pattern of CNCCs in the

morphants compared to UICs (quantified fluorescence, $p < 0.0001$). At 3 dpf the morphants showed reduced CNCCs compared to both the UICs and MMs ($p < 0.0001$ and $p = 0.002$ respectively). These differences became more pronounced at 5 dpf, as evidenced by a significant decrease of *sox10*.GFP fluorescence in morphants compared to controls ($p < 0.0001$) (**Figure 23**). Similar results were observed when CRISPR guides were injected into this transgenic line, with *fos* F0 mutants showing both reduction and abnormal migration of neural crest cells at 48 hpf and 5 dpf (**Figure 23**, bottom panel). These alterations were also confirmed by quantification of average fluorescence ($p < 0.0001$ for both developmental time points). *Fos* morphants and *fos* F0 mutants were not significantly different at any of the time points assessed.

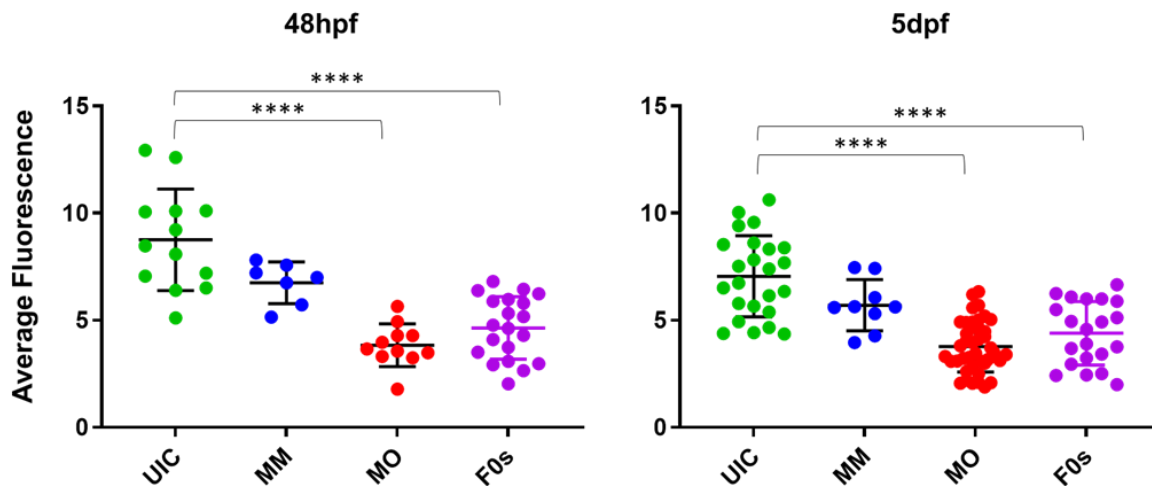


Figure 23. Sox10 expression was significantly reduced in *fos* morphants and mutants.

4.3 Discussion

Fos, a proto-oncogene, has a known but poorly defined role in embryonic development and specifically, craniofacial development [158-160, 163]. In this study, we show that reduction or absence of *fos* in zebrafish embryos resulted in a wide array of craniofacial phenotypic abnormalities, including a keyhole shaped mouth, abnormal face shape and missing or smaller teeth. These gross anomalies resulted from abnormal skeletal and cartilage elements, caused by dysregulation in specific cranial neural crest (CNCC) populations that are necessary for normal facial and oropharynx patterning. This study provides new information about the specific contributions *fos* makes to vertebrate craniofacial development.

Previously, we identified *fos* in a network of differentially expressed genes in a *crispld2* zebrafish model of orofacial clefts, which was confirmed by association with NSCLP in a family-based dataset [33]. Different genetic approaches, employing *fos* morphants and F0 mutants, were used to determine the effects of *fos* perturbation in craniofacial morphogenesis. Starting at 48 hpf, *fos* morphants and mutants had smaller head and eyes, cardiac edema, abnormal yolk extension and missing swim bladder. Close analysis of bone and cartilage showed smaller ethmoid plate, reduced Meckel's and palatoquadrate cartilages and missing basibranchial cartilages. The most dramatic phenotype observed was a keyhole-shaped mouth at 5 and 6 dpf, similar to a hypoplastic lip phenotype observed in a zebrafish model of orofacial clefts [169]. Using zFACE morphometrics, regional facial alterations were identified in the mouth, olfactory pits (nasal cavities) and midface neuromasts among other features, strongly supporting the role of *fos* in the morphogenesis of these structures. Furthermore, additional analyses with zFACE data showed the most robust changes resulting from *fos* disruption were to the oral cavity and midface. Interestingly, changes in the dimensions of the maxillae and nasal pits have been reported to correlate with the development of cleft lip and palate in mice [171-173]. Additionally, human morphometric studies have shown facial

differences in individuals predisposed to orofacial clefts as well as their unaffected relatives, including differences in the upper lip, philtrum and nasolabial angles [12, 174-177]. These morphometric differences observed in mice and humans, which are similar to alterations in facial structures in the current zebrafish model, further support the role of *fos* in the etiology of orofacial clefts. Additionally, because zFACE uses similar anatomical landmarks to those in mouse and human studies, it offers comparability across different species, an important advantage for a better understanding in this area of research.

Rodent models to understand *Fos* function have shown that *Fos* is expressed in some orofacial tissues such as the medial edge epithelium (MEE) of the palate, the dental papilla mesenchyme, the periderm, and cells at the midline of the nasal septum [166, 167]. Given this expression pattern, it is not surprising that *fos* knockout mice develop craniofacial abnormalities such as a domed skull, shorter snout and abnormal maxillas, mandibles and dentition [163, 164]. Data from the zebrafish model in this study recapitulates these craniofacial abnormalities, signifying the conserved nature of *Fos* function across all vertebrates. Even though we observed reduced, and not increased bone like the osteopetrotic *fos* null mice, our results are not necessarily in contradiction because *fos* has also been shown to control endochondral ossification and is highly expressed in osteoblast precursors at critical stages when mineralization takes place [158]. Additionally, an avian embryonic model showed that viral injection of *fos* caused chondrodysplasia with a delay in chondrocyte differentiation and subsequent ossification, further signifying that precise levels of *fos* are necessary for correct skeletal development [178]. The decreased ossification we observed in the head could be a consequence of abnormal endochondral, perichondral and direct ossification because jawbones, pharyngeal bones and dermal bones were all affected.

Fos null mice also have smaller teeth that fail to erupt and form roots [163]. Even though the process of tooth eruption in mice is different from pharyngeal tooth attachment to a

mineralized ceratobranchial arch 5 (CB5) in zebrafish, zebrafish *fos* morphants also had abnormal tooth development with marked delays in formation, abnormal tooth size, shape and number, as well as increased asymmetry between left and right sides of the pharyngeal jaw. The teeth that did form by 8 dpf were either beginning to attach around unmineralized CB5 or not attached at all, likely impacting the functionality of the pharyngeal jaw. Together, the skeletal and dental abnormalities observed in *fos* morphants/mutants parallel the abnormalities seen in *fos* null mice and these findings together enhance our understanding of the importance of *fos* in the development of these structures [163, 164, 179-181]

The abnormalities observed in both craniofacial and dental morphogenesis pointed to a common developmental program involving the cranial neural crest cells (CNCCs). Craniofacial development in vertebrates is highly dependent on the correct formation, proliferation, differentiation and migration of NCCs [41]. Transgenic zebrafish lines labeling premigratory and migrating NCCs were used to show that both *fos* morpholino knockdown and deletion by CRISPR/Cas9 caused a reduction in cranial NCCs starting at 48 hpf. This is a critical time point during which the CNCCs populate the seven pharyngeal arches of the zebrafish viscerocranium and the ethmoid plate in the neurocranium [182]. They begin to form the facial skeletal elements by adopting chondrocyte and osteoblast cell fates [182]. The reduction of CNCCs likely led to the abnormal arches observed starting at 3 dpf, and the abnormal jaw skeletal elements observed at 5 dpf. We have previously demonstrated that *crispld2* knockdown affects the viability and migration of NCCs in the early zebrafish embryo [155, 156]. However, *fos* did not affect the early migration of NCCs, which starts around 14 hpf [156]. The loss of CNCCs observed in the current study could result from disruption of several cellular process that *fos* has been shown to regulate [158, 159, 165, 183]. For example, perturbation of *fos* could disrupt NCC populations by impacting the function of AP1, which regulates gene expression to control cell proliferation, survival and migration [183]. In

trophoblasts, expression of *fos* contributes to the robust activity of AP1 regulated gene expression [183]. Additionally, *fos* knockdown in vitro inhibits cell migration and invasion while inhibiting proliferation and promoting apoptosis, while *fos* overexpression interferes with the equilibrium of cell proliferation and induces transformation and tumor formation [184]. In *c. elegans*, *fos* is also a cell autonomous regulator of cell invasion, a process critical for many cell types and also NCCs, as they have to invade through extracellular matrix, mesoderm and migrating endothelial cells to reach their destination making their motility and invasive ability crucial [185, 186]. The exact cause of loss of CNCCs in *fos* morphants/mutants warrants additional study.

The strengths of using zebrafish include optically clear embryos, which allow the observation of biological processes, and ease of genetic modifications using morpholino and CRISPR/Cas9 technology [182, 187]. While other studies have relied on lateral and ventral imaging to assess zebrafish craniofacial development, these orientations miss critical facial phenotypic information. In contrast, the rostral mounting technique used in this study enabled detailed assessment of facial structures for a more direct comparison to human phenotypes. Additionally, specific alterations of facial dimensions were captured by zFACE, providing an unbiased assessment of the changes in morphants and mutants and lack of changes in rescued embryos. This novel morphometric program will be highly advantageous for studying the effects of genetic manipulation of other craniofacial genes.

In conclusion, the results of this study demonstrate that *fos* is critical for NCCs and craniofacial development. Importantly, absence of *fos* leads to abnormal bone and cartilage development, causing a mouth shape that resembles an orofacial cleft phenotype. Moreover, the findings suggest that perturbations in genes that regulate NCCs, such as *fos*, can have a detrimental effect on NCC-derived tissues and alter normal craniofacial development, thereby contributing to NSCLP. Further work is needed, in both zebrafish and humans, to identify other genes and

pathways by which *fos* is regulating craniofacial development. Our study also provides a model to test putative genes associated with NSCLP in vivo, explore their molecular mechanism in early orofacial development and identify new targets that can be tested in human NSCLP populations.

CHAPTER 5: The role of regulatory variants in *FZD6* and interacting genes in nonsyndromic cleft lip and palate

Note: The information presented in this chapter is based on a manuscript being prepared for submission, for which I am first author. Additional coauthors include Syed Hashmi, Susan Blanton, Bhavna Tandon, Brett Chiquet, George Eisenhoffer, Ariadne Letra and Jaqueline Hecht.

5.0 Introduction

As part of our ongoing genetic studies, GWAS in a large multiplex NSCLP family identified a linkage region harboring rs138557689, a functional noncoding single nucleotide variant (SNV) upstream of the frizzled-6 (*FZD6*) gene which segregated with NSCLP in all the affected individuals in the family [65]. This SNV created a novel TF binding site resulting in an 80% reduction in luciferase reporter activity and suggesting that it affects *FZD6* expression. Interestingly, *Fzd6* null mice have claw and hair patterning defects while *Fzd3/Fzd6* double knockout animals display midbrain morphogenesis defects [188-190]. Knockdown and overexpression of *fzd6* in zebrafish both led to severe craniofacial abnormalities confirming that tightly regulated *fzd6* expression is necessary for correct craniofacial development [65]. Collectively, these studies implicated *FZD6*, a receptor in the Wnt pathway, as an important NSCLP candidate gene.

Wnt signaling is one of the key pathways in craniofacial development, directing migration of NCCs and subsequent growth and fusion of the facial prominences[49]. Wnt pathway genes are highly expressed in both the ectoderm and underlying mesenchyme of the facial prominences and palatal shelves. Wnt activity in mammals is high in areas of rapid growth, specifically in lateral regions such as the maxilla, and is low or absent in the frontonasal prominence [49, 52]. In order to transmit Wnt signaling, the FZD receptor requires the coupling of either co-receptor low-density lipoprotein-related protein 5 (LRP5) or LRP6, which is inhibited by dickopff (DKK) family members [191]. Intriguingly, *lrp6* is expressed in the murine orofacial primordia and null mutant embryos show reduced Wnt signaling, bilateral cleft lip and mandible defects [75]. Recently, a mutation in *LRP6* was identified in a multiplex NSCLP family with tooth agenesis [74]. *LRP5* mutations in humans are associated with syndromic craniofacial bone abnormalities and zebrafish *lrp5* morphant and mutant models show abnormal craniofacial cartilage phenotypes [71-73]. During early development, the

head and other anterior structures form under a gradient of increased *Dkk1* expression and decreased Wnt signaling [76]. *Dkk1* null mice display severe craniofacial abnormalities and completely lack facial structures, while overexpression of *Dkk1* in Wnt reporter mice causes altered Wnt activation pattern in the developing craniofacies and affects the dimensions of the facial prominences [76, 77] [52]. Together, these studies show that the interacting partners of *FZD6* are also critical for normal craniofacial development and perturbation of their expression leads to orofacial phenotypes, making them important NSCLP candidate genes.

Results from GWASs of complex disorders (adult complex disorders and birth defects) show that the majority of risk variants are located in the noncoding regulatory landscape of the genome [192]. Importantly, this finding is also observed in NSCLP, where the majority of GWAS “hits” also fall in noncoding regions [35, 40, 150, 193, 194]. These regions may harbor functional genetic elements, which are often characterized by open chromatin structures, allowing the binding of transcription factors (TF) and coactivator proteins to regulate gene expression [37]. Since variation in these regions contributes to the heritability of NSLCP, their functional characterization is a new and exciting research focus that may uncover missing contributory genetic variation [35, 40]. In the current study, putative noncoding variants upstream of *FZD6*, *LRP5*, *LRP6* and *DKK1* were prioritized using bioinformatic evidence and assayed for functionality in cell-based and zebrafish assays before being tested for association, alone and in combination, in a large and well-characterized NSCLP family dataset.

5.1 Materials and methods

A detailed description of methods used can be found in Chapter 2. A workflow of the methodology is presented in Figure 24.

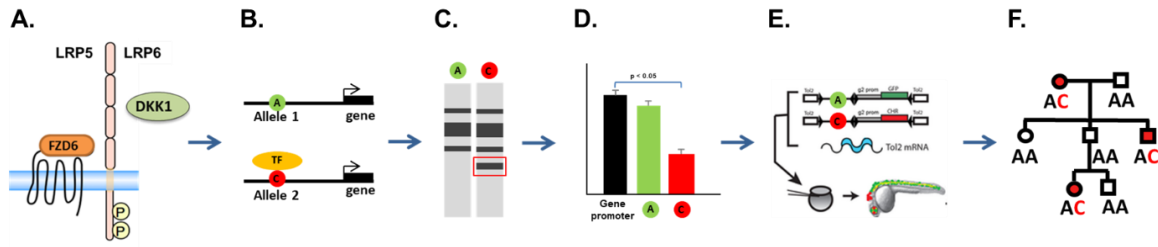


Figure 24. Approach to identify and test noncoding variants in *FZD6* and related genes.

5.2 Results

5.2.1 Twenty one putatively functional variants prioritized for study

Our bioinformatic prioritization approach identified 21 potentially functional SNVs in all four genes. Information on the number of variants that were evaluated using the prioritization method is presented in **Table 10**. Interestingly, the majority of the candidate functional SNVs were predicted to bind TFs that have been implicated in craniofacial development, such as AP2 α , RAR α , and GR β [40, 195-198]. **Table 11** lists the minor allele frequency (MAF), base-wise genomic evolutionary rate profiling (GERP) scores and predicted TFs for the selected SNVs.

Table 10. Bioinformatic prioritization results

		SNVs IDed		Annotation			Pos GERP and open chromatin	<i>In silico</i> TF binding	Prioritized SNVs
Gene	Chrom	dbSNP	Total 5'	GWAVA	VEF				
		total	variants	SNPs w info	Modifier	Promoter			
FZD6	8	1801	227	72	227	57	13	9	6
LRP5	11	8979	200	57	200	56	12	6	5
LRP6	12	8595	267	69	267	102	23	12	5
DKK1	10	447	385*	101	427	248	18	6	5

Table 11. Details of selected variants and predicted TFBSs

	Variant	MAF	GERP	In Silico Prediction	
				Ancestral	Alternate
FZD6	rs75892544	0.06	1.3	--	RAR α , RAR β , c-Myc
	rs1522711	0.45	1.08	GR β	FoxP3
	rs80084586	0.46	1.5	--	AP-2 α
	rs827525	0.02	0.9	p300	MyoD, c-Myc, AP-2, RXR α
	rs74949239	0.03	2.1	--	AP-2, Sp1
	rs827526	0.25	1.8	p300	AP-2, RXR α
LRP6	rs115369160	0.02	1.76	AP-2 α	NF-kappaB, GR β
	rs7136900	0.28	1.04	GR β , Pit-1a	c-Fos, c-Jun
	rs79239491	0.03	3.53	C/Ebalpha	Sp1, Pax5, GR- α , AP-2
	rs7302808	0.47	2.61	--	c-Myb
	rs7136380	0.26	1.36	Sp-1	AP-2 α , RAR α
LRP5	rs58529904	0.04	2.95	--	RAR α , RAR β
	rs4988325	0.17	0.785	NF-1	VDR, RAR α , GR
	rs312009	0.19	1.19	AP-2, NF-1, AP-2 α	RAR β
	rs77394830	0.03	0.937	GR	c-Myb
	rs4988327	0.03	0.937	C/EBP α	--
DKK1	rs7069912	0.12	1.89	RXR α	c-Fos, c-Jun
	rs114971851	0.02	1.54	MEF-2A	GR
	rs114205486	0.01	2.71	Pit-1a, IRF-1, IRF-2	GR α
	rs75526820	0.03	2.08	HNF-1	Sp1, Pax-5
	rs1528879	0.07	2.17	GR α , Pax-5	Foxp3

5.2.2 Protein-DNA binding assays showed allele-specific effects for ten variants

SNVs prioritized using in silico tools were tested for allele-specific binding with electrophoretic mobility shift assays (EMSAs). Screening of the 21 putatively functional SNVs identified 10 variants that displayed allele-specific binding patterns: 1 variant in *FZD6*, 3 variants in *LRP5*, 3 in *LRP6* and 3 in *DKK1* (**Table 2, Figure 25A**). A summary and results for *LRP6* rs7136380 are presented in **Figure 25**. These results suggested that 10 variants created allele-specific protein binding sites giving them the potential to affect gene transcription and expression.

5.2.3 Luciferase assays identified six variants with allele-specific effects on expression

Cloned reporter constructs containing each variant and flanking region in front of the respective gene promoter driving luciferase expression were transfected into 3 different cell lines in order to examine allele and cell-specific influences on gene expression.

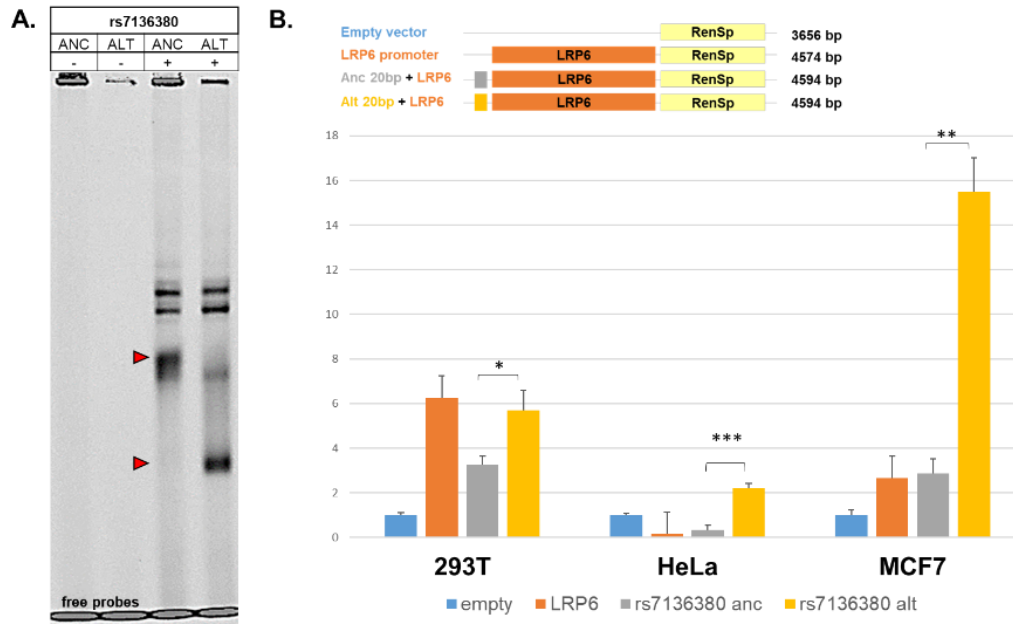


Figure 25. Results for *LRP6* rs7136380 showed allele-specific banding and luciferase expression.

Interestingly, while *FZD6* rs75892544 did not show an effect in 293T cells, both HeLa and MCF7 cells showed that the alternate allele significantly increased promoter activity ($p = 0.02$ for both). The *LRP5* promoter and experimental variant constructs all showed comparatively low luciferase expression in all 3 cell lines. Only one *LRP5* variant, rs4988327, showed an effect: the ancestral allele led to higher promoter activity in 293T cells and this effect was replicated in the MCF7 cells ($p = 0.02$ and $p = 0.03$ respectively). For *LRP6*, 293T cells showed an effect for all 3 SNVs: the rs115369160 alternate allele reduced activity ($p = 0.005$), the alternate rs7136900 allele reduced activity ($p = 0.0004$), and the alternate rs7136380 allele

increased activity ($p= 0.03$) (**Figure 25**). HeLa and MCF7 cells only replicated this effect for rs7136380 ($p= 0.0003$ and $p= 0.001$ respectively). All three *DKK1* variants showed an allele-specific effect in 293T cells. The rs7069912 alternate allele showed higher activity than the ancestral ($p= 0.002$), for rs114205486 the alternate allele showed lower activity ($p=0.001$) and for rs114971851 the alternate allele was significantly lower than the ancestral ($p=0.00002$). For rs7069912, the alternate allele showed higher activity in the HeLa cells but the p value was marginal ($p=0.050$) and in MCF7 cells the alternate allele led to lower activity ($p=0.001$). Both other SNVs showed consistent effects in HeLa and MCF7 cells. These differences in the various cell lines for each study variant were expected for noncoding variation, which is known to have cell-specific effects [35, 37]. A summary of the findings from the EMSA and Luciferase assays is shown in **Table 12**.

Table 12. Summary of EMSA and luciferase assay results for prioritized variants.

Gene	Variant	EMSA	Luciferase Assay		
			293T	HeLa	MCF7
<i>FZD6</i>	rs75892544	Y	N	Y	Y
<i>LRP6</i>	rs115369160	Y	N	N	N
<i>LRP6</i>	rs7136900	Y	Y	N	N
<i>LRP6</i>	rs7136380	Y	Y	Y	Y
<i>LRP5</i>	rs58529904	Y	N	N	N
<i>LRP5</i>	rs4988325	Y	N	N	N
<i>LRP5</i>	rs4988327	Y	Y	N	Y
<i>DKK1</i>	rs7069912	Y	Y	Y	Y
<i>DKK1</i>	rs114971851	Y	Y	Y	Y
<i>DKK1</i>	rs114205486	Y	Y	Y	Y

5.2.4 Establishment of timeline for mouth development and β -catenin expression

Time course analysis was performed utilizing two stable Wnt reporter lines, Tg(7xTCF-Xla.Siam:nlsMCherry)^{ia4} and Tg(7xTCF-Xla.Siam:GFP)^{ia4} to establish regional and temporal Wnt activation in zebrafish [92]. These transgenic reporter animals have 7 tcf binding sites driving mcherry or gfp expression, which allow for the visualization of activated β -catenin Wnt signaling during embryonic development, making these lines β -catenin biosensors [92]. Reporter embryos were collected from 1 to 7 days post fertilization (dpf), fixed in 4% PFA, stained with DAPI to visualize the nuclei of each cell, and then mounted in 1% agarose for confocal imaging. The novel rostral mounting technique developed in the Eisenhoffer lab was used to capture important facial features such as the neuromasts, olfactory pits, oral cavity and jaws. Results showed robust β -catenin Wnt signaling in the craniofacial region, specifically in the developing oral cavity by 3 dpf (**Figure 26**). Expression was also observed in the developing brain starting at 24 hpf through 7 dpf. A summary of the results for embryos 48 hpf to 5 dpf, where the gfp channel indicates β -catenin activation (bottom panel) and the merged DAPI and gfp channels image visualize facial structures where expression is

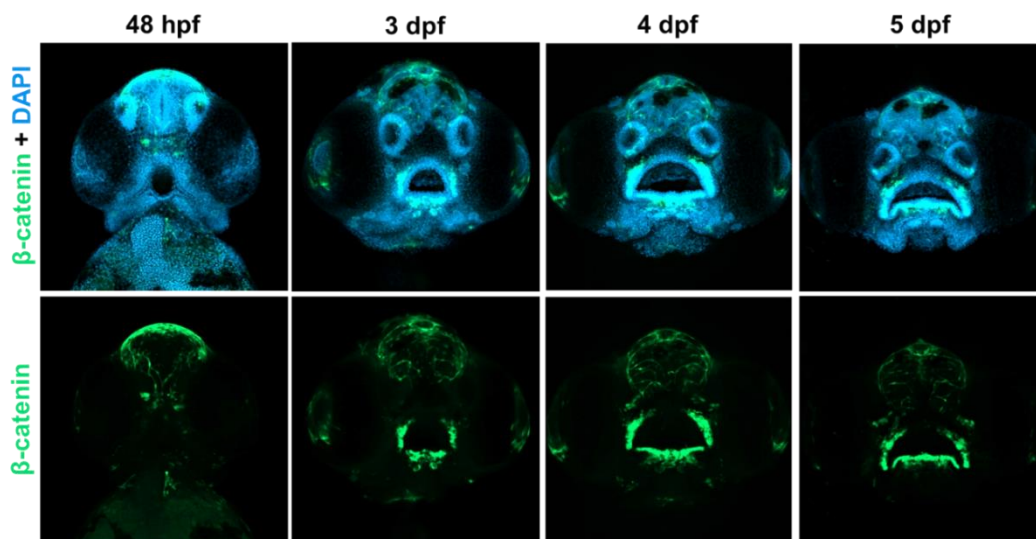


Figure 26. β -catenin activation during orofacial development in zebrafish embryos.

observed (top panel) is shown in **Figure 26**. This pattern was observed up to 7 dpf and these results were also confirmed using the same reporter attached to a different fluorophore (the mCherry line with the nuclear localization signal).

5.2.5 Knockdown of *FZD6* and related genes caused similarly abnormal facial phenotypes

Morpholino knockdown was performed for each study gene to determine its importance to craniofacial development, facial morphogenesis and to identify facial structures affected by perturbations in gene expression. Knockdown of all four genes altered the pattern of β -catenin expression in the head starting at 3 days post fertilization, however a significant difference in β -catenin levels was not observed at this timepoint (**Figure 27**). Evaluation of craniofacial morphology at 5 dpf using zFACE revealed ten altered facial measurements after *fzd6* knockdown, 17 after *lrp5*, 23 after *lrp6* and 26 after *dkk1* knockdown. Intriguingly, 7 facial dimensions were commonly altered after all four gene knockdowns and included mouth height, mouth width, and various oral cavity angles ($p < 0.0013$), shown in **Table 13**). Measures of differences between left and right side facial angles were not different in any of the knockdowns.

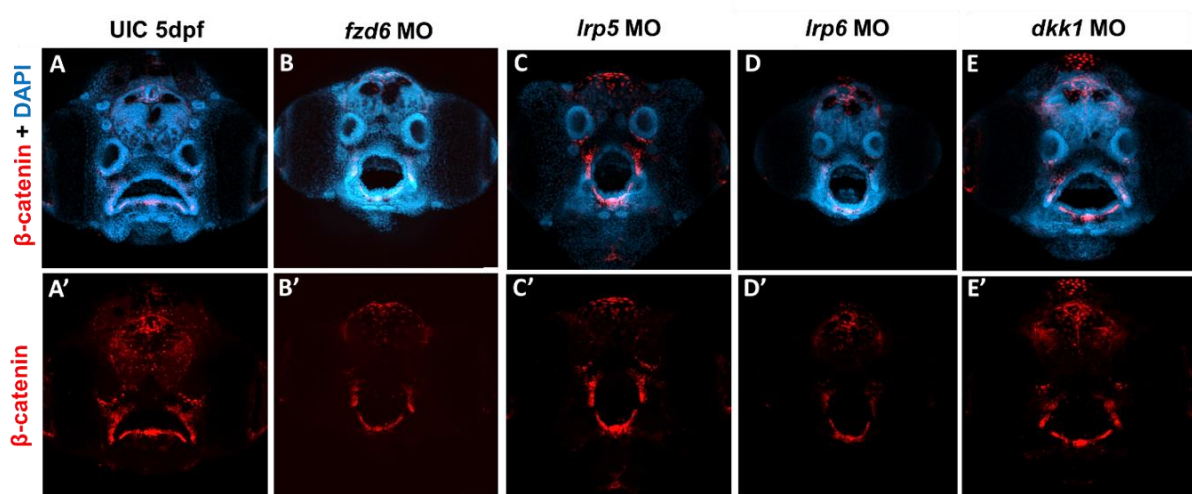


Figure 27. Knockdown of *FZD6* and related genes caused abnormal faical phenotypes.

Table 13. ZFACE morphometric results in *FZD6*, *LRP5*, *LRP6* and *DKK1* morphants.

zFACE feature	UIC vs. <i>FZD6</i>	UIC vs. <i>LRP6</i>	UIC vs. <i>LRP5</i>	UIC vs. <i>DKK1</i>
Width	**	****	ns	****
Height	ns	****	ns	***
Olfactory Distance	****	****	ns	****
Upper Lip Width	ns	ns	ns	ns
Lower Lip Width	ns	****	ns	ns
Mouth Width	****	****	**	****
Olfactory to Mouth	****	****	ns	****
Olfactory to Mouth 2	****	***	ns	****
Difference	ns	**	ns	ns
Olfactory to Mouth 3	****	****	ns	****
Chin Width	ns	*	ns	***
Mouth to Chin	ns	**	ns	**
Alternate Height	*	**	ns	**
Mouth Height	****	***	***	**
Neuromast Angle 1	*	**	ns	****
Neuromast Angle 2	***	****	ns	****
Difference	ns	ns	ns	ns
Neuromast Height	**	***	ns	****
Neuromast Width	**	****	ns	****
Mid Neuromast Width	ns	****	**	***
Average Length Olfactory to mouth	ns	****	ns	****
Area Top	ns	****	ns	****
Area Bottom	*	***	ns	****
Area Combined	ns	****	ns	****
Mid Olfactory to Chin height	ns	*	ns	ns
Mouth Area	ns	ns	**	ns
Mouth Perimeter	****	****	ns	****
Libiale Superius Angle	ns	ns	ns	**
Chelion Left Angle	ns	ns	ns	**
Chelion Right Angle	ns	ns	ns	**
Chelion Diff	ns	ns	ns	ns
Labiale Inferius Angle	****	****	***	****
Crista Philtri Left Angle	****	****	**	****
Crista Philtri Right Angle	****	****	**	****
Crista Philtri Diff	****	ns	ns	ns
Labiale Superius Mid Angle	****	****	****	****
Labiale Inferius Left Angle	****	****	****	****
Labiale Inferius Right Angle	****	****	***	****
Labiale Inferius Diff	ns	ns	ns	ns

* p < 0.05, ** p < 0.01, *** p < 0.001, **** p < 0.0001

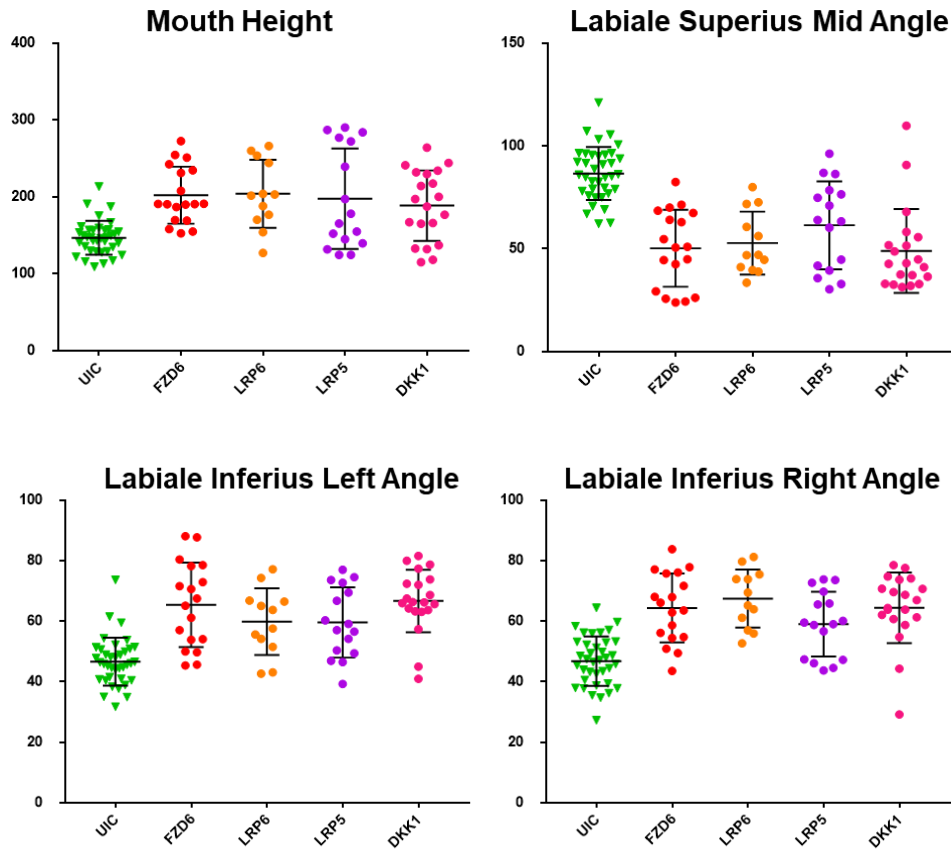


Figure 28. Morphometric results showed common alterations after knockdown of *fzd6*, *lrp5*, *lrp6* and *dkk1*.

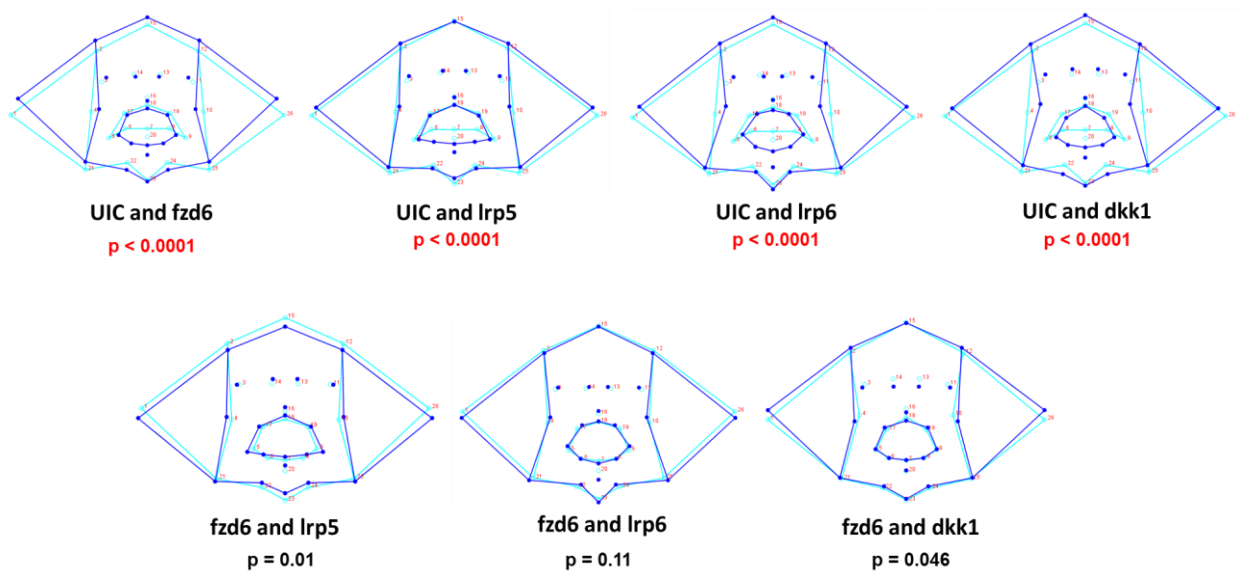


Figure 29. DFA results showed that all morphants had a significantly different face shape compared to controls but a similar face shape compared to each other.

5.2.6 Small molecule inhibition and activation of WNT signaling alters facial phenotype

Two small molecule Wnt modulators, the antagonist IWR-1 and agonist BIO were used to treat zebrafish embryos starting at 24 hpf up to the time of collection in order to examine the effects of β -catenin inhibition and activation on facial morphogenesis. Both treatments altered the facial and mouth phenotype at 3 and 5 dpf (**Figure 30A**). Importantly, these phenotypes were similar to the morpholino knockdowns, displaying abnormally oval and elongated oral cavities. These experiments were repeated in the Wnt reporter lines and showed a significant reduction of β -catenin activation in the craniofacial region after IWR treatment compared to both the untreated control (UTC) and DMSO treated control ($p = 0.0002$). BIO treatment, on the other hand, led to an increase β -catenin activation, however, this difference was only significant in the UTC comparison ($p = 0.01$). These results further indicated that perturbation of β -catenin activation results in craniofacial and mouth abnormalities, similar to knockdowns of the study genes, which code for receptors upstream in the signaling of this pathway.

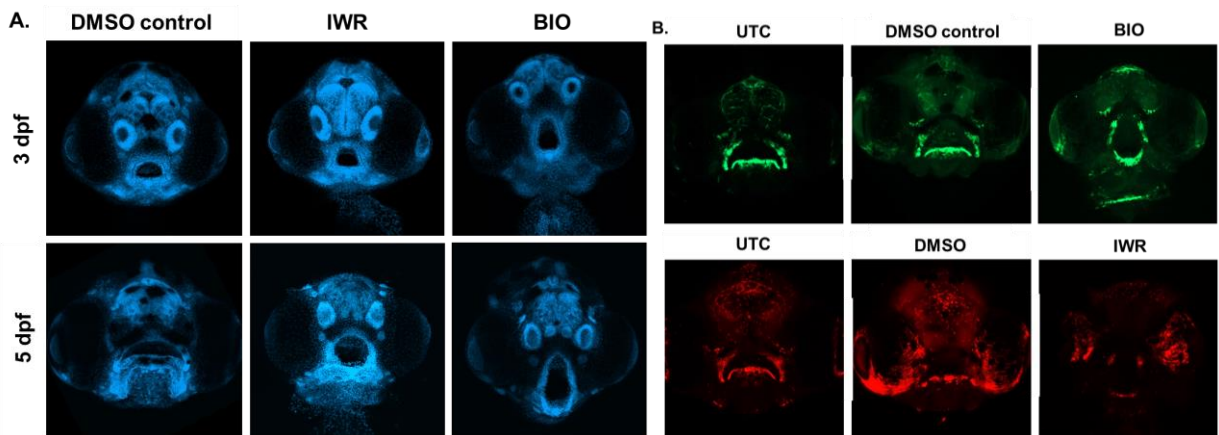


Figure 30. Wnt drugs altered facial phenotype and β -catenin activation in the oral cavity. A. Both IWR and BIO treatment altered the face at 3 and 5 dpf. **B.** IWR led to a decrease in beta catenin while BIO led to an increase.

5.2.7 Transgenic reporter zebrafish assays supported functionality of four variants

Zebrafish were generated to further test variants showing functionality in the cell based assays in order to examine allele-specific expression in craniofacial structures during embryonic development. Two control variant constructs were also generated to compare experimental results: a) *FZD6* rs138557689 which we identified in the African American NSCLP family, for which the alternate allele led to decreased luciferase expression and b) *IRF6* rs642961, for which the alternate allele led to decreased expression in developing zebrafish in the publication describing this transgenesis method [36]. This *IRF6* variant was also associated with NSCLP in our family dataset [132, 199] (also see CHAPTER 3). Surprisingly, transgenic *FZD6* rs13855768 animals showed increased expression driven by the alternate allele (mCherry) compared to the ancestral allele (gfp) in the brain, upper lip and lower jaw in F0 embryos from 2- 5 days post fertilization (dpf). Stable F1s confirmed this expression pattern, further showing strong regional expression in the midbrain-hindbrain boundary and the lower oral cavity starting at 48 hpf up to 5 dpf (**Figure 31**). The ancestral allele drove expression in some regions of the face in F0 embryos but was not detected in F1s.

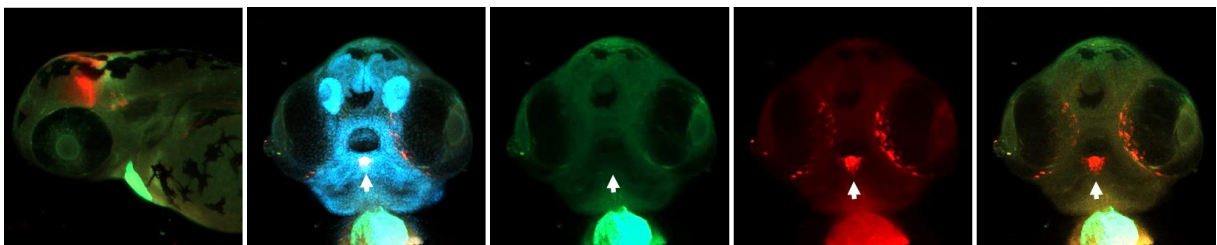


Figure 31. F1 *FZD6* rs139557689 expression results showed higher alternate allele (mCherry) expression in the oral cavity (white arrowhead).

IRF6 rs642961, on the other hand, showed a consistent expression pattern in F0 and F1 embryos, with both the ancestral and alternate alleles driving expression in the brain but only ancestral- gfp expression seen in the lower jaw and oral cavity at both 3 and 5 dpf ($p = 0.0009$).

These results are in agreement overall with Bhatia *et al* findings but the craniofacial structures where expression was observed differed slightly [199].

The experimental study variants all showed stronger ancestral compared to alternate allele-driven reporter expression in developing craniofacial structures at 3 and 5 dpf. The *FZD6* rs75892444 ancestral allele drove reporter expression in the lower jaw cartilages, near the oral cavity and in the brain while the alteranate construct showed weak expression near the oral cavity and in the lower jaw cartilages ($p < 0.0001$, **Figure 32**). The *LRP5* rs4988327 ancestral allele showed strong expression around the mouth and in the brain while the alternate allele didn't show expression in the craniofacial region ($p < 0.0001$). The *LRP6* rs7136380 ancestral allele drove expression around the oral cavity and in the lower jaw while alterante allele-driven expression was not detected in these structures but was detected in the brain ($p = 0.002$). Lastly, *DKK1* rs7069912 showed strong ancestral allele expression in lower jaw structures and stong alternate allele-driven expression in the brain, however gfp experssion was comparatively higher ($p = 0.006$) (**Figure 32**).

Results from stable F1 reporter embryos agreed with F0 results but additionally showed more specific expression compared to the dispersed expression in the chimeric F0s. *FZD6* rs75892544 showed ancestral allele-driven expression in the brain and the corners of the oral cavity (**Figure 33**). *LRP5* rs4988327 showed very high expression in the brain, olfactory pits and some expression in the lower oral cavity edges, while the *LRP6* rs7136380 ancestral allele drove more robust and diffuse expression in the brain compared to the alternate allele which drove weaker expression in a smaller area (**Figure 33**). Lastly, *DKK1* rs7069912 showed expression in the facial muscles including ones in the lower and upper jaw (**Figure 33**). These dual transgenic reporter zebrafish experiments further nominated 4 variants, one in each gene, for further study.

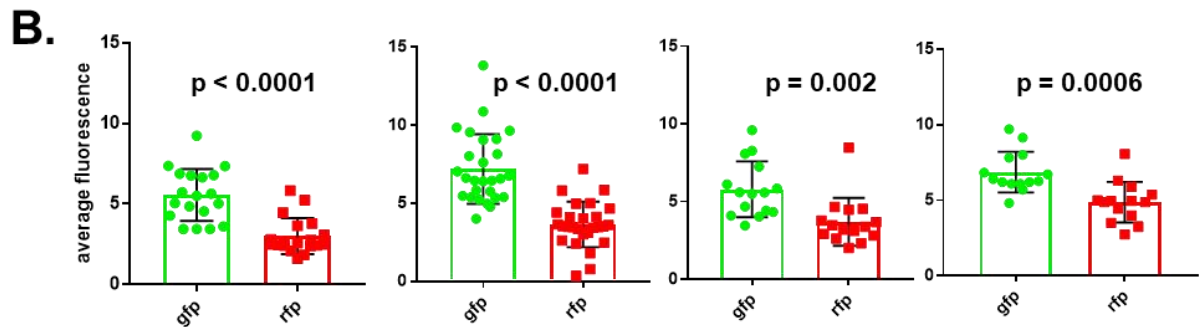
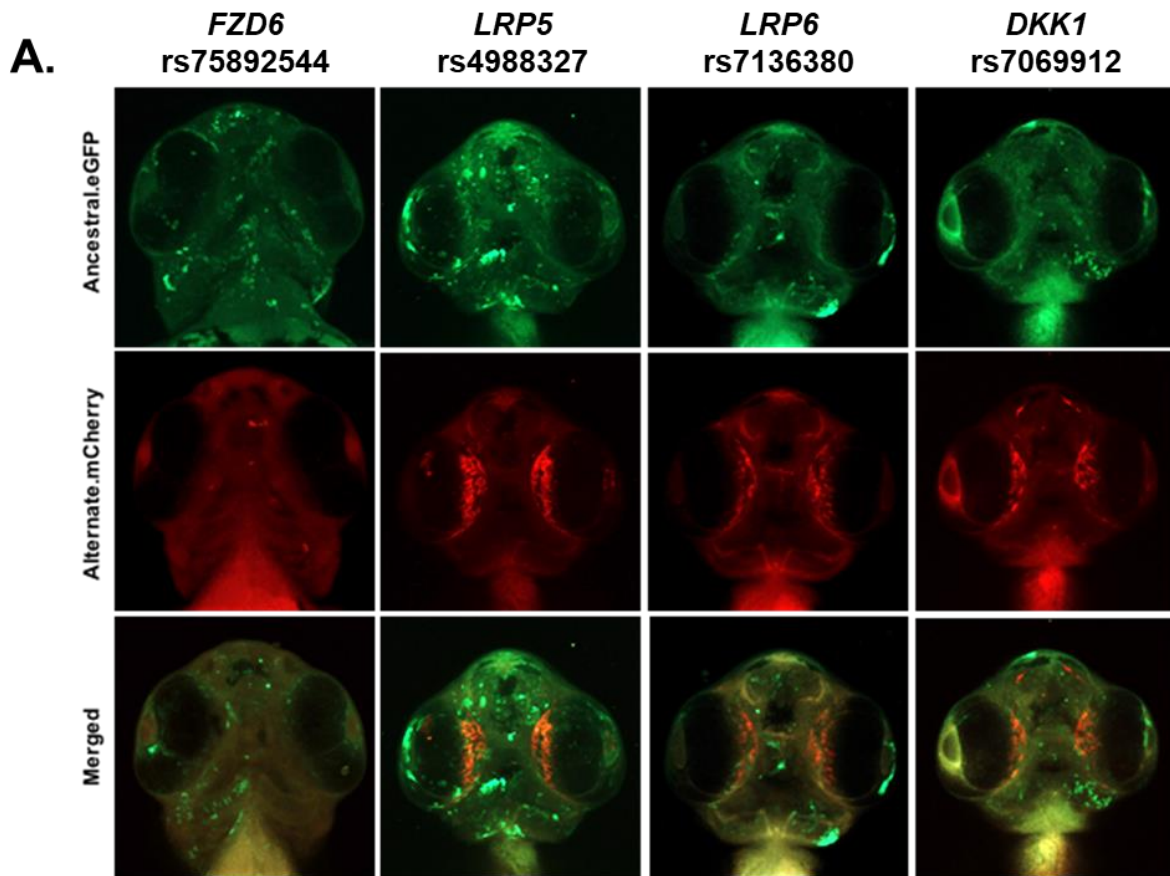


Figure 32. Transgenic reporter expression results at 3 dpf. A. Comparison of ancestral-driven *gfp* expression and alternate-driven *mCherry* expression in the craniofacial regions of F0 transgenic embryos for each study variant. **B.** Increased *gfp* expression was observed for all study variants after fluorescence was quantified.

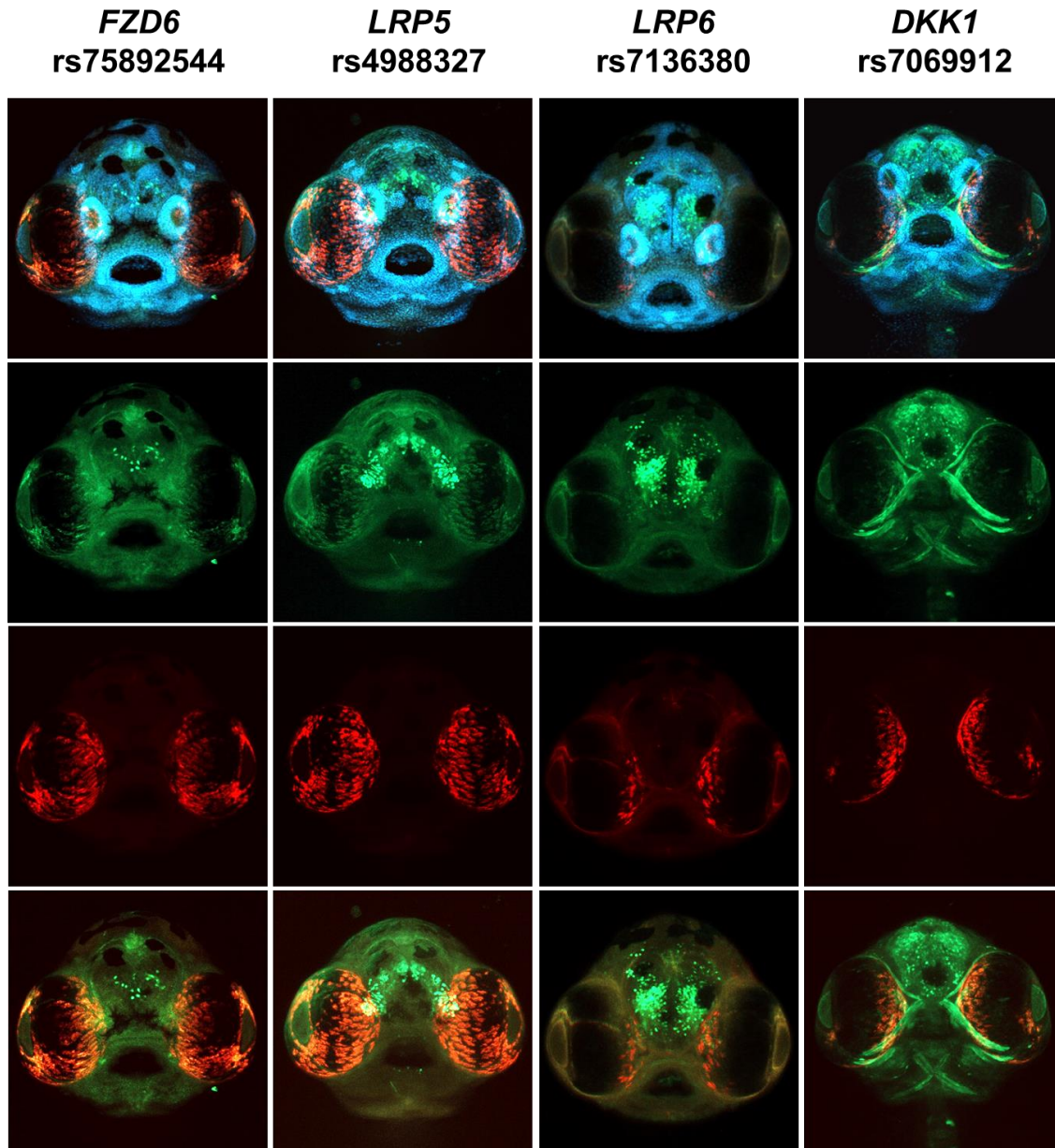


Figure 33. Transgenic reporter expression results at 3 dpf in stable F1 reporter zebrafish.

5.2.5 Association in NSCLP families

All SNVs were in Hardy-Weinberg equilibrium. Variants in all four genes met the nominal association threshold of $p \leq 0.05$ (**Table 14**). After Bonferroni correction, associations between variants in *LRP5* and *LPR6* and NSCLP were observed in the NHW white families while association of variants in *FZD6*, *LPR5* and *DKK1* were observed in the Hispanic families (**Table 14**). *FZD6* rs75892544 was associated with NSCLP in combined Hispanic ($p = 4.70E-07$), multiplex Hispanic ($p = 3.00E-05$) and simplex Hispanic ($p = 0.002$) families and no association was observed in the NHW families. *LRP5* rs49883257 and NSCLP association was observed in both ethnic groups, specifically in all NHW families combined ($p = 1.49E-04$) multiplex NHW families ($p = 8.24E-06$), combined Hispanic families ($p = 0.004$) and simplex Hispanic families ($p = 5.95E-04$). *LRP6* rs7136380 showed association in combined NHW ($p = 4.4E-05$) and multiplex NHW families ($p = 5.95E-04$), while simplex NHW and simplex Hispanic families showed nominal association ($p = 0.014$ and $p = 0.04$, respectively). Lastly, *DKK1* rs7069912 was associated with NSCLP in the combined Hispanic families ($p = 0.002$) and showed suggestive association in the multiplex and simplex Hispanic families ($p = 0.03$ and $p = 0.03$, respectively).

Pair-wise gene-gene interactions were also examined in FBAT. In the NHW families, interactions were found between *FZD6* and *LRP5* ($p = 0.001$), *LRP5* and *LRP6* ($p = 2.14E-06$), *LRP5* and *DKK1* ($p = 1.69E-04$) and *LRP6* and *DKK1* ($p = 2.90E-05$) (**Table 15**). In Hispanics, evidence of interaction was found between *FZD6* and the other 3 genes, *FZD6* and *LRP5* ($p = 2.47E-06$), *FZD6* and *LRP6* ($p = 4.85E-04$), *FZD6* and *DKK1* ($p = 1.06E-07$), as well as *LRP5* and *DKK1* ($p = 5.30E-05$).

Table 14. FBAT results on *FZD6*, *LRP5*, *LRP6* and *DKK1* variants

	GENE	SNP	All		Multiplex		Simplex	
			FBAT	FBAT-e	FBAT	FBAT-e	FBAT	FBAT-e
NHW Families	<i>FZD6</i>	rs75892544						
	<i>LRP5</i>	rs4899327	1.49E-04	8.60E-05			8.24E-06	4.03E-06
	<i>LRP6</i>	rs7136380	4.40E-05	1.01E-04	7.05E-04	0.001	0.01	0.02
	<i>DKK1</i>	rs7069912						
Hispanic Families	<i>FZD6</i>	rs75892544	4.70E-07	2.80E-06	3.00E-05	1.94E-04	0.002	0.003
	<i>LRP5</i>	rs4899327	0.004	0.004			5.95E-04	7.49E-04
	<i>LRP6</i>	rs7136380					0.04	0.05
	<i>DKK1</i>	rs7069912	0.002	0.003	0.03	0.04	0.03	0.03

Table 15. Gene-gene interaction results for *FZD6*, *LRP5*, *LRP6* and *DKK1* variants.

Gene 1	Gene 2	Families	NHW			Families	Hispanic		
			All	Multiplex	Simplex		All	Multiplex	Simplex
<i>FZD6</i>	<i>LRP5</i>	225	0.006	--	0.001	124	2.47E-06	0.002	3.43E-04
	<i>LRP6</i>	233	--	--	--	177	4.85E-04	--	0.002
	<i>DKK1</i>	174	--	--	--	101	1.06E-07	1.10E-05	0.001
<i>LRP5</i>	<i>LRP6</i>	241	2.14E-06	0.004	1.93E-04	187	--	--	0.007
	<i>DKK1</i>	143	1.69E-04	--	2.20E-05	96	5.30E-05	--	1.31E-04
<i>LRP6</i>	<i>DKK1</i>	208	2.90E-05	5.15E-04	0.01	159	--	--	--

5.3 Discussion

Variants in noncoding regions of the genome have been consistently associated with NSCLP in GWASs and candidate gene studies examining SNVs [35]. One limitation in these studies is that the biological contributions of the identified/associated variants are difficult to interpret without follow up functional experiments to provide context and possible explanations for their etiologic roles. Here we employed an approach where noncoding variants were first prioritized and tested for functionality and then examined for association with NSCLP, thereby increasing statistical power by focusing only on variants with strong evidence of functionality. The results showed that variants with allele-specific protein binding, promoter activity and reporter expression during vertebrate craniofacial development in *FZD6*, *LRP5*, *LRP6* and *DKK1* were associated with NSCLP.

NSCLP is a complex disorder that follows a multifactorial model of inheritance, under which multiple genetic variables are thought to contribute to susceptibility risk [13]. Results showed support for the association of *FZD6*, *LRP5* and *DKK1* in Hispanic families and for *LRP5* and *LRP6* in NHW families. The proteins encoded by these four genes, which work at the receptor level of the Wnt pathway, all influence Wnt signaling [31, 51]. Additionally, significant statistical interactions were observed between *FZD6* - *LRP5* and *LRP5* - *DKK1* in both ethnic populations. These statistical interactions supported known biological links between FZD receptors and LRP5/LRP6 co-receptors and between LRP5/6 and their antagonist DKK1 [67]. Differences in the single variant and gene-gene association results between the NHW and Hispanic families further emphasize the heterogeneity of NSCLP heritability and are in agreement with other findings of ethnic population-specific genetic liability. These results are also consistent with the multifactorial model and support the contributions of multiple genes in susceptibility risk [6, 16, 200].

Craniofacial morphogenesis is highly regulated and perturbations in gene expression at any stage of development can alter the resulting facial phenotype. Genetic manipulations to β -catenin mediated Wnt signaling illustrate this point, as overexpression of *Dkk1* in Wnt reporter mice leads to altered Wnt signaling and resulting changes to the morphology of the facial prominences, thereby increasing the likelihood that an abnormality such as a cleft will occur (25). To understand how variation in *FZD6*, *LRP5*, *LRP6* and *DKK1* can potentially affect craniofacial morphology we first characterized β -catenin signaling in developing zebrafish embryos by examining rostral images of the developing face in a Wnt reporter line. Intriguingly, β -catenin was highly active in the developing oral cavity starting at 3 dpf and persisting to 7 dpf. This pattern of expression is in agreement with findings in TOPGAL/BATGAL mice where β -catenin signaling is high at the edges of the facial prominences and observed later in development in the maxilla and lower lip [52, 75]. The transgenic reporter zebrafish for each study variant also largely drove expression in these craniofacial regions in both F0 and F1 animals, with the exception of *DKK1* rs7069912, which drove expression in facial muscles.

Genes in the Wnt pathway are known to play crucial roles in craniofacial development and to contribute to orofacial disorders such as NSCLP [31]. Given the specific expression pattern of active β -catenin signaling around the oral cavity, it was not surprising that abnormal mouth phenotypes resulted from both knockdown of each gene and from pharmacological perturbations of this pathway. Applying ZFACE morphometric analysis allowed the comparison of phenotypes from each condition and the identification of oral-cavity related measurements altered by all 4 genes and by activation or inhibition of Wnt signaling. Together these results suggest that dysregulation of β -catenin signaling in the oral cavity and other craniofacial structures leads to the formation of abnormal mouth phenotypes and dysmorphic

craniofacies, signifying possible mechanisms by which differences in gene expression driven by noncoding variation can contribute to phenotypic changes in orofacial development.

Noncoding variants fine-tune transcription and expression of genes by creating or abolishing transcription factor binding sites (TFBSs) [37]. The transcription factors by which these noncoding variants are thought to confer their effects are important and warrant further study. For example, the *FZD6* rs75892544 alternate allele was predicted to create binding sites for RAR α and RAR β , known transcriptional repressors, suggesting lower gene transcription/ expression expected when the alternate allele is present. This was supported by the transgenic zebrafish reporter results, where the alternate allele drove diminished mCherry expression. The cell-based results, however, showed increased alternate allele expression in HeLa and MCF7 cells, while the 293T cells did not show an effect. Retinoic acid is a well-known teratogen that causes cleft palate in both mice and humans, suggesting that this variant is a good candidate for examining gene-environment interaction effects, another component of the multifactorial model of NSCLP [201]. We still do not fully understand how noncoding variants enact their effects and further studies are needed to elucidate this. Our findings in the cell-based and zebrafish reporter assays indicate that both in vitro and in vivo assays are needed to fully evaluate potential effects of noncoding variants.

The strengths of this study come from focused analysis of a set of genes with strong biological evidence in craniofacial development that act together in the same signaling pathway. Statistical power was increased by prioritizing and testing noncoding variants in multiple ways, including in silico, in vitro, and in vivo approaches before examining them in human NSCLP populations. The use of zebrafish embryos offered the opportunity to interrogate these variants in high resolution in a developmental time line and allowed the opportunity to perform supporting expression and perturbation studies to understand the consequences and context of variant-specific alterations in gene expression. In summary, this study identified 4

functional noncoding variants in Wnt pathway genes that contribute to NSCLP etiology. These results strengthen the evidence for an etiologic role of *FZD6* and *LRP6* and provide the first evidence for *LRP5* and *DKK1* in NSCLP. They also begin to fill the gap in our knowledge about the genetic underpinnings of this common birth defect. Our novel approach can be used in future studies to begin the construction of a map of noncoding genetic contributions to NSCLP and may ultimately be translated for use in determining individual and family risk for NSCLP.

CHAPTER 6: Summary and Future Directions

Nonsyndromic cleft lip and palate is the most common craniofacial birth defect occurring in 1 in 700 live births, affecting more than 4000 individuals in the US, and approximately 130,000 individuals worldwide each year [2, 202]. Although surgical therapies have improved facial outcomes, the associated long-term abnormalities impose significant psychosocial and financial burdens that negatively impact quality of life [146]. Despite numerous decades of research, only 20% of the genetic contributions have been identified, explaining only a small part of NSCLP's heritability and leaving a large gap in knowledge.

The familial aggregation of orofacial clefts has been recognized since the 1700s, and Fogh Anderson first documented the birth prevalence, male/female skewing, and segregation within a Danish family cohort in 1942 [24, 203]. Studies using twin pairs have estimated a high heritability and NSCLP is classified as a complex disorder following multifactorial inheritance, where multiple genetic and environmental factors that each have a small effect, act together in an additive manner [16]. Multifactorial model specifications include: 1) affected children are most often born to unaffected parents, 2) the risk of recurrence increases with the number of affected individuals in the family, by severity of the condition, and by gender with the least often affected sex (in this case females) having a higher liability, and 3) the risk declines by degree of relationship [6].

Efforts to identify the underlying genetic components have utilized both simplex and multiplex families and case-control populations, yielding evidence for the involvement of over 40 genes [24]. Parallel studies in animal models with sporadic clefting, teratogenic causes of cleft phenotypes and genetic mutations that recapitulate syndromic presentations of orofacial clefts have yielded support for the involvement of even more genes, environmental factors and signaling pathways [4].

More recently, with the feasibility of sequencing the entire genome of an individual, the focus of human studies is shifting towards in depth genetic interrogation of affected individuals and their families by whole genome sequencing [204, 205]. This will aid in characterizing variation in noncoding regions, which is a new direction and may uncover unknown genetic contributors underlying NSCLP.

The current work examined gene regulatory pathways that are known to be important in craniofacial development. The first pathway examined was a Pbx-driven regulatory network that alters Wnt ligand gene expression and controls facial morphogenesis. When this network is disrupted, it leads to completely penetrant bilateral cleft lip in mice [59]. We followed up on these exciting results by examining the components of this proposed pathway, both individually and together, in human NSCLP in Chapter 3. Our results with two independent datasets found support for the contribution of variation in *PBX2* in NSCLP families and *PBX1* in case-control comparisons. We also observed significant gene-gene interactions between *PBX2-IRF6*, *PBX1-WNT9B-IRF6*, and *TP63-IRF6*, further supporting the combinatorial effects of genetic components of this regulatory pathway and confirming for the first time the contributions of this pathway to NSCLP risk.

Chapter 4 presented continuing work in our efforts to understand how *CRISPLD2*, an NSCLP gene discovered in our lab and confirmed by studies in different populations, contributes to craniofacial morphogenesis and leads to a cleft when disrupted. We focused on a novel gene, *fos*, which was shown to be differentially expressed upon *crispld2* knockdown in zebrafish, and confirmed to play a role in our NSCLP families [33, 151-156, 206]. Although well characterized as an oncogene and for its regulatory role in bone biology, *FOS* has not been studied in the context of orofacial clefting. Our work utilized zebrafish as a powerful model to show that reduction or absence of *fos* results in a wide array of craniofacial abnormalities, including an abnormal mouth and face shape, defects in skeletal components of the

neurocranium and viscerocranium and tooth anomalies. These novel findings hold promise for further interrogations of this gene in human NSCLP and for further exploration of the molecular mechanisms conferred by its dysregulation in the context of *CRISPLD2*.

Finally, in Chapter 5, we examined noncoding variation in 4 genes that control WNT signaling at the receptor level that are strongly implicated in regulating craniofacial development and contributing to NSCLP. We used a novel top-down approach that prioritized and tested noncoding variants in these genes and shortlisted variants that affect gene expression during orofacial development in an allele-specific way. After testing these functional variants in a large dataset of NSCLP families, we observed individual and combinatorial contributions to NSCLP, paving the way for future studies of these genes and the identification of genetic signatures that increase NSCLP risk in individuals and families.

Altogether, results from this work enhance our knowledge of regulatory gene pathways in NSCLP and further the understanding of craniofacial genetics. They present new candidate genes for replication studies in different ethnic and geographic populations. These results also have the potential to be translated in the clinical setting for the purposes of providing improved genetic counseling and assessing individual risk for NSCLP.

BIBLIOGRAPHY

1. *Improved national prevalence estimates for 18 selected major birth defects--United States, 1999-2001.* MMWR Morb Mortal Wkly Rep, 2006. **54**(51): p. 1301-5.
2. Hashmi, S.S., D.K. Waller, P. Langlois, M. Canfield, and J.T. Hecht, *Prevalence of nonsyndromic oral clefts in Texas: 1995-1999.* Am J Med Genet A, 2005. **134**(4): p. 368-72.
3. Parker, S.E., C.T. Mai, M.A. Canfield, R. Rickard, Y. Wang, R.E. Meyer, P. Anderson, C.A. Mason, J.S. Collins, R.S. Kirby, A. Correa, and N. National Birth Defects Prevention, *Updated National Birth Prevalence estimates for selected birth defects in the United States, 2004-2006.* Birth Defects Res A Clin Mol Teratol, 2010. **88**(12): p. 1008-16.
4. Dixon, M.J., M.L. Marazita, T.H. Beaty, and J.C. Murray, *Cleft lip and palate: understanding genetic and environmental influences.* Nat Rev Genet, 2011. **12**(3): p. 167-78.
5. Marazita, M.L. and M.P. Mooney, *Current concepts in the embryology and genetics of cleft lip and cleft palate.* Clin Plast Surg, 2004. **31**(2): p. 125-40.
6. Grosen, D., C. Chevrier, A. Skytthe, C. Bille, K. Molsted, A. Sivertsen, J.C. Murray, and K. Christensen, *A cohort study of recurrence patterns among more than 54,000 relatives of oral cleft cases in Denmark: support for the multifactorial threshold model of inheritance.* J Med Genet, 2010. **47**(3): p. 162-8.
7. Stuppia, L., M. Capogreco, G. Marzo, D. La Rovere, I. Antonucci, V. Gatta, G. Palka, C. Mortellaro, and S. Tete, *Genetics of syndromic and nonsyndromic cleft lip and palate.* J Craniofac Surg, 2011. **22**(5): p. 1722-6.

8. Yuzuriha, S. and J.B. Mulliken, *Minor-form, microform, and mini-microform cleft lip: anatomical features, operative techniques, and revisions*. *Plast Reconstr Surg*, 2008. **122**(5): p. 1485-1493.
9. Suzuki, S., M.L. Marazita, M.E. Cooper, N. Miwa, A. Hing, A. Jugessur, N. Natsume, K. Shimozato, N. Ohbayashi, Y. Suzuki, T. Niimi, K. Minami, M. Yamamoto, T.J. Altannamar, T. Erkhembaatar, H. Furukawa, S. Daack-Hirsch, J. L'Heureux, C.A. Brandon, S.M. Weinberg, K. Neiswanger, F.W. Deleyiannis, J.E. de Salamanca, A.R. Vieira, A.C. Lidral, J.F. Martin, and J.C. Murray, *Mutations in BMP4 are associated with subepithelial, microform, and overt cleft lip*. *Am J Hum Genet*, 2009. **84**(3): p. 406-11.
10. Mulliken, J.B., J.K. Wu, and B.L. Padwa, *Repair of bilateral cleft lip: review, revisions, and reflections*. *J Craniofac Surg*, 2003. **14**(5): p. 609-20.
11. Marazita, M.L., *Subclinical features in non-syndromic cleft lip with or without cleft palate (CL/P): review of the evidence that subepithelial orbicularis oris muscle defects are part of an expanded phenotype for CL/P*. *Orthodontics & craniofacial research*, 2007. **10**(2): p. 82-7.
12. Weinberg, S.M., K. Neiswanger, R.A. Martin, M.P. Mooney, A.A. Kane, S.L. Wenger, J. Losee, F. Deleyiannis, L. Ma, J.E. De Salamanca, A.E. Czeizel, and M.L. Marazita, *The Pittsburgh Oral-Facial Cleft study: expanding the cleft phenotype. Background and justification*. *Cleft Palate Craniofac J*, 2006. **43**(1): p. 7-20.
13. Carter, C.O., *Genetics of common disorders*. *Brit Med Bull*, 1969. **25**: p. 52-57.
14. Carter, C.O., *Genetics of Common Congenital Malformations in Man*. *Proc.Roy.Soc.Med.*, 1976. **69**: p. 6-8.
15. Wyszynski, D.F. and T.H. Beaty, *Phenotypic discordance in a family with monozygotic twins and nonsyndromic cleft lip and palate: follow-up*. *Am J Med Genet*, 2002. **110**(2): p. 182-3.

16. Fraser, F.C., *The genetics of cleft lip and palate*. Am J Hum Genet, 1970. **22**: p. 336-352.
17. Grosen, D., C. Bille, I. Petersen, A. Skytthe, J. Hjelmberg, J.K. Pedersen, J.C. Murray, and K. Christensen, *Risk of oral clefts in twins*. Epidemiology, 2011. **22**(3): p. 313-9.
18. Grosen, D., C. Bille, J.K. Pedersen, A. Skytthe, J.C. Murray, and K. Christensen, *Recurrence risk for offspring of twins discordant for oral cleft: a population-based cohort study of the Danish 1936-2004 cleft twin cohort*. Am J Med Genet A, 2010. **152A**(10): p. 2468-74.
19. Sivertsen, A., A.J. Wilcox, R. Skjaerven, H.A. Vindenes, F. Abyholm, E. Harville, and R.T. Lie, *Familial risk of oral clefts by morphological type and severity: population based cohort study of first degree relatives*. BMJ, 2008. **336**(7641): p. 432-4.
20. Wyszynski, D.F., ed. *Cleft lip and palate : from origin to treatment*. 2002, Oxford University Press: Oxford ; New York. xviii, 518 p., 4 p. of plates.
21. Lidral, A.C. and J.C. Murray, *Genetic approaches to identify disease genes for birth defects with cleft lip/palate as a model*. Birth Defects Res A Clin Mol Teratol, 2004. **70**(12): p. 893-901.
22. Leslie, E.J. and M.L. Marazita, *Genetics of cleft lip and cleft palate*. Am J Med Genet C Semin Med Genet, 2013. **163C**(4): p. 246-58.
23. Vieira, A.R. and I.M. Orioli, *Candidate genes for nonsyndromic cleft lip and palate*. ASDC J Dent Child, 2001. **68**(4): p. 272-9, 229.
24. Marazita, M.L., *The evolution of human genetic studies of cleft lip and cleft palate*. Annu Rev Genomics Hum Genet, 2012. **13**: p. 263-83.
25. Cox, L.L., T.C. Cox, L.M. Moreno Uribe, Y. Zhu, C.T. Richter, N. Nidey, J.M. Standley, M. Deng, E. Blue, J.X. Chong, Y. Yang, R.P. Carstens, D. Anand, S.A. Lachke, J.D. Smith, M.O. Dorschner, B. Bedell, E. Kirk, A.V. Hing, H. Venselaar, L.C.

- Valencia-Ramirez, M.J. Bamshad, I.A. Glass, J.A. Cooper, E. Haan, D.A. Nickerson, H. van Bokhoven, H. Zhou, K.N. Krahn, M.F. Buckley, J.C. Murray, A.C. Lidral, and T. Roscioli, *Mutations in the Epithelial Cadherin-p120-Catenin Complex Cause Mendelian Non-Syndromic Cleft Lip with or without Cleft Palate*. *Am J Hum Genet*, 2018. **102**(6): p. 1143-1157.
26. Vieira, A.R., *Unraveling human cleft lip and palate research*. *J Dent Res*, 2008. **87**(2): p. 119-25.
27. Younkin, S.G., R.B. Scharpf, H. Schwender, M.M. Parker, A.F. Scott, M.L. Marazita, T.H. Beaty, and I. Ruczinski, *A genome-wide study of de novo deletions identifies a candidate locus for non-syndromic isolated cleft lip/palate risk*. *BMC Genet*, 2014. **15**: p. 24.
28. Leslie, E.J., J.C. Carlson, J.R. Shaffer, C.J. Buxo, E.E. Castilla, K. Christensen, F.W.B. Deleyiannis, L.L. Field, J.T. Hecht, L. Moreno, I.M. Orioli, C. Padilla, A.R. Vieira, G.L. Wehby, E. Feingold, S.M. Weinberg, J.C. Murray, and M.L. Marazita, *Association studies of low-frequency coding variants in nonsyndromic cleft lip with or without cleft palate*. *Am J Med Genet A*, 2017. **173**(6): p. 1531-1538.
29. Scapoli, L., F. Carinci, A. Palmieri, F. Cura, A. Baj, G. Beltramini, R. Docimo, and M. Martinelli, *Copy number variation analysis of twin pairs discordant for cleft lip with or without cleft palate*. *Int J Immunopathol Pharmacol*, 2019. **33**: p. 2058738419855873.
30. Conte, F., M. Oti, J. Dixon, C.E. Carels, M. Rubini, and H. Zhou, *Systematic analysis of copy number variants of a large cohort of orofacial cleft patients identifies candidate genes for orofacial clefts*. *Hum Genet*, 2016. **135**(1): p. 41-59.
31. Reynolds, K., P. Kumari, L. Sepulveda Rincon, R. Gu, Y. Ji, S. Kumar, and C.J. Zhou, *Wnt signaling in orofacial clefts: crosstalk, pathogenesis and models*. *Dis Model Mech*, 2019. **12**(2).

32. Kousa, Y.A. and B.C. Schutte, *Toward an orofacial gene regulatory network*. Dev Dyn, 2016. **245**(3): p. 220-32.
33. Chiquet, B.T., Q. Yuan, E.C. Swindell, L. Maili, R. Plant, J. Dyke, R. Boyer, J.F. Teichgraeber, M.R. Greives, J.B. Mulliken, A. Letra, S.H. Blanton, and J.T. Hecht, *Knockdown of Crispld2 in zebrafish identifies a novel network for nonsyndromic cleft lip with or without cleft palate candidate genes*. Eur J Hum Genet, 2018. **26**(10): p. 1441-1450.
34. Letra, A., L. Maili, J.B. Mulliken, E. Buchanan, S.H. Blanton, and J.T. Hecht, *Further evidence suggesting a role for variation in ARHGAP29 variants in nonsyndromic cleft lip/palate*. Birth Defects Res A Clin Mol Teratol, 2014. **100**(9): p. 679-85.
35. Thieme, F. and K.U. Ludwig, *The Role of Noncoding Genetic Variation in Isolated Orofacial Clefts*. J Dent Res, 2017. **96**(11): p. 1238-1247.
36. Bhatia, S. and D.A. Kleinjan, *Disruption of long-range gene regulation in human genetic disease: a kaleidoscope of general principles, diverse mechanisms and unique phenotypic consequences*. Hum Genet, 2014. **133**(7): p. 815-45.
37. Spielmann, M. and S. Mundlos, *Structural variations, the regulatory landscape of the genome and their alteration in human disease*. Bioessays, 2013. **35**(6): p. 533-43.
38. Attanasio, C., A.S. Nord, Y. Zhu, M.J. Blow, Z. Li, D.K. Liberton, H. Morrison, I. Plajzer-Frick, A. Holt, R. Hosseini, S. Phouanavong, J.A. Akiyama, M. Shoukry, V. Afzal, E.M. Rubin, D.R. FitzPatrick, B. Ren, B. Hallgrimsson, L.A. Pennacchio, and A. Visel, *Fine tuning of craniofacial morphology by distant-acting enhancers*. Science, 2013. **342**(6157): p. 1241006.
39. Morris, V.E., S.S. Hashmi, L. Zhu, L. Maili, C. Urbina, S. Blackwell, M.R. Greives, E.P. Buchanan, J.B. Mulliken, S.H. Blanton, W.J. Zheng, J.T. Hecht, and A. Letra, *Evidence for craniofacial enhancer variation underlying nonsyndromic cleft lip and palate*. Hum Genet, 2020. **139**(10): p. 1261-1272.

40. Leslie, E.J., M.A. Taub, H. Liu, K.M. Steinberg, D.C. Koboldt, Q. Zhang, J.C. Carlson, J.B. Hetmanski, H. Wang, D.E. Larson, R.S. Fulton, Y.A. Kousa, W.D. Fakhouri, A. Naji, I. Ruczinski, F. Begum, M.M. Parker, T. Busch, J. Standley, J. Rigdon, J.T. Hecht, A.F. Scott, G.L. Wehby, K. Christensen, A.E. Czeizel, F.W. Deleyiannis, B.C. Schutte, R.K. Wilson, R.A. Cornell, A.C. Lidral, G.M. Weinstock, T.H. Beaty, M.L. Marazita, and J.C. Murray, *Identification of functional variants for cleft lip with or without cleft palate in or near PAX7, FGFR2, and NOG by targeted sequencing of GWAS loci*. *Am J Hum Genet*, 2015. **96**(3): p. 397-411.
41. Cordero, D.R., S. Brugmann, Y. Chu, R. Bajpai, M. Jame, and J.A. Helms, *Cranial neural crest cells on the move: their roles in craniofacial development*. *Am J Med Genet A*, 2011. **155A**(2): p. 270-9.
42. Twigg, S.R. and A.O. Wilkie, *New insights into craniofacial malformations*. *Hum Mol Genet*, 2015. **24**(R1): p. R50-9.
43. Jiang, R., J.O. Bush, and A.C. Lidral, *Development of the upper lip: morphogenetic and molecular mechanisms*. *Dev Dyn*, 2006. **235**(5): p. 1152-66.
44. Marcucio, R., B. Hallgrimsson, and N.M. Young, *Facial Morphogenesis: Physical and Molecular Interactions Between the Brain and the Face*. *Curr Top Dev Biol*, 2015. **115**: p. 299-320.
45. Marcucio, R.S., N.M. Young, D. Hu, and B. Hallgrimsson, *Mechanisms that underlie co-variation of the brain and face*. *Genesis*, 2011. **49**(4): p. 177-89.
46. Parsons, T.E., E.J. Schmidt, J.C. Boughner, H.A. Jamniczky, R.S. Marcucio, and B. Hallgrimsson, *Epigenetic integration of the developing brain and face*. *Dev Dyn*, 2011. **240**(10): p. 2233-44.
47. Nopoulos, P., S. Berg, J. Canady, L. Richman, D. Van Demark, and N.C. Andreasen, *Abnormal brain morphology in patients with isolated cleft lip, cleft palate, or both: a preliminary analysis*. *Cleft Palate Craniofac J*, 2000. **37**(5): p. 441-6.

48. Weinberg, S.M., T.E. Parsons, M.R. Fogel, C.P. Walter, A.L. Conrad, and P. Nopoulos, *Corpus callosum shape is altered in individuals with nonsyndromic cleft lip and palate*. Am J Med Genet A, 2013. **161A**(5): p. 1002-7.
49. He, F. and Y. Chen, *Wnt signaling in lip and palate development*. Front Oral Biol, 2012. **16**: p. 81-90.
50. Clevers, H. and R. Nusse, *Wnt/beta-catenin signaling and disease*. Cell, 2012. **149**(6): p. 1192-205.
51. Niehrs, C., *The complex world of WNT receptor signalling*. Nat Rev Mol Cell Biol, 2012. **13**(12): p. 767-79.
52. Brugmann, S.A., L.H. Goodnough, A. Gregorieff, P. Leucht, D. ten Berge, C. Fuerer, H. Clevers, R. Nusse, and J.A. Helms, *Wnt signaling mediates regional specification in the vertebrate face*. Development, 2007. **134**(18): p. 3283-95.
53. Juriloff, D.M. and M.J. Harris, *Mouse genetic models of cleft lip with or without cleft palate*. Birth defects research. Part A, Clinical and molecular teratology, 2008. **82**(2): p. 63-77.
54. Juriloff, D.M., M.J. Harris, D.L. Mager, and L. Gagnier, *Epigenetic mechanism causes Wnt9b deficiency and nonsyndromic cleft lip and palate in the A/WySn mouse strain*. Birth Defects Res A Clin Mol Teratol, 2014. **100**(10): p. 772-88.
55. Plamondon, J.A., M.J. Harris, D.L. Mager, L. Gagnier, and D.M. Juriloff, *The clf2 gene has an epigenetic role in the multifactorial etiology of cleft lip and palate in the A/WySn mouse strain*. Birth Defects Res A Clin Mol Teratol, 2011. **91**(8): p. 716-27.
56. Juriloff, D.M., M.J. Harris, A.P. McMahon, T.J. Carroll, and A.C. Lidral, *Wnt9b is the mutated gene involved in multifactorial nonsyndromic cleft lip with or without cleft palate in A/WySn mice, as confirmed by a genetic complementation test*. Birth Defects Res A Clin Mol Teratol, 2006. **76**(8): p. 574-9.

57. Juriloff, D.M., M.J. Harris, S.L. Dewell, C.J. Brown, D.L. Mager, L. Gagnier, and D.G. Mah, *Investigations of the genomic region that contains the clf1 mutation, a causal gene in multifactorial cleft lip and palate in mice*. Birth Defects Res A Clin Mol Teratol, 2005. **73**(2): p. 103-13.
58. Juriloff, D.M., M.J. Harris, and S.L. Dewell, *A digenic cause of cleft lip in A-strain mice and definition of candidate genes for the two loci*. Birth Defects Res A Clin Mol Teratol, 2004. **70**(8): p. 509-18.
59. Ferretti, E., B. Li, R. Zewdu, V. Wells, J.M. Hebert, C. Karner, M.J. Anderson, T. Williams, J. Dixon, M.J. Dixon, M.J. Depew, and L. Selleri, *A conserved Pbx-Wnt-p63-Irf6 regulatory module controls face morphogenesis by promoting epithelial apoptosis*. Dev Cell, 2011. **21**(4): p. 627-41.
60. Uslu, V.V., M. Petretich, S. Ruf, K. Langenfeld, N.A. Fonseca, J.C. Marioni, and F. Spitz, *Long-range enhancers regulating Myc expression are required for normal facial morphogenesis*. Nat Genet, 2014.
61. Mostowska, A., K.K. Hozyasz, B. Biedziak, P. Wojcicki, M. Lianeri, and P.P. Jagodzinski, *Genotype and haplotype analysis of WNT genes in non-syndromic cleft lip with or without cleft palate*. Eur J Oral Sci, 2012. **120**(1): p. 1-8.
62. Chiquet, B.T., S.H. Blanton, A. Burt, D. Ma, S. Stal, J.B. Mulliken, and J.T. Hecht, *Variation in WNT genes is associated with non-syndromic cleft lip with or without cleft palate*. Hum Mol Genet, 2008. **17**(14): p. 2212-8.
63. Yao, T., L. Yang, P.Q. Li, H. Wu, H.B. Xie, X. Shen, and X.D. Xie, *Association of Wnt3A gene variants with non-syndromic cleft lip with or without cleft palate in Chinese population*. Arch Oral Biol, 2011. **56**(1): p. 73-8.
64. Menezes, R., A. Letra, A.H. Kim, E.C. Kuchler, A. Day, P.N. Tannure, L. Gomes da Motta, K.B. Paiva, J.M. Granjeiro, and A.R. Vieira, *Studies with Wnt genes and*

- nonsyndromic cleft lip and palate*. Birth Defects Res A Clin Mol Teratol, 2010. **88**(11): p. 995-1000.
65. Cvjetkovic, N., L. Maili, K.S. Weymouth, S.S. Hashmi, J.B. Mulliken, J. Topczewski, A. Letra, Q. Yuan, S.H. Blanton, E.C. Swindell, and J.T. Hecht, *Regulatory variant in FZD6 gene contributes to nonsyndromic cleft lip and palate in an African-American family*. Mol Genet Genomic Med, 2015. **3**(5): p. 440-51.
66. Tokuhara, M., M. Hirai, Y. Atomi, M. Terada, and M. Katoh, *Molecular cloning of human Frizzled-6*. Biochem Biophys Res Commun, 1998. **243**(2): p. 622-7.
67. MacDonald, B.T., K. Tamai, and X. He, *Wnt/beta-catenin signaling: components, mechanisms, and diseases*. Dev Cell, 2009. **17**(1): p. 9-26.
68. Borello, U., V. Buffa, C. Sonnino, R. Melchionna, E. Vivarelli, and G. Cossu, *Differential expression of the Wnt putative receptors Frizzled during mouse somitogenesis*. Mech Dev, 1999. **89**(1-2): p. 173-7.
69. Golan, T., A. Yaniv, A. Bafico, G. Liu, and A. Gazit, *The human Frizzled 6 (HFz6) acts as a negative regulator of the canonical Wnt. beta-catenin signaling cascade*. J Biol Chem, 2004. **279**(15): p. 14879-88.
70. He, X., M. Semenov, K. Tamai, and X. Zeng, *LDL receptor-related proteins 5 and 6 in Wnt/beta-catenin signaling: arrows point the way*. Development, 2004. **131**(8): p. 1663-77.
71. Kwee, M.L., W. Balemans, E. Cleiren, J.J. Gille, F. Van Der Blij, J.M. Sepers, and W. Van Hul, *An autosomal dominant high bone mass phenotype in association with craniosynostosis in an extended family is caused by an LRP5 missense mutation*. J Bone Miner Res, 2005. **20**(7): p. 1254-60.
72. Boyden, L.M., J. Mao, J. Belsky, L. Mitzner, A. Farhi, M.A. Mitnick, D. Wu, K. Insogna, and R.P. Lifton, *High bone density due to a mutation in LDL-receptor-related protein 5*. N Engl J Med, 2002. **346**(20): p. 1513-21.

73. Willems, B., S. Tao, T. Yu, A. Huysseune, P.E. Witten, and C. Winkler, *The Wnt Co-Receptor Lrp5 Is Required for Cranial Neural Crest Cell Migration in Zebrafish*. PLoS One, 2015. **10**(6): p. e0131768.
74. Basha, M., B. Demeer, N. Revencu, R. Helaers, S. Theys, S. Bou Saba, O. Boute, B. Devauchelle, G. Francois, B. Bayet, and M. Vikkula, *Whole exome sequencing identifies mutations in 10% of patients with familial non-syndromic cleft lip and/or palate in genes mutated in well-known syndromes*. J Med Genet, 2018. **55**(7): p. 449-458.
75. Song, L., Y. Li, K. Wang, Y.Z. Wang, A. Molotkov, L. Gao, T. Zhao, T. Yamagami, Y. Wang, Q. Gan, D.E. Pleasure, and C.J. Zhou, *Lrp6-mediated canonical Wnt signaling is required for lip formation and fusion*. Development, 2009. **136**(18): p. 3161-71.
76. Fossat, N., V. Jones, M.J. Garcia-Garcia, and P.P. Tam, *Modulation of WNT signaling activity is key to the formation of the embryonic head*. Cell Cycle, 2012. **11**(1): p. 26-32.
77. Mukhopadhyay, M., Shtrom, S., Rodriguez-Esteban, C., Chen, L., Tsukui, T., Gomer, L., Dorward, D.W., Glinka, A., Grinberg, A., Huang, S.P., Niehrs, C., Izpisua Belmonte, J.C., Westphal, H., *Dickkopf1 is required for embryonic head induction and limb morphogenesis in the mouse*. Dev Cell, 2001. **3**: p. 423-34.
78. Online Mendelian Inheritance in Man, O.T., *The Human Genome Data Base Project, Johns Hopkins University, Baltimore, MD World Wide Web*<URL:<http://gdbwww.gdb.org/omim/docs/omimtop.html>>,. 1995.
79. Orioli, I.M. and E.E. Castilla, *Clinical epidemiologic study of holoprosencephaly in South America*. Am J Med Genet A, 2007. **143A**(24): p. 3088-99.
80. Lidral, A.C., H. Liu, S.A. Bullard, G. Bonde, J. Machida, A. Visel, L.M. Uribe, X. Li, B. Amendt, and R.A. Cornell, *A single nucleotide polymorphism associated with isolated*

- cleft lip and palate, thyroid cancer and hypothyroidism alters the activity of an oral epithelium and thyroid enhancer near FOXE1. Hum Mol Genet, 2015. 24(14): p. 3895-907.*
81. Smigielski, E.M., K. Sirotkin, M. Ward, and S.T. Sherry, *dbSNP: a database of single nucleotide polymorphisms. Nucleic Acids Res, 2000. 28(1): p. 352-5.*
 82. Barrett, J.C., B. Fry, J. Maller, and M.J. Daly, *Haploview: analysis and visualization of LD and haplotype maps. Bioinformatics, 2005. 21(2): p. 263-5.*
 83. Cooper, G.M., E.A. Stone, G. Asimenos, N.C.S. Program, E.D. Green, S. Batzoglou, and A. Sidow, *Distribution and intensity of constraint in mammalian genomic sequence. Genome Res, 2005. 15(7): p. 901-13.*
 84. Davydov, E.V., D.L. Goode, M. Sirota, G.M. Cooper, A. Sidow, and S. Batzoglou, *Identifying a high fraction of the human genome to be under selective constraint using GERP++. PLoS Comput Biol, 2010. 6(12): p. e1001025.*
 85. Ritchie, G.R., I. Dunham, E. Zeggini, and P. Flicek, *Functional annotation of noncoding sequence variants. Nat Methods, 2014. 11(3): p. 294-6.*
 86. Ward, L.D. and M. Kellis, *HaploReg v4: systematic mining of putative causal variants, cell types, regulators and target genes for human complex traits and disease. Nucleic Acids Res, 2016. 44(D1): p. D877-81.*
 87. Ward, L.D. and M. Kellis, *HaploReg: a resource for exploring chromatin states, conservation, and regulatory motif alterations within sets of genetically linked variants. Nucleic Acids Res, 2012. 40(Database issue): p. D930-4.*
 88. Consortium, G.T., D.A. Laboratory, G. Coordinating Center -Analysis Working, G. Statistical Methods groups-Analysis Working, G.g. Enhancing, N.I.H.C. Fund, Nih/Nci, Nih/Nhgri, Nih/Nimh, Nih/Nida, N. Biospecimen Collection Source Site, R. Biospecimen Collection Source Site, V. Biospecimen Core Resource, B. Brain Bank Repository-University of Miami Brain Endowment, M. Leidos Biomedical-Project, E.

- Study, I. Genome Browser Data, E.B.I. Visualization, I. Genome Browser Data, U.o.C.S.C. Visualization-Ucsc Genomics Institute, a. Lead, D.A. Laboratory, C. Coordinating, N.I.H.p. management, c. Biospecimen, Pathology, Q.T.L.m.w.g. e, A. Battle, C.D. Brown, B.E. Engelhardt, and S.B. Montgomery, *Genetic effects on gene expression across human tissues*. Nature, 2017. **550**(7675): p. 204-213.
89. Wang, J., E.R. Gamazon, B.L. Pierce, B.E. Stranger, H.K. Im, R.D. Gibbons, N.J. Cox, D.L. Nicolae, and L.S. Chen, *Imputing Gene Expression in Uncollected Tissues Within and Beyond GTEx*. Am J Hum Genet, 2016. **98**(4): p. 697-708.
90. Grabe, N., *AliBaba2: context specific identification of transcription factor binding sites*. In Silico Biol, 2002. **2**(1): p. S1-15.
91. Messeguer, X., R. Escudero, D. Farre, O. Nunez, J. Martinez, and M.M. Alba, *PROMO: detection of known transcription regulatory elements using species-tailored searches*. Bioinformatics, 2002. **18**(2): p. 333-4.
92. Moro, E., G. Ozhan-Kizil, A. Mongera, D. Beis, C. Wierzbicki, R.M. Young, D. Bournele, A. Domenichini, L.E. Valdivia, L. Lum, C. Chen, J.F. Amatruda, N. Tiso, G. Weidinger, and F. Argenton, *In vivo Wnt signaling tracing through a transgenic biosensor fish reveals novel activity domains*. Dev Biol, 2012. **366**(2): p. 327-40.
93. Klingenberg, C.P., *MorphoJ: an integrated software package for geometric morphometrics*. Mol Ecol Resour, 2011. **11**(2): p. 353-7.
94. Kimmel, C.B., W.W. Ballard, S.R. Kimmel, B. Ullmann, and T.F. Schilling, *Stages of embryonic development of the zebrafish*. Dev Dyn, 1995. **203**(3): p. 253-310.
95. Schneider, C.A., W.S. Rasband, and K.W. Eliceiri, *NIH Image to ImageJ: 25 years of image analysis*. Nat Methods, 2012. **9**(7): p. 671-5.
96. Laird, N.M. and C. Lange, *Family-based methods for linkage and association analysis*. Adv Genet, 2008. **60**: p. 219-52.

97. Laird, N.M. and C. Lange, *Family-based designs in the age of large-scale gene-association studies*. Nat Rev Genet, 2006. **7**(5): p. 385-94.
98. Chung, R.H., M.A. Schmidt, and E.R. Martin, *CAPL: an efficient association software package using family and case-control data and accounting for population stratification*. BMC Bioinformatics, 2011. **12**: p. 201.
99. Chung, R.H., E.R. Hauser, and E.R. Martin, *The APL test: extension to general nuclear families and haplotypes and examination of its robustness*. Human Heredity, 2006. **61**(4): p. 189-99.
100. Lange, C., D. DeMeo, ., E.K. Silverman, S.T. Weiss, and N.M. Laird, *PBAT: Tools for family-based association studies*. Am J Hum Genet, 2004. **74**: p. 367-369.
101. Horvath, S., X. Xu, and N.M. Laird, *The family based association test method: strategies for studying general genotype-phenotype associations*. Eur J Hum Genet, 2001. **9**: p. 301-306.
102. Laird, N.M., S. Horvath, and X. Xu, *Implementing a unified approach to family-based tests of association*. Genet Epidemiol, 2000. **19 Suppl 1**: p. S36-42.
103. Carter, C.O., *Genetics of common congenital malformations in man*. Proc R Soc Med, 1976. **69**(1): p. 38-40.
104. Mossey, P.A., J. Little, R.G. Munger, M.J. Dixon, and W.C. Shaw, *Cleft lip and palate*. Lancet, 2009. **374**(9703): p. 1773-85.
105. Beaty, T.H., M.L. Marazita, and E.J. Leslie, *Genetic factors influencing risk to orofacial clefts: today's challenges and tomorrow's opportunities*. F1000Res, 2016. **5**: p. 2800.
106. Leoyklang, P., P. Siriwan, and V. Shotelersuk, *A mutation of the p63 gene in non-syndromic cleft lip*. J Med Genet, 2006. **43**(6): p. e28.

107. Barrow, L.L., H. van Bokhoven, S. Daack-Hirsch, T. Andersen, S.E. van Beersum, R. Gorlin, and J.C. Murray, *Analysis of the p63 gene in classical EEC syndrome, related syndromes, and non-syndromic orofacial clefts*. J Med Genet, 2002. **39**(8): p. 559-66.
108. Pengelly, R.J., R. Upstill-Goddard, L. Arias, J. Martinez, J. Gibson, M. Knut, A.L. Collins, S. Ennis, A. Collins, and I. Briceno, *Resolving clinical diagnoses for syndromic cleft lip and/or palate phenotypes using whole-exome sequencing*. Clin Genet, 2015. **88**(5): p. 441-9.
109. Bureau, A., M.M. Parker, I. Ruczinski, M.A. Taub, M.L. Marazita, J.C. Murray, E. Mangold, M.M. Noethen, K.U. Ludwig, J.B. Hetmanski, J.E. Bailey-Wilson, C.D. Cropp, Q. Li, S. Szymczak, H. Albacha-Hejazi, K. Alqosayer, L.L. Field, Y.H. Wu-Chou, K.F. Doheny, H. Ling, A.F. Scott, and T.H. Beaty, *Whole exome sequencing of distant relatives in multiplex families implicates rare variants in candidate genes for oral clefts*. Genetics, 2014. **197**(3): p. 1039-44.
110. Zhou, R., M. Wang, W. Li, S. Wang, Z. Zhou, J. Li, T. Wu, H. Zhu, and T.H. Beaty, *Gene-Gene Interactions among SPRYs for Nonsyndromic Cleft Lip/Palate*. J Dent Res, 2019. **98**(2): p. 180-185.
111. Velazquez-Aragon, J.A., M.A. Alcantara-Ortigoza, B. Estandia-Ortega, M.E. Reyna-Fabian, C.D. Mendez-Adame, and A. Gonzalez-Del Angel, *Gene Interactions Provide Evidence for Signaling Pathways Involved in Cleft Lip/Palate in Humans*. J Dent Res, 2016. **95**(11): p. 1257-64.
112. Li, Q., Y. Kim, B. Suktitipat, J.B. Hetmanski, M.L. Marazita, P. Duggal, T.H. Beaty, and J.E. Bailey-Wilson, *Gene-Gene Interaction Among WNT Genes for Oral Cleft in Trios*. Genet Epidemiol, 2015. **39**(5): p. 385-94.
113. Liu, D., H. Schwender, M. Wang, H. Wang, P. Wang, H. Zhu, Z. Zhou, J. Li, T. Wu, and T.H. Beaty, *Gene-gene interaction between MSX1 and TP63 in Asian case-*

- parent trios with nonsyndromic cleft lip with or without cleft palate*. Birth Defects Res, 2018. **110**(4): p. 317-324.
114. Carlson, J.C., J. Standley, A. Petrin, J.R. Shaffer, A. Butali, C.J. Buxo, E. Castilla, K. Christensen, F.W. Deleyiannis, J.T. Hecht, L.L. Field, A. Garidkhuu, L.M. Moreno Uribe, N. Nagato, I.M. Orioli, C. Padilla, F. Poletta, S. Suzuki, A.R. Vieira, G.L. Wehby, S.M. Weinberg, T.H. Beaty, E. Feingold, J.C. Murray, M.L. Marazita, and E.J. Leslie, *Identification of 16q21 as a modifier of nonsyndromic orofacial cleft phenotypes*. Genet Epidemiol, 2017. **41**(8): p. 887-897.
115. Tumpel, S., L.M. Wiedemann, and R. Krumlauf, *Hox genes and segmentation of the vertebrate hindbrain*. Curr Top Dev Biol, 2009. **88**: p. 103-37.
116. Capellini, T.D., R. Zewdu, G. Di Giacomo, S. Ascitti, J.E. Kugler, A. Di Gregorio, and L. Selleri, *Pbx1/Pbx2 govern axial skeletal development by controlling Polycomb and Hox in mesoderm and Pax1/Pax9 in sclerotome*. Dev Biol, 2008. **321**(2): p. 500-14.
117. Capellini, T.D., G. Di Giacomo, V. Salsi, A. Brendolan, E. Ferretti, D. Srivastava, V. Zappavigna, and L. Selleri, *Pbx1/Pbx2 requirement for distal limb patterning is mediated by the hierarchical control of Hox gene spatial distribution and Shh expression*. Development, 2006. **133**(11): p. 2263-73.
118. Purcell, S., B. Neale, K. Todd-Brown, L. Thomas, M.A. Ferreira, D. Bender, J. Maller, P. Sklar, P.I. de Bakker, M.J. Daly, and P.C. Sham, *PLINK: a tool set for whole-genome association and population-based linkage analyses*. Am J Hum Genet, 2007. **81**(3): p. 559-75.
119. Blanton, S.H., A. Burt, E. Garcia, J.B. Mulliken, S. Stal, and J.T. Hecht, *Ethnic heterogeneity of IRF6 AP-2a binding site promoter SNP association with nonsyndromic cleft lip and palate*. Cleft Palate Craniofac J, 2010. **47**(6): p. 574-7.

120. Liu, N., K. Zhang, and H. Zhao, *Haplotype-association analysis*. Adv Genet, 2008. **60**: p. 335-405.
121. Evangelou, E., T.A. Trikalinos, G. Salanti, and J.P. Ioannidis, *Family-based versus unrelated case-control designs for genetic associations*. PLoS Genet, 2006. **2**(8): p. e123.
122. Igl, B.W., I.R. Konig, and A. Ziegler, *What do we mean by 'replication' and 'validation' in genome-wide association studies?* Hum Hered, 2009. **67**(1): p. 66-8.
123. Liu, H., E.J. Leslie, Z. Jia, T. Smith, M. Eshete, A. Butali, M. Dunnwald, J. Murray, and R.A. Cornell, *Irf6 directly regulates Klf17 in zebrafish periderm and Klf4 in murine oral epithelium, and dominant-negative KLF4 variants are present in patients with cleft lip and palate*. Hum Mol Genet, 2016. **25**(4): p. 766-76.
124. Warner, D.R., S.C. Smith, I.A. Smolenkova, M.M. Pisano, and R.M. Greene, *Inhibition of p300 histone acetyltransferase activity in palate mesenchyme cells attenuates Wnt signaling via aberrant E-cadherin expression*. Exp Cell Res, 2016. **342**(1): p. 32-8.
125. Bhattacharjee, V., K.H. Horn, S. Singh, C.L. Webb, M.M. Pisano, and R.M. Greene, *CBP/p300 and associated transcriptional co-activators exhibit distinct expression patterns during murine craniofacial and neural tube development*. Int J Dev Biol, 2009. **53**(7): p. 1097-104.
126. Uslu, V.V., M. Petretich, S. Ruf, K. Langenfeld, N.A. Fonseca, J.C. Marioni, and F. Spitz, *Long-range enhancers regulating Myc expression are required for normal facial morphogenesis*. Nat Genet, 2014. **46**(7): p. 753-8.
127. Xu, P., B. Balczerski, A. Ciozda, K. Louie, V. Oralova, A. Huysseune, and J.G. Crump, *Fox proteins are modular competency factors for facial cartilage and tooth specification*. Development, 2018. **145**(12).

128. Xu, J., H. Liu, Y. Lan, B.J. Aronow, V.V. Kalinichenko, and R. Jiang, *A Shh-Foxf-Fgf18-Shh Molecular Circuit Regulating Palate Development*. PLoS Genet, 2016. **12**(1): p. e1005769.
129. Leslie, E.J., J.C. Carlson, J.R. Shaffer, A. Butali, C.J. Buxo, E.E. Castilla, K. Christensen, F.W. Deleyiannis, L. Leigh Field, J.T. Hecht, L. Moreno, I.M. Orioli, C. Padilla, A.R. Vieira, G.L. Wehby, E. Feingold, S.M. Weinberg, J.C. Murray, T.H. Beaty, and M.L. Marazita, *Genome-wide meta-analyses of nonsyndromic orofacial clefts identify novel associations between FOXE1 and all orofacial clefts, and TP63 and cleft lip with or without cleft palate*. Hum Genet, 2017. **136**(3): p. 275-286.
130. Minocha, S., D. Valloton, Y. Arsenijevic, J.R. Cardinaux, R. Guidi, J.P. Hornung, and C. Lebrand, *Nkx2.1 regulates the generation of telencephalic astrocytes during embryonic development*. Sci Rep, 2017. **7**: p. 43093.
131. Manoli, M. and W. Driever, *nkx2.1 and nkx2.4 genes function partially redundant during development of the zebrafish hypothalamus, preoptic region, and pallidum*. Front Neuroanat, 2014. **8**: p. 145.
132. Blanton, S.H., A. Cortez, S. Stal, J.B. Mulliken, R.H. Finnell, and J.T. Hecht, *Variation in IRF6 contributes to nonsyndromic cleft lip and palate*. Am J Med Genet A, 2005. **137A**(3): p. 259-62.
133. Zuccherro, T.M., M.E. Cooper, B.S. Maher, S. Daack-Hirsch, B. Nepomuceno, L. Ribeiro, D. Caprau, K. Christensen, Y. Suzuki, J. Machida, N. Natsume, K. Yoshiura, A.R. Vieira, I.M. Orioli, E.E. Castilla, L. Moreno, M. Arcos-Burgos, A.C. Lidral, L.L. Field, Y.E. Liu, A. Ray, T.H. Goldstein, R.E. Schultz, M. Shi, M.K. Johnson, S. Kondo, B.C. Schutte, M.L. Marazita, and J.C. Murray, *Interferon regulatory factor 6 (IRF6) gene variants and the risk of isolated cleft lip or palate*. N Engl J Med, 2004. **351**(8): p. 769-80.

134. Zuccherro, T.M., M.E. Cooper, B.S. Maher, S. Daack-Hirsch, N. B., L. Ribeiro, D. Caprau, K. Christensen, Y. Suzuki, J. Machida, N. Natsume, K. Yoshiura, A.R. Vieira, I.M. Orioli, E.E. Castilla, L. Moreno, M. Arcos-Burgos, A.C. Lidral, L.L. Field, Y. Liu, A. Ray, T.H. Goldstein, R.E. Schultz, M. Shi, S. Kondo, B.C. Schutte, M. Marazita, and J. Murray, *Interferon Regulatory Factor 6 (IRF6) is a Modifier for Isolated Cleft Lip and Palate*. *Am J Human Genet*, 2003. **73**: p. 162.
135. Birnbaum, S., K.U. Ludwig, H. Reutter, S. Herms, N.A. de Assis, A. Diaz-Lacava, S. Barth, C. Lauster, G. Schmidt, M. Scheer, M. Saffar, M. Martini, R.H. Reich, F. Schiefke, A. Hemprich, S. Potzsch, B. Potzsch, T.F. Wienker, P. Hoffmann, M. Knapp, F.J. Kramer, M.M. Nothen, and E. Mangold, *IRF6 gene variants in Central European patients with non-syndromic cleft lip with or without cleft palate*. *Eur J Oral Sci*, 2009. **117**(6): p. 766-9.
136. Jugessur, A., F. Rahimov, R.T. Lie, A.J. Wilcox, H.K. Gjessing, R.M. Nilsen, T.T. Nguyen, and J.C. Murray, *Genetic variants in IRF6 and the risk of facial clefts: single-marker and haplotype-based analyses in a population-based case-control study of facial clefts in Norway*. *Genet Epidemiol*, 2008. **32**(5): p. 413-24.
137. Park, J.W., I. McIntosh, J.B. Hetmanski, E.W. Jabs, C.A. Vander Kolk, Y.H. Wu-Chou, P.K. Chen, S.S. Chong, V. Yeow, S.H. Jee, B.Y. Park, M.D. Fallin, R. Ingersoll, A.F. Scott, and T.H. Beaty, *Association between IRF6 and nonsyndromic cleft lip with or without cleft palate in four populations*. *Genetics in Medicine*, 2007. **9**(4): p. 219-27.
138. Mani, P., A. Jarrell, J. Myers, and R. Atit, *Visualizing canonical Wnt signaling during mouse craniofacial development*. *Dev Dyn*, 2010. **239**(1): p. 354-63.
139. Mazemondet, O., R. Hubner, J. Frahm, D. Koczan, B.M. Bader, D.G. Weiss, A.M. Uhrmacher, M.J. Frech, A. Rolfs, and J. Luo, *Quantitative and kinetic profile of*

- Wnt/beta-catenin signaling components during human neural progenitor cell differentiation.* Cell Mol Biol Lett, 2011. **16**(4): p. 515-38.
140. Wang, Y., L. Song, and C.J. Zhou, *The canonical Wnt/beta-catenin signaling pathway regulates Fgf signaling for early facial development.* Dev Biol, 2011. **349**(2): p. 250-60.
141. Gritli-Linde, A., *p63 and IRF6: brothers in arms against cleft palate.* J Clin Invest, 2010. **120**(5): p. 1386-9.
142. Ionita-Laza, I., S. Lee, V. Makarov, J.D. Buxbaum, and X. Lin, *Family-based association tests for sequence data, and comparisons with population-based association tests.* Eur J Hum Genet, 2013. **21**(10): p. 1158-62.
143. Gorlin, R.J., Cohen, M.M., Hennekam, R.C.M, *Syndromes of the Head and Neck.* Fourth Edition ed. 2011, New York Oxford University Press.
144. Letra, A., R. Menezes, J.M. Granjeiro, and A.R. Vieira, *Defining subphenotypes for oral clefts based on dental development.* Journal of dental research, 2007. **86**(10): p. 986-91.
145. Yates, D., V. Allareddy, J. Caplin, S. Yadav, and M.R. Markiewicz, *An Overview of Timeline of Interventions in the Continuum of Cleft Lip and Palate Care.* Oral Maxillofac Surg Clin North Am, 2020. **32**(2): p. 177-186.
146. Wehby, G.L. and C.H. Cassell, *The impact of orofacial clefts on quality of life and healthcare use and costs.* Oral Dis, 2010. **16**(1): p. 3-10.
147. Brito, L.A., L.A. Cruz, K.M. Rocha, L.K. Barbara, C.B. Silva, D.F. Bueno, M. Aguenta, D.R. Bertola, D. Franco, A.M. Costa, N. Alonso, P.A. Otto, and M.R. Passos-Bueno, *Genetic contribution for non-syndromic cleft lip with or without cleft palate (NS CL/P) in different regions of Brazil and implications for association studies.* Am J Med Genet A, 2011. **155A**(7): p. 1581-7.

148. Christensen, K. and P. Fogh-Andersen, *Cleft lip (+/- cleft palate) in Danish twins, 1970-1990*. Am J Med Genet, 1993. **47**(6): p. 910-6.
149. Jugessur, A., M. Shi, H.K. Gjessing, R.T. Lie, A.J. Wilcox, C.R. Weinberg, K. Christensen, A.L. Boyles, S. Daack-Hirsch, T.N. Trung, C. Bille, A.C. Lidral, and J.C. Murray, *Genetic determinants of facial clefting: analysis of 357 candidate genes using two national cleft studies from Scandinavia*. PLoS One, 2009. **4**(4): p. e5385.
150. Ludwig, K.U., A.C. Bohmer, J. Bowes, M. Nikolic, N. Ishorst, N. Wyatt, N.L. Hammond, L. Golz, F. Thieme, S. Barth, H. Schuenke, J. Klamt, M. Spielmann, K. Aldhoreae, A. Rojas-Martinez, M.M. Nothen, A. Rada-Iglesias, M.J. Dixon, M. Knapp, and E. Mangold, *Imputation of orofacial clefting data identifies novel risk loci and sheds light on the genetic background of cleft lip +/- cleft palate and cleft palate only*. Hum Mol Genet, 2017. **26**(4): p. 829-842.
151. Chiquet, B.T., A.C. Lidral, S. Stal, J.B. Mulliken, L.M. Moreno, M. Arcos-Burgos, C. Valencia-Ramirez, S.H. Blanton, and J.T. Hecht, *CRISPLD2: a novel NSCLP candidate gene*. Hum Mol Genet, 2007. **16**(18): p. 2241-8.
152. Mijiti, A., W. Ling, A. Maimaiti, M. Tuerdi, J. Tuerxun, and A. Moming, *Preliminary evidence of an interaction between the CRISPLD2 gene and non-syndromic cleft lip with or without cleft palate (nsCL/P) in Xinjiang Uyghur population, China*. Int J Pediatr Otorhinolaryngol, 2015. **79**(2): p. 94-100.
153. Shen, X., R.M. Liu, L. Yang, H. Wu, P.Q. Li, Y.L. Liang, X.D. Xie, T. Yao, T.T. Zhang, and M. Yu, *The CRISPLD2 gene is involved in cleft lip and/or cleft palate in a Chinese population*. Birth defects research. Part A, Clinical and molecular teratology, 2011. **91**(10): p. 918-24.
154. Letra, A., R. Menezes, M. Cooper, R. Fonseca, S. Tropp, M. Govil, J. Granjeiro, S. Imoehl, M. Mansilla, J. Murray, E. Castilla, I. Orioli, A.E. Czeizel, L. Ma, B. Chiquet, J. Hecht, A. Vieira, and M. Marazita, *Crispld2 Variants Including a C471t Silent*

- Mutation May Contribute to Nonsyndromic Cleft Lip with or without Cleft Palate.* Cleft Palate Craniofac J, 2010.
155. Yuan, Q., B.T. Chiquet, L. Devault, M.L. Warman, Y. Nakamura, E.C. Swindell, and J.T. Hecht, *Craniofacial abnormalities result from knock down of nonsyndromic clefting gene, crispld2, in zebrafish.* Genesis, 2012. **50**(12): p. 871-81.
156. Swindell, E.C., Q. Yuan, L.E. Maili, B. Tandon, D.S. Wagner, and J.T. Hecht, *Crispld2 is required for neural crest cell migration and cell viability during zebrafish craniofacial development.* Genesis, 2015. **53**(10): p. 660-7.
157. Rodriguez-Berdini, L., G.O. Ferrero, F. Bustos Plonka, A.M. Cardozo Gizzi, C.G. Prucca, S. Quiroga, and B.L. Caputto, *The moonlighting protein c-Fos activates lipid synthesis in neurons, an activity that is critical for cellular differentiation and cortical development.* J Biol Chem, 2020. **295**(26): p. 8808-8818.
158. Wagner, E.F., *Functions of AP1 (Fos/Jun) in bone development.* Ann Rheum Dis, 2002. **61 Suppl 2**: p. ii40-2.
159. Durchdewald, M., P. Angel, and J. Hess, *The transcription factor Fos: a Janus-type regulator in health and disease.* Histol Histopathol, 2009. **24**(11): p. 1451-61.
160. Velazquez, F.N., C.G. Prucca, O. Etienne, D.S. D'Astolfo, D.C. Silvestre, F.D. Boussin, and B.L. Caputto, *Brain development is impaired in c-fos -/- mice.* Oncotarget, 2015. **6**(19): p. 16883-901.
161. Chen, J., E. Zhang, W. Zhang, Z. Liu, P. Lu, T. Zhu, Z. Yin, L.J. Backman, H. Liu, X. Chen, and H. Ouyang, *Fos Promotes Early Stage Teno-Lineage Differentiation of Tendon Stem/Progenitor Cells in Tendon.* Stem Cells Transl Med, 2017. **6**(11): p. 2009-2019.

162. Milde-Langosch, K., *The Fos family of transcription factors and their role in tumorigenesis*. Eur J Cancer, 2005. **41**(16): p. 2449-61.
163. Alfaqeeh, S., V. Oralova, M. Foxworthy, E. Matalova, A.E. Grigoriadis, and A.S. Tucker, *Root and Eruption Defects in c-Fos Mice Are Driven by Loss of Osteoclasts*. J Dent Res, 2015. **94**(12): p. 1724-31.
164. Johnson, R.S., B.M. Spiegelman, and V. Papaioannou, *Pleiotropic effects of a null mutation in the c-fos proto-oncogene*. Cell, 1992. **71**(4): p. 577-86.
165. Smeyne, R.J., M. Vendrell, M. Hayward, S.J. Baker, G.G. Miao, K. Schilling, L.M. Robertson, T. Curran, and J.I. Morgan, *Continuous c-fos expression precedes programmed cell death in vivo*. Nature, 1993. **363**(6425): p. 166-9.
166. Smeyne, R.J., K. Schilling, J. Oberdick, L. Robertson, D. Luk, T. Curran, and J.I. Morgan, *A fos-lac Z transgenic mouse that can be used for neuroanatomic mapping*. Adv Neurol, 1993. **59**: p. 285-91.
167. Yano, H., A. Ohtsuru, M. Ito, T. Fujii, and S. Yamashita, *Involvement of c-Fos proto-oncogene during palatal fusion and interdigital space formation in the rat*. Development, Growth & Differentiation, 1996. **38**(4): p. 351-357.
168. Dickinson, A.J., *Using frogs faces to dissect the mechanisms underlying human orofacial defects*. Semin Cell Dev Biol, 2016. **51**: p. 54-63.
169. Eberhart, J.K., X. He, M.E. Swartz, Y.L. Yan, H. Song, T.C. Boling, A.K. Kunerth, M.B. Walker, C.B. Kimmel, and J.H. Postlethwait, *MicroRNA Mirn140 modulates Pdgf signaling during palatogenesis*. Nat Genet, 2008. **40**(3): p. 290-8.
170. Carney, T.J., K.A. Dutton, E. Greenhill, M. Delfino-Machin, P. Dufourcq, P. Blader, and R.N. Kelsh, *A direct role for Sox10 in specification of neural crest-derived sensory neurons*. Development, 2006. **133**(23): p. 4619-30.

171. Young, N.M., S. Wat, V.M. Diewert, L.W. Browder, and B. Hallgrimsson, *Comparative morphometrics of embryonic facial morphogenesis: implications for cleft-lip etiology*. *Anatomical Record* (Hoboken, N.J.: 2007), 2007. **290**(1): p. 123-39.
172. Parsons, T.E., E. Kristensen, L. Hornung, V.M. Diewert, S.K. Boyd, R.Z. German, and B. Hallgrimsson, *Phenotypic variability and craniofacial dysmorphology: increased shape variance in a mouse model for cleft lip*. *J Anat*, 2008. **212**(2): p. 135-43.
173. Green, R.M., W. Feng, T. Phang, J.L. Fish, H. Li, R.A. Spritz, R.S. Marcucio, J. Hooper, H. Jamniczky, B. Hallgrimsson, and T. Williams, *Tfap2a-dependent changes in mouse facial morphology result in clefting that can be ameliorated by a reduction in Fgf8 gene dosage*. *Dis Model Mech*, 2015. **8**(1): p. 31-43.
174. Weinberg, S.M., S.D. Naidoo, K.M. Bardi, C.A. Brandon, K. Neiswanger, J.M. Resick, R.A. Martin, and M.L. Marazita, *Face shape of unaffected parents with cleft affected offspring: combining three-dimensional surface imaging and geometric morphometrics*. *Orthod Craniofac Res*, 2009. **12**(4): p. 271-81.
175. Weinberg, S.M., B.S. Maher, and M.L. Marazita, *Parental craniofacial morphology in cleft lip with or without cleft palate as determined by cephalometry: a meta-analysis*. *Orthod Craniofac Res*, 2006. **9**(1): p. 18-30.
176. Fraser, F.C. and H. Pashayan, *Relation of face shape to susceptibility to congenital cleft lip. A preliminary report*. *J Med Genet*, 1970. **7**(2): p. 112-7.
177. El Sergani, A.M., S. Brandebura, C. Padilla, A. Butali, W.L. Adeyemo, C. Valencia-Ramirez, C.P.R. Muneton, L.M. Moreno, C.J. Buxo, R.E. Long, Jr., K. Neiswanger, J.R. Shaffer, M.L. Marazita, and S.M. Weinberg, *Parents of Children With Nonsyndromic Orofacial Clefting Show Altered Palate Shape*. *Cleft Palate Craniofac J*, 2020: p. 1055665620967235.

178. Watanabe, H., K. Saitoh, T. Kameda, M. Murakami, Y. Niikura, S. Okazaki, Y. Morishita, S. Mori, Y. Yokouchi, A. Kuroiwa, and H. Iba, *Chondrocytes as a specific target of ectopic Fos expression in early development*. Proc Natl Acad Sci U S A, 1997. **94**(8): p. 3994-9.
179. Caubet, J.F. and J.F. Bernaudin, *Expression of the c-fos proto-oncogene in bone, cartilage and tooth forming tissues during mouse development*. Biol Cell, 1988. **64**(1): p. 101-4.
180. Sandberg, M., H. Autio-Harminen, and E. Vuorio, *Localization of the expression of types I, III, and IV collagen, TGF-beta 1 and c-fos genes in developing human calvarial bones*. Dev Biol, 1988. **130**(1): p. 324-34.
181. Dony, C. and P. Gruss, *Proto-oncogene c-fos expression in growth regions of fetal bone and mesodermal web tissue*. Nature, 1987. **328**(6132): p. 711-4.
182. Mork, L. and G. Crump, *Zebrafish Craniofacial Development: A Window into Early Patterning*. Curr Top Dev Biol, 2015. **115**: p. 235-69.
183. Hess, J., P. Angel, and M. Schorpp-Kistner, *AP-1 subunits: quarrel and harmony among siblings*. J Cell Sci, 2004. **117**(Pt 25): p. 5965-73.
184. Wang, Q., H. Liu, Q. Wang, F. Zhou, Y. Liu, Y. Zhang, H. Ding, M. Yuan, F. Li, and Y. Chen, *Involvement of c-Fos in cell proliferation, migration, and invasion in osteosarcoma cells accompanied by altered expression of Wnt2 and Fzd9*. PLoS One, 2017. **12**(6): p. e0180558.
185. Sherwood, D.R., J.A. Butler, J.M. Kramer, and P.W. Sternberg, *FOS-1 promotes basement-membrane removal during anchor-cell invasion in C. elegans*. Cell, 2005. **121**(6): p. 951-62.
186. McLennan, R., M.C. McKinney, J.M. Teddy, J.A. Morrison, J.C. Kasemeier-Kulesa, D.A. Ridenour, C.A. Manthe, R. Giniunaite, M. Robinson, R.E. Baker, P.K. Maini, and

- P.M. Kulesa, *Neural crest cells bulldoze through the microenvironment using Aquaporin 1 to stabilize filopodia*. *Development*, 2020. **147**(1).
187. Duncan, K.M., K. Mukherjee, R.A. Cornell, and E.C. Liao, *Zebrafish models of orofacial clefts*. *Dev Dyn*, 2017. **246**(11): p. 897-914.
188. Guo, N., C. Hawkins, and J. Nathans, *Frizzled6 controls hair patterning in mice*. *Proc Natl Acad Sci U S A*, 2004. **101**(25): p. 9277-81.
189. Frojmark, A.S., J. Schuster, M. Sobol, M. Entesarian, M.B. Kilander, D. Gabrikova, S. Nawaz, S.M. Baig, G. Schulte, J. Klar, and N. Dahl, *Mutations in Frizzled 6 cause isolated autosomal-recessive nail dysplasia*. *Am J Hum Genet*, 2011. **88**(6): p. 852-60.
190. Stuebner, S., T. Faus-Kessler, T. Fischer, W. Wurst, and N. Prakash, *Fzd3 and Fzd6 deficiency results in a severe midbrain morphogenesis defect*. *Dev Dyn*, 2010. **239**(1): p. 246-60.
191. Wang, Y., H. Chang, A. Rattner, and J. Nathans, *Frizzled Receptors in Development and Disease*. *Curr Top Dev Biol*, 2016. **117**: p. 113-39.
192. Maurano, M.T., R. Humbert, E. Rynes, R.E. Thurman, E. Haugen, H. Wang, A.P. Reynolds, R. Sandstrom, H. Qu, J. Brody, A. Shafer, F. Neri, K. Lee, T. Kutayavin, S. Stehling-Sun, A.K. Johnson, T.K. Canfield, E. Giste, M. Diegel, D. Bates, R.S. Hansen, S. Neph, P.J. Sabo, S. Heimfeld, A. Raubitschek, S. Ziegler, C. Cotsapas, N. Sotoodehnia, I. Glass, S.R. Sunyaev, R. Kaul, and J.A. Stamatoyannopoulos, *Systematic localization of common disease-associated variation in regulatory DNA*. *Science*, 2012. **337**(6099): p. 1190-5.
193. Birnbaum, S., K.U. Ludwig, H. Reutter, S. Herms, M. Steffens, M. Rubini, C. Baluardo, M. Ferrian, N. Almeida de Assis, M.A. Alblas, S. Barth, J. Freudenberg, C. Lauster, G. Schmidt, M. Scheer, B. Braumann, S.J. Berge, R.H. Reich, F. Schiefke, A. Hemprich, S. Potzsch, R.P. Steegers-Theunissen, B. Potzsch, S. Moebus, B.

- Horsthemke, F.J. Kramer, T.F. Wienker, P.A. Mossey, P. Propping, S. Cichon, P. Hoffmann, M. Knapp, M.M. Nothen, and E. Mangold, *Key susceptibility locus for nonsyndromic cleft lip with or without cleft palate on chromosome 8q24*. *Nat Genet*, 2009. **41**(4): p. 473-7.
194. Grant, S.F., K. Wang, H. Zhang, W. Glaberson, K. Annaiah, C.E. Kim, J.P. Bradfield, J.T. Glessner, K.A. Thomas, M. Garris, E.C. Frackelton, F.G. Otieno, R.M. Chiavacci, H.D. Nah, R.E. Kirschner, and H. Hakonarson, *A genome-wide association study identifies a locus for nonsyndromic cleft lip with or without cleft palate on 8q24*. *J Pediatr*, 2009. **155**(6): p. 909-13.
195. Brewer, S., W. Feng, J. Huang, S. Sullivan, and T. Williams, *Wnt1-Cre-mediated deletion of AP-2alpha causes multiple neural crest-related defects*. *Dev Biol*, 2004. **267**(1): p. 135-52.
196. Milunsky, J.M., T.A. Maher, G. Zhao, A.E. Roberts, H.J. Stalker, R.T. Zori, M.N. Burch, M. Clemens, J.B. Mulliken, R. Smith, and A.E. Lin, *TFAP2A mutations result in branchio-oculo-facial syndrome*. *American journal of human genetics*, 2008. **82**(5): p. 1171-7.
197. Corradin, O. and P.C. Scacheri, *Enhancer variants: evaluating functions in common disease*. *Genome Med*, 2014. **6**(10): p. 85.
198. Betancur, P., M. Simoes-Costa, T. Sauka-Spengler, and M.E. Bronner, *Expression and function of transcription factor cMyb during cranial neural crest development*. *Mech Dev*, 2014. **132**: p. 38-43.
199. Bhatia, S., C.T. Gordon, R.G. Foster, L. Melin, V. Abadie, G. Baujat, M.P. Vazquez, J. Amiel, S. Lyonnet, V. van Heyningen, and D.A. Kleinjan, *Functional assessment of disease-associated regulatory variants in vivo using a versatile dual colour transgenesis strategy in zebrafish*. *PLoS Genet*, 2015. **11**(6): p. e1005193.

200. Carter, C.O., *The inheritance of common congenital malformations*. Prog Med Genet, 1965. **5**: p. 59-84.
201. Okano, J., J. Udagawa, and K. Shiota, *Roles of retinoic acid signaling in normal and abnormal development of the palate and tongue*. Congenit Anom (Kyoto), 2014. **54**(2): p. 69-76.
202. CDC, *Hospital stays, hospital charges, and in-hospital deaths among infants with selected birth defects--United States, 2003*. MMWR Morb Mortal Wkly Rep, 2007. **56**(2): p. 25-9.
203. Greene, J.C., *Epidemiology of congenital clefts of the lip and palate*. Public Health Rep, 1963. **78**: p. 589-602.
204. Mukhopadhyay, N., M. Bishop, M. Mortillo, P. Chopra, J.B. Hetmanski, M.A. Taub, L.M. Moreno, L.C. Valencia-Ramirez, C. Restrepo, G.L. Wehby, J.T. Hecht, F. Deleyiannis, A. Butali, S.M. Weinberg, T.H. Beaty, J.C. Murray, E.J. Leslie, E. Feingold, and M.L. Marazita, *Whole genome sequencing of orofacial cleft trios from the Gabriella Miller Kids First Pediatric Research Consortium identifies a new locus on chromosome 21*. Hum Genet, 2020. **139**(2): p. 215-226.
205. Bishop, M.R., K.K. Diaz Perez, M. Sun, S. Ho, P. Chopra, N. Mukhopadhyay, J.B. Hetmanski, M.A. Taub, L.M. Moreno-Urbe, L.C. Valencia-Ramirez, C.P. Restrepo Muneton, G. Wehby, J.T. Hecht, F. Deleyiannis, S.M. Weinberg, Y.H. Wu-Chou, P.K. Chen, H. Brand, M.P. Epstein, I. Ruczinski, J.C. Murray, T.H. Beaty, E. Feingold, R.J. Lipinski, D.J. Cutler, M.L. Marazita, and E.J. Leslie, *Genome-wide Enrichment of De Novo Coding Mutations in Orofacial Cleft Trios*. Am J Hum Genet, 2020. **107**(1): p. 124-136.
206. Shi, J., X. Jiao, T. Song, B. Zhang, C. Qin, and F. Cao, *CRISPLD2 polymorphisms are associated with non-syndromic cleft lip with or without cleft palate in a northern Chinese population*. European journal of oral sciences, 2010. **118**(4): p. 430-3.

Vita

Lorena Maili was born the daughter of Eduard Maili and Zhaneta Maili. After completing her work at Cypress Falls High School, Houston, Texas, she entered Baylor University in Waco, Texas. She received the degree of Bachelor of Science with a major in neuroscience from Baylor in May, 2007. She then received a Master of Science in biomedical sciences from The University of Texas MD Anderson Cancer Center UTHealth Graduate School of Biomedical Sciences in May 2011. For the next three years, she worked as a research assistant in the Department of Pediatrics at McGovern Medical School. In August of 2014 she entered The University of Texas MD Anderson Cancer Center UTHealth Graduate School of Biomedical Sciences.

Permanent address:

8903 Green Ray Drive
Houston, Texas 77095